Malagasy *Conostigmus* (Hymenoptera: Ceraphronoidea) and the secret of scutes

István Mikó Corresp., [1] , **Carolyn Trietsch** [1] , **Emily Sandall** [1] , **Matthew Jon Yoder** [2] , **Heather Hines** [3] , **Andrew Robert Deans** [1]

[1] Frost Entomological Museum, Department of Entomology, Pennsylvania State University, University Park, PA, United States

[2] Illinois Natural History Survey, University of Illinois at Urbana-Champaign, Champaign, Illinois, United States

[3] Department of Biology, Pennsylvania State University, University Park, Pennsylvania, United States

Corresponding Author: István Mikó
Email address: izm2@psu.edu

We revise the genus *Conostigmus Dahlbom* 1858 occurring in Madagascar, based on data from more specimens than were examined for the latest world revision of the genus. Our results yield new information about intraspecific variability and the nature of the atypical latitudinal diversity gradient observed in Ceraphronoidea. We also investigate cellular processes that underlie body size polyphenism, by utilizing the correspondence between epidermal cells and scutes, polygonal units of leather-like microsculpture. Our results reveal that body size polyphenism in Megaspilidae is most likely related to cell number and not cell size variation, and that cell size differs between epithelial fields of the head and that of the mesosoma. Three species, *Conostigmus ballescoracas* Dessart 1997, C. babaiax Dessart 1996 and *C. longulus* Dessart 1997, are redescribed. Females of *C. longulus* is described for the first time, as are nine new species: *C. bucephalus* Mikó and Trietsch **sp. nov.**, *C. clavatus* Mikó and Trietsch **sp. nov.**, *C. fianarantsoaensis* Mikó and Trietsch **sp. nov.**, *C. lucidus* Mikó and Trietsch **sp. nov.**, *C. macrocupula,* Mikó and Trietsch **sp. nov.**, *C. madagascariensis* Mikó and Trietsch **sp. nov.**, *C. missyhazenae* Mikó and Trietsch **sp. nov.**, *C. pseudobabaiax* Mikó and Trietsch **sp. nov.**, and *C. toliaraensis* Mikó and Trietsch **sp. nov..** A fully illustrated identification key for *Malagasy Conostigmus* species and a Web Ontology Language (OWL) representation of the taxonomic treatment, including specimen data, nomenclature, and phenotype descriptions, in both natural and formal languages, are provided.

Malagasy *Conostigmus* (Hymenoptera: Ceraphronoidea) and the secret of scutes

István Mikó[1], Carolyn Trietsch[1], Emily L. Sandall[1], Matthew J. Yoder[2], Heather M. Hines[1,3], and Andrew R. Deans[1]

[1]Frost Entomological Museum, Department of Entomology, Pennsylvania State University, University Park, PA, USA
[2]Illinois Natural History Survey, University of Illinois, Champaign, IL, USA
[3]Department of Biology, Pennsylvania State University, University Park, PA, USA

ABSTRACT

We revise the genus *Conostigmus* Dahlbom 1858 occurring in Madagascar, based on data from more specimens than were examined for the latest world revision of the genus. Our results yield new information about intraspecific variability and the nature of the atypical latitudinal diversity gradient observed in Ceraphronoidea. We also investigate cellular processes that underlie body size polyphenism, by utilizing the correspondence between epidermal cells and scutes, polygonal units of leather-like microsculpture. Our results reveal that body size polyphenism in Megaspilidae is most likely related to cell number and not cell size variation, and that cell size differs between epithelial fields of the head and that of the mesosoma. Three species, *Conostigmus ballescoracas* Dessart 1997, *C. babaiax* Dessart 1996 and *C. longulus* Dessart 1997, are redescribed. Females of *C. longulus* is described for the first time, as are nine new species: *C. bucephalus* Mikó and Trietsch **sp. nov.**, *C. clavatus* Mikó and Trietsch **sp. nov.**, *C. fianarantsoaensis* Mikó and Trietsch **sp. nov.**, *C. lucidus* Mikó and Trietsch **sp. nov.**, *C. macrocupula* Mikó and Trietsch **sp. nov.**, *C. madagascariensis* Mikó and Trietsch **sp. nov.**, *C. missyhazenae* Mikó and Trietsch **sp. nov.**, *C. pseudobabaiax* Mikó and Trietsch **sp. nov.**, and *C. toliaraensis* Mikó and Trietsch **sp. nov.**. A fully illustrated identification key for Malagasy *Conostigmus* species and a Web Ontology Language (OWL) representation of the taxonomic treatment, including specimen data, nomenclature, and phenotype descriptions, in both natural and formal languages, are provided.

Keywords: taxonomy, morphology, microscopy, male genitalia, phenotypic plasticity, imaginal disks, CLSM, LDG

INTRODUCTION

With 162 extant species, *Conostigmus* Dahlbom 1858 is the second most species-rich genus of Megaspilidae (Ceraphronoidea), a hymenopteran family showing a reverse latitudinal diversity gradient (LDG) in species richness (Johnson and Musetti, 2004; Noyes, 1989). Since ceraphronoid faunistic and taxonomic studies mostly focuse on the Holarctic fauna, it is possible that sample bias is the reason for this atypical distribution. This might be especially true for *Conostigmus*, given that the only revision of the genus focused exclusively on non-American and non-European species (n=36) and was based on only 145 specimens (Dessart, 1997). The large number of Malagasy specimens examined in the present study will not only double the number of specimens of non-American and non-European *Conostigmus* but will also provide a reasonable data set for comparing the Malagasy fauna with that of a similarly sized area in Europe, the Atlantic Archipelago (British Isles; Broad and Livermore, 2014). Madagascar is considered a hotspot of biodiversity (Myers et al., 2000), and if reverse LDG is false and based on sample bias, we would be able to document more species in Madagascar than in the AA.

Ceraphronoids likely belong to the basal apocritan Evaniomorpha, and exhibit mostly ancestral sets of phenotypes (Heraty et al., 2011; Vilhelmsen et al., 2010). The complexity of the ceraphronoid ovipositor system and male genitalia is unparalleled among Apocritans (Mikó et al., 2013; Ernst et al., 2013), and the leather-like microsculpture covering their head and mesosoma (Mikó et al., 2011; Burks et al., 2016) is hypothesized to be an ancestral trait in Insecta (Hinton, 1970).

Besides the ten-fold interspecific body length variability from 0.37 mm (*Microceraphron subterraneus*

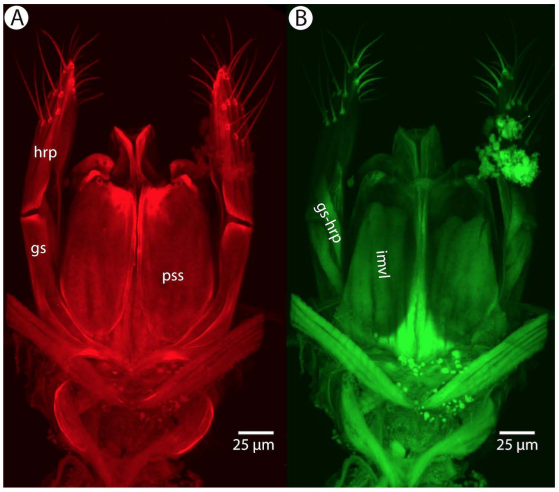

Figure 1. CLSM volume rendered micrographs showing the skeletomuscular system of the male genitalia of *Conostigmus longulus* Dessart 1997. A. Excitation wavelength=631 nm, emission wavelength=647 nm. B. Excitation wavelength=499 nm, emission wavelength=520 nm. Abbreviations: pss=parossiculus; gs=gonostipes; hrp=harpe; gs-hrp=proximal gonostyle/volsella complex-harpal muscle; imvl=medial gonostyle volsella complex-volsellal muscle.

Szelényi 1935) to 4.5 mm, (*Megaspilus armatus* Say 1836), up to four-fold intraspecific variability has been reported in Ceraphronoidea (Mackauer and Chow, 2015; Dessart and Gärdenfors, 1985; Liebscher, 1972). Similar intraspecific variability is common among microhymenoptera and can be stimulated by alternative host species with different nutritional quality, gregariousness with variable nest sizes, and climatic differences, such as temperature. Ceraphronoids are ectoparasitoids on insect parasitoid and predator larvae (Haviland, 1920; Withycombe, 1924; Kamal, 1939) and have a broad host range (Gilkeson et al., 1993; Sullivan and Völkl, 1999). *Dendrocerus carpenteri*, for example, has been reared from >70 aphidiine (Braconidae) species (Fergusson, 1980). Based on the few studies with appropriate rearing experiences, gregariousness might also be not uncommon among Ceraphronoidea (Kamal, 1939; Bennett and Sullivan, 1978; Mackauer and Chow, 2015; Cooper and Dessart, 1975; Dessart, 1997; Liebscher, 1972)).

Environmental factors impact development and determine final adult body size (Nijhout and Callier, 2015) by altering different cellular processes. Temperature and oxygen level usually impact cell size (Azevedo et al., 2002; Harrison and Haddad, 2011; Heinrich et al., 2011), while nutrition mostly regulates cell division (Emlen et al., 2007) . *Conostigmus* species are relatively large ceraphronoids (0.8–2.2 mm) making them feasible to observe and examine scutes (Meyer, 1842; Cals, 1974; Krell, 1994), elements of the aforementioned leather like sculpture. Scutes likely have a one to one correspondence to epidermal cells in arthropods (Moretto et al., 2015; Hinton, 1970; Cals, 1973, 1974; Blaney and Chapman, 1969) and thus should provide information about the cellular basis of body size polyphenism.

Research related to geographic distribution and polyphenism requires a stable taxonomic framework. We revise the Malagasy *Conostigmus*, Dahlbom 1858 and use this system to explore the anomalous ceraphronoid diversity patterns and possible reasons for body size polyphenism.

MATERIALS AND METHODS

Specimens for the present study (Table S1) were obtained from Malaise trap samples and were loaned to the authors from the California Academy of Sciences. Morphological characters were scored with an Olympus SZX16 stereo-microscope equipped with an Olympus SDF PLAPO 2XPFC objective, resulting in 230× magnification. Specimens are deposited in the California Academy of Sciences (CAS), in the Frost Entomological Museum (FEM) and in the Royal Museum of Central Africa (MRAC) (Table S1).

Brightfield images of dried specimens were taken with an Olympus BX43 compound microscope equipped with an Olympus DP73 digital camera. Image stacking was performed with Zerene Stacker (Version 1.04 Build T201404082055, Zerene Systems LLC, Richland, WA) and extended focus images

were annotated and modified with Adobe Photoshop 6^{TM} (Adobe Systems, San Jose, California) using Adjust/Filter/Unsharp mask and Image/Adjustments/Exposure (Gamma correction) tools.

Metasomata were removed from the specimens and placed in 35% H_2O_2 for 20 minutes, rinsed in distilled water for 30 minutes and dehydrated with 25% and 50% ethanol for 15–15 minutes, then transferred to a glycerol droplet on a concavity slide (Sail Brand Ltd., West Yorkshire, UK) and dissected. This protocol preserves muscle tissue while bleaching melanized structures, making them transparent for confocal laser scanning microscopy (CLSM).

Sample preparation for CLSM followed Mikó and Deans (2013): male genitalia was temporarily mounted between two coverslips (1.5 µm, 22×60) in a glycerin droplet, which did not reach the edge of the coverslip. We used Blu-tack (Bostik, Wauwatosa, WI, USA) as spacer as this material does not interact with glycerol and provides an adjustable, appropriate distance between the coverslips. Specimens were examined with an Olympus FV10i desktop CLSM.

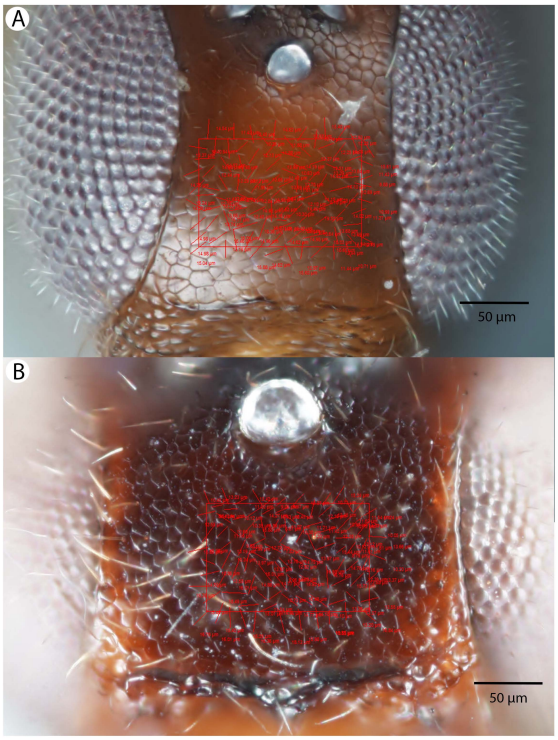

Figure 2. Brightfield image showing the median region of the cranium of *Conostigmus longulus* Dessart 1997, anterior view. The measured scute lengths and values and borders of measured rectangle are annotated in red color. Size of rectangular area=9636 µm².

Soft and sclerotized anatomical structures in arthropods tend to fluoresce with different intensities at different wavelength intervals (Mikó and Deans, 2013). CLSM tissue-specific contrast is gained by exciting specimens using multiple excitation wavelengths and/or recording the fluorescence on multiple channels assigned to different laser wavelength intervals. In previous research (Mikó et al., 2013; Popovici et al., 2014; Ernst et al., 2013), specimens were excited with only one blue laser (480 nm) and the auto-fluorescence was detected with two channels (500–580 nm and 580–800 nm). Although the resulting micrographs had differences in their intensity patterns, data from the two channels largely overlapped. In the present paper, we use two different lasers (631 nm and 499 nm) and set filters (644 nm and 520 nm respectively; narrow green and narrow red presets in Olympus Fluoview viewer software version 4.2) with narrow wavelength windows that result a much higher tissue-specific contrast, almost perfectly separating muscle tissue and skeletal components (Fig. 1).

For the morphometric analysis on scute patterns, extended focal images of the frons and the mesocutellar-axillar complex of 14 *Conostigmus longulus* Dessart 1997 specimens were taken using an Olympus BX43 compound microscope equipped with an Olympus DP73 digital camera on 200× magnification. Extended focal images were generated using the online "extended focal imaging" (efi)

tool of an Olympus Cellsens™ software. Measurements (Table S2) were taken using the same software. First, a 9636 µm² rectangular area was assigned on the extended focal images for recording scute pattern. The lateral vertices of the medially-positioned rectangle were adjacent with the scutoscutellar sulcus on the mesonotum, while the rectangle was positioned medially on the frons with equal distance from the anterior ocellus and the intertorular carina. Scutes overlapping this area (including scutes adjacent to the margin of the rectangle) were counted and the longest diameter of each scute was measured. Measurements were taken on the images while constantly checking their accuracy on live view at 200–500× magnification (Figures 2A, B). Body length largely depends on the relative orientations of the tagmata. The head of most species is flattened dorsoventrally and attached at its posterior end to the thorax (compare the position of the head on Figs 31A and B). We used the IOS (interorbital distance (IOS, http://purl.obolibrary.org/obo/HAO_0000432) to refer body size in our statistical analysis.

Bright field images, volume rendered CLSM micrographs and media files and scaleable vector (.msi) annotated extended focal images of the frons and mesoscutum, complete with scute measurements, IOS and rectangles can be accessed from Figshare (http://dx.doi.org/10.6084/m9.figshare.xxxxxxxx).

Abbreviations of anatomical structures used in Figures are listed in Table S3.

Intraspecific variation in scute diameter and relative size was scrutinized by linear regression analyses. Intra-individual variation was scrutinized via Mann-Whitney sum-rank test (Mann and Whitney, 1947). The relationship between morphometric variables was inspected through linear regression analyses. Statistical analyses were carried out and Boxplots were generated in R version 3.2.2 (Core Team, 2015) (Figure S1-S.

Taxonomic nomenclature, specimen information, OTU concepts and natural language (NL) phenotype representations were compiled in mx (http://purl.org/NET/mx-database). Taxonomic history, description, and material examined sections (Table S1) were rendered from the same software. Terminology of the phenotype statements used in descriptions, identification key and diagnoses are mapped to the Hymenoptera Anatomy Ontology (HAO, available at the), Phenotypic Quality Ontology (PATO, available at http://purl.obolibrary.org/obo/pato.owl), Biospatial Ontology (BSPO, available at http://purl.obolibrary.org/obo/bspo.owl) and Common Anatomy Reference Ontology (CARO, available at http://obofoundry.org/).

Natural language phenotypes are represented in "Entity attribute: value" format. Semantic statements for phenotype descriptions were created in Protégé 5.0.0-beta-16 (http://protege.stanford.edu/) using the OWL Manchester syntax (http://www.w3.org/TR/owl2-manchester-syntax/) following Balhoff et al. (2013), Mikó et al. (2015) and Mikó et al. (2014) (Table S4). The OWL (http://www.w3.org/TR/owl2-overview/; accessed February 4, 2014) representation of the full data set was deposited as a single Resource Description Framework (RDF)-XML file (http://www.w3.org/TR/REC-rdf-syntax/; accessed March 12) in the Github repository (https://github.com/hymao/hymao-data/blob/master/miko2016_malagasy.owl).

RESULTS

Body size polyphenism in *Conostigmus longulus* Mikó and Trietsch sp. nov.

Intraspecific variation in scute diameter and relative scute size

Fourteen specimens were measured and are represented in analysis of frons measurement distribution. Ten of these specimens were also measured on the mesoscutellum and make up the mesoscutellar analysis. Four specimens could not be measured for both regions due to inaccessibility of all scutes required for mesoscutellar measurements (*i.e.*, the specimen preparation obscured these parts). One specimen was found to have measurements four standard deviations from the mean, and was removed from subsequent analyses. Removal of this influential point from linear regression and further statistical analyses was justified by the reduction in statistical power caused by its inclusion in our small sample size (Osborne and Overbay, 2008).

Measurements were tested for normalcy and found to not follow the normal distribution, even after removal of the outlier from analyses. The scutes in a 9636 µm² rectangular region of the frons and mesoscutellum were counted and measured. It was found that maximum scute length varied from 6.6 µm to 19.5 µm. on the frons (Table 1). On the mesoscutellum, maximum scute length varied from 8.8 µm to 23.4 µm (Table 2). Median cell length of each specimen was used as a variable in statistical analyses.

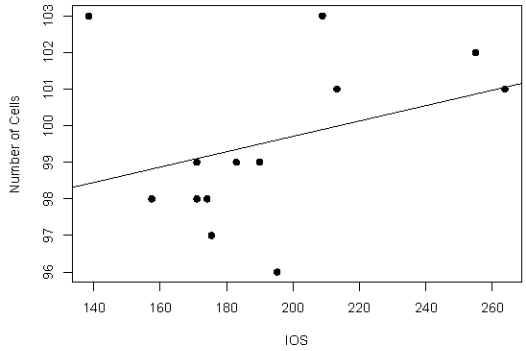

Figure 3. Relationship between body size and number of cells as linear regression. Interorbital space length (IOS), measured in μm, stands as a proxy for body size. Number of cells refers to the number of scutes/cells of a standard sized rectangular area. The size of these cells is not correlated to significant body size differences (Figure S4).

Linear regression analyses were carried out independently on both the frons and mesoscutellar fields. There was a weak negative correlation between median scute length and scute number in the frons region (R^2= 0.1369023). In the mesoscutellar region, scute length had a stronger negative correlation with scute number (R^2=0.7149943).

Table 1. Mesoscutellar average scute size, length and scute number in *Conostigmus longulus* Dessart 1997. ID: CASENT identifier for specimen, aCS: average cell size in μm², mCL: median cell length in μm, nS: number of scutes (cells) in a rectangular area of 9636 μm².

mesoscutellum	ID	aCS	mCL	nS
	2041918	119.02	17.13	81
	2003474	109.56	17.22	88
	2044193	107.12	14.52	90
	2044825	101.48	15.19	95
	2040900	101.48	16.01	95
	2009756	101.48	16.01	95
	2002193	101.48	16.01	95
	2044755	94.52	14.09	102
	2040771	91.82	13.02	105
	2053554	90.95	13.635	106
median		101.48	15.60	95
mean		101.89	15.28	95.2
s.d.		2.188891	1.437595	7.743097

Intraindividual variation in scute size: frons vs. mesoscutellum

In individuals where average scute size and diameter were measured on both the frons and the mesoscutellum, we found a variation in median cell length ranging from 11.43 μm to 17.22 μm. Wilcoxon rank-sum test revealed a significant difference in cell length between the frons and mesoscutellar regions (p-value=0.0004011). Measurements of average scute size varied from 90.95 μm² to 119.02 μm². There was no significant difference in average scute size between the frons and mesoscutellar regions in this sample when analyzed by Wilcoxon rank-sum test (p-value=0.0809).

Table 2. Frontal average scute size, length and scute number in *Conostigmus longulus* Dessart 1997. ID: CASENT identifier for specimen, IOS: interorbital space (referring to body size) in µm, aCS: average scute (cell) size in µm², mCL: median cell length in µm, nS: number of scutes (cells) in a rectangular area of 9636 µm². Note the outlier 2002193 with significantly larger average cell size and median cell length as well as a lower number of scutes.

	ID	IOS	aCS	mCL	nS
	2003474	182.91	97.38	12.78	99
	2009756	157.42	98.38	13.655	98
	2040771	174.12	98.38	12.195	98
	2040900	171.04	98.38	13.12	98
	2002193	251.06	133.90	16.195	72
	2053688	195.22	100.43	13.695	96
	2053554	189.95	97.38	13.55	99
	2053308	175.44	99.39	12.32	97
	2046100	208.85	93.60	11.43	103
	2041918	213.25	95.46	12.68	101
	2044193	263.82	95.46	13.37	101
	2044511	138.51	93.60	13.02	103
	2044755	171.04	97.38	12.75	99
	2044825	255.02	94.52	12.82	102
median		186.4	97.38	12.92	99
mean		196.3	99.55	13.11	97.57
s.d.		37.95319	10.10979	1.081914	7.673273

Body size vs. scute size

Interorbital space was used as a measure of body size for all 14 specimens examined. Linear regression analysis for the relationship between scute size and body size was carried out using measurements for interorbital space and the measurements of average frons scute size, which were available for all measured specimens (Figure 3). Correlation between median cell length and IOS was extremely weak and negative (R^2=0.001341984). The correlation between cell number and IOS was much stronger and weakly positive (R^2=0.1114898).

Taxonomic treatment of Malagasy *Conostigmus*

Conostigmus babaiax **Dessart, 1997**

Conostigmus babaiax **Dessart, 1997** *Conostigmus babaiax*: Dessart, 1997 (original description)

Figures 4, 5, 6

Diagnosis

Conostigmus babaiax Dessart 1996 shares the presence of a prognathous head (dorsal-most point of occipital carina is dorsal to posterior ocellus in lateral view) and the presence of transverse scutes on the ventral region of frons with *Conostigmus longulus* Dessart 1997, *C. toliaraensis* sp. nov. and *C. pseudobabaiax* sp. nov.*Conostigmus babaiax*, *C. toliaraensis* sp. nov. and *C. pseudobabaiax* differ from all other *Conostigmus* species by the presence of ventromedian and ventrolateral white, setiferous patches on the frons. The LOL is longer than OOL in *Conostigmus babaiax* and the LOL is shorter than OOL in *C. toliaraensis* sp. nov. and *C. pseudobabaiax* sp. nov.

Description

Body length: 2200 µm. Color intensity pattern: NOT CODED. Color hue pattern: scape, pedicel, F1-3, head, anterior mesosoma ochre, F4-F9, posterior mesosoma, metasoma brown, legs except darker proximal regions of meso and metacoxae yellow. Occipital carina sculpture: smooth. Median flange of occipital

carina count: absent. Submedial flange of occipital carina count: absent. Dorsal margin of occipital carina vs. dorsal margin of lateral ocellus in lateral view: occipital carina is dorsal to lateral ocellus in lateral view. Preoccipital lunula count: NOT CODED. Preoccipital carina count: absent. Preoccipital carina shape: NOT CODED. Preoccipital furrow count: present. Preoccipital furrow anterior end: Preoccipital furrow ends inside ocellar triangle. Postocellar carina count: absent. Male ocular ocellar line (OOL): posterior ocellar line (POL): lateral ocellar line (LOL): NOT CODED. Female ocular ocellar line (OOL): posterior ocellar line (POL): lateral ocellar line (LOL): 0.85:0.85:1.00. Head width vs. interorbital space (HW/IOS) Male: NOT CODED. Head width vs. interorbital space (HW/IOS) Female : 2.65. Setal pit on vertex size: smaller than diameter of scutes. Transverse frontal carina count: absent. Transverse scutes on frons count: present. Rugose region on frons count: absent. Randomly sized areolae around setal pits on frons count: absent. Antennal scrobe count: absent. Ventromedian setiferous patch and ventrolateral setiferous patch count: present. Facial pit count: no external corresponding structure present. Supraclypeal depression count: absent. Supraclypeal depression structure: NOT CODED. Intertorular carina count: present. Intertorular area count: present. Median region of intertorular area shape: flat. Ventral margin of antennal rim vs. dorsal margin of clypeus: not adjacent. Torulo-clypeal carina count: absent. Subtorular carina count: absent. Mandibular tooth count: 2. Female flagellomere 1 length vs. pedicel: 1.09. Female ninth flagellomere length: F9 less than F7+F8. Sensillar patch of the male flagellomere pattern: NOT CODED. Length of setae on male flagellomere vs. male flagellomere width: NOT CODED. Male flagellomere 1 length vs. male second flagellomere length: NOT CODED. Male flagellomere 1 length vs. pedicel length: NOT CODED. Ventrolateral invagination of the pronotum count: present. Scutes on posterior region of mesoscutum and dorsal region of mesoscutellum convexity: flat. Notaulus posterior end location: adjacent to transscutal articulation. Median mesoscutal sulcus posterior end: not adjacent to transscutal articulation (ends anterior to transscutal articulation). Scutoscutellar sulcus vs. transscutal articulation: adjacent. Axillular carina count: absent. Axillular carina shape: NOT CODED. Epicnemium posterior margin shape: anterior discrimenal pit absent; epicnemial carina interrupted medially. Epicnemial carina count: present only laterally. Sternaulus count: absent. Sternaulus length: NOT CODED. Speculum ventral limit: not extending ventrally of pleural pit line. Mesometapleural sulcus count: present. Metapleural carina count: present. Transverse line of the metanotum-propodeum vs. antecostal sulcus of the first abdominal tergum: adjacent sublaterally. Lateral propodeal carina count: present. Lateral propodeal carina shape: inverted "U" (left and right lateral propodeal carina are adjacent to the antecostal sulcus of the first abdominal tergumsubmedially). Anteromedian projection of the metanoto-propodeo-metapecto-mesopectal complex count: absent. S1 length vs. shortest width: S1 wider than long. Transverse carina on petiole shape: concave. Distal margin of male S9 shape: NOT CODED. Proximolateral corner of male S9 shape: NOT CODED. Cupula length vs. gonostyle-volsella complex length: NOT CODED. Proximodorsal notch of cupula count: NOT CODED. Proximodorsal notch of cupula shape: NOT CODED. Proximolateral projection of the cupula shape: NOT CODED. Proximodorsal notch of cupula width vs length: NOT CODED. Distodorsal margin of cupula shape: NOT CODED. Dorsomedian conjunctiva of the gonostyle-volsella complex length relative to length of gonostyle-volsella complex: NOT CODED. Dorsomedian conjunctiva of the gonostyle-volsella complex count: NOT CODED. Distal end of dorsomedian conjunctiva of the gonostyle-volsella complex shape: NOT CODED. Parossiculus count (parossiculus and gonostipes fusion): NOT CODED. Apical parossicular seta number: NOT CODED. Distal projection of the parossiculus count: NOT CODED. Distal projection of the penisvalva count: NOT CODED. Dorsal apodeme of penisvalva count: NOT CODED. Harpe length: NOT CODED. Distodorsal setae of sensillar ring of harpe length vs. harpe width in lateral view: NOT CODED. Distodorsal setae of sensillar ring of harpe orientation: NOT CODED. Sensillar ring area of harpe orientation: NOT CODED. Lateral setae of harpe count: NOT CODED. Lateral setae of harpe orientation: NOT CODED. Distal margin of harpe in lateral view: shape: NOT CODED. Lateral margin of harpe shape: NOT CODED.

Material Examined

Holotype female: MADAGASCAR: PSUC_FEM 000006723, COLL. MUS. Congo Madagascar: Mandraka II-1944 A. Seyrig HOLOTYPUS Holotype Prep. micros-copique n 9508/051 (deposited in MRAC)

***Conostigmus ballescoracas* Dessart, 1997**

Conostigmus ballescoracas: Dessart, 1997 (original description)

Figures 7, 8, 9

Diagnosis

Conostigmus ballescoracas Dessart 1997 differs from other *Conostigmus* species by the presence of a strong preoccipital carina that is continuous with the orbital carina, the presence of randomly sized areolae around the setal bases on the frons (shared with the ceraphronid *Masner lubomirus* Deans and Mikó 2009) and the posteromedially adjacent axillular carinae (left and right axillar carinae compose a U-shaped carina that surrounds the mesoscutellar disc).

Description

Body length: 1650-1875 µm. Color intensity pattern: NOT CODED. Color hue pattern: Cranium black; mesosoma, metasoma, F4-F9 brown; rest of antenna, legs and mandible ochre; Cranium brown; mesosoma except legs, metasoma ochre; F4-F9 brown; rest of antenna ochre, legs yellow. Occipital carina sculpture: crenulate. Median flange of occipital carina count: absent. Submedial flange of occipital carina count: absent. Dorsal margin of occipital carina vs. dorsal margin of lateral ocellus in lateral view: occipital carina is ventral to lateral ocellus in lateral view. Preoccipital lunula count: present. Preoccipital carina count: present. Preoccipital carina shape: complete. Preoccipital furrow count: present. Preoccipital furrow anterior end: Preoccipital furrow ends inside ocellar triangle. Postocellar carina count: absent. Male ocular ocellar line (OOL): posterior ocellar line (POL): lateral ocellar line (LOL): NOT CODED. Female ocular ocellar line (OOL): posterior ocellar line (POL): lateral ocellar line (LOL): 2.5-3.0:1.9-2.0:1.0. Head width vs. interorbital space (HW/IOS) Male: NOT CODED. Head width vs. interorbital space (HW/IOS) Female : 1.7-1.8. Setal pit on vertex size: smaller than diameter of scutes. Transverse frontal carina count: absent. Transverse scutes on frons count: absent. Rugose region on frons count: absent. Randomly sized areolae around setal pits on frons count: present. Antennal scrobe count: absent. Ventromedian setiferous patch and ventrolateral setiferous patch count: absent. Facial pit count: facial pit present. Supraclypeal depression count: absent. Supraclypeal depression structure: NOT CODED. Intertorular carina count: present. Intertorular area count: present. Median region of intertorular area shape: convex. Ventral margin of antennal rim vs. dorsal margin of clypeus: adjacent. Torulo-clypeal carina count: absent. Subtorular carina count: absent. Mandibular tooth count: 2. Female flagellomere 1 length vs. pedicel: 0.8-0.9. Female ninth flagellomere length: F9 less than F7+F8. Sensillar patch of the male flagellomere pattern: NOT CODED. Length of setae on male flagellomere vs. male flagellomere width: NOT CODED. Male flagellomere 1 length vs. male second flagellomere length: NOT CODED. Male flagellomere 1 length vs. pedicel length: NOT CODED. Ventrolateral invagination of the pronotum count: present. Scutes on posterior region of mesoscutum and dorsal region of mesoscutellum convexity: flat. Notaulus posterior end location: adjacent to transscutal articulation. Median mesoscutal sulcus posterior end: adjacent to transscutal articulation. Scutoscutellar sulcus vs. transscutal articulation: adjacent. Axillular carina count: present. Axillular carina shape: left and right carina continuous posteromedially forming a U-shape carina on the mesoscutellar axillar complex. Epicnemium posterior margin shape: anterior discrimenal pit present; epicnemial carina curved. Epicnemial carina count: complete. Sternaulus count: present. Sternaulus length: elongate, exceeding 3/4 of mesopleuron length at level of sternaulus. Speculum ventral limit: not extending ventrally of pleural pit line. Mesometapleural sulcus count: present. Metapleural carina count: present. Transverse line of the metanotum-propodeum vs. antecostal sulcus of the first abdominal tergum: adjacent sublaterally. Lateral propodeal carina count: present. Lateral propodeal carina shape: NOT CODED. Anteromedian projection of the metanoto-propodeo-metapecto-mesopectal complex count: present. S1 length vs. shortest width: S1 wider than long. Transverse carina on petiole shape: straight. Distal margin of male S9 shape: NOT CODED. Proximolateral corner of male S9 shape: NOT CODED. Cupula length vs. gonostyle-volsella complex length: NOT CODED. Proximodorsal notch of cupula count: NOT CODED. Proximodorsal notch of cupula shape: NOT CODED. Proximolateral projection of the cupula shape: NOT CODED. Proximodorsal notch of cupula width vs length: NOT CODED. Distodorsal margin of cupula shape: NOT CODED. Dorsomedian conjunctiva of the gonostyle-volsella complex length relative to length of gonostyle-volsella complex: NOT CODED. Dorsomedian conjunctiva of the gonostyle-volsella complex count: NOT CODED. Distal end of dorsomedian conjunctiva of the gonostyle-volsella complex shape: NOT CODED. Parossiculus count (parossiculus and gonostipes fusion): NOT CODED. Apical parossicular seta number: NOT CODED. Distal projection of the parossiculus count: NOT CODED. Distal projection of the penisvalva count: NOT CODED. Dorsal

apodeme of penisvalva count: NOT CODED. Harpe length: NOT CODED. Distodorsal setae of sensillar ring of harpe length vs. harpe width in lateral view: NOT CODED. Distodorsal setae of sensillar ring of harpe orientation: NOT CODED. Sensillar ring area of harpe orientation: NOT CODED. Lateral setae of harpe count: NOT CODED. Lateral setae of harpe orientation: NOT CODED. Distal margin of harpe in lateral view: shape: NOT CODED. Lateral margin of harpe shape: NOT CODED.

Material Examined
Holotype female: CONGO: PSUC_FEM 8883 Congo Belge : P.N.A 7-XIII-1953 H. Synave 6853 Massif Ruwenzori Mont Ngulingo pres Nyamgaleke, 2.500m, ex P.N.A HOLOTYPE Prep. micros-copique n 9507/241 (deposited in MRAC).
Other material (2 females): MADAGASCAR: 2 females. CASENT 2001391, 2016542 (CAS).

Conostigmus bucephalus Mikó and Trietsch sp. nov.

Figures 15, 16, 17

Diagnosis
Conostigmus bucephalus sp. nov. differs from other *Conostigmus* species in the presence of the antennal scrobe and the size of impressions around the setal bases on the head: impressions are larger than scutes on cranium and mesonotum in *Conostigmus bucephalus* sp. nov. whereas in other Malagasy species depressions are smaller than scutes on cranium and mesonotum.

Description
Body length: 2575 µm. Color intensity pattern: distal scape, legs except hind coxa lighter than metasoma. Color hue pattern: Cranium, mesosoma brown; antenna, legs except brown metacoxa, metasoma ochre. Occipital carina sculpture: crenulate. Median flange of occipital carina count: absent. Submedial flange of occipital carina count: absent. Dorsal margin of occipital carina vs. dorsal margin of lateral ocellus in lateral view: occipital carina is dorsal to lateral ocellus in lateral view. Preoccipital lunula count: absent. Preoccipital carina count: absent. Preoccipital carina shape: NOT CODED. Preoccipital furrow count: present. Preoccipital furrow anterior end: Preoccipital furrow ends posterior to ocellar triangle. Postocellar carina count: absent. Male ocular ocellar line (OOL): posterior ocellar line (POL): lateral ocellar line (LOL): NOT CODED. Female ocular ocellar line (OOL): posterior ocellar line (POL): lateral ocellar line (LOL): 1.0:1.2:1.0. Head width vs. interorbital space (HW/IOS) Male: NOT CODED. Head width vs. interorbital space (HW/IOS) Female : 2.2. Setal pit on vertex size: larger than diameter of scutes. Transverse frontal carina count: absent. Transverse scutes on frons count: present. Rugose region on frons count: absent. Randomly sized areolae around setal pits on frons count: absent. Antennal scrobe count: present. Ventromedian setiferous patch and ventrolateral setiferous patch count: absent. Facial pit count: no external corresponding structure present. Supraclypeal depression count: present. Supraclypeal depression structure: present medially, inverted U-shaped. Intertorular carina count: present. Intertorular area count: absent. Median region of intertorular area shape: NOT CODED. Ventral margin of antennal rim vs. dorsal margin of clypeus: adjacent. Torulo-clypeal carina count: absent. Subtorular carina count: absent. Mandibular tooth count: 2. Female flagellomere 1 length vs. pedicel: 0.7. Female ninth flagellomere length: F9 less than F7+F8. Sensillar patch of the male flagellomere pattern: NOT CODED. Length of setae on male flagellomere vs. male flagellomere width: NOT CODED. Male flagellomere 1 length vs. male second flagellomere length: NOT CODED. Male flagellomere 1 length vs. pedicel length: NOT CODED. Ventrolateral invagination of the pronotum count: present. Scutes on posterior region of mesoscutum and dorsal region of mesoscutellum convexity: flat. Notaulus posterior end location: adjacent to transscutal articulation. Median mesoscutal sulcus posterior end: adjacent to transscutal articulation. Scutoscutellar sulcus vs. transscutal articulation: adjacent. Axillular carina count: absent. Axillular carina shape: NOT CODED. Epicnemium posterior margin shape: anterior discrimenal pit absent; epicnemial carina interrupted medially. Epicnemial carina count: present only laterally. Sternaulus count: absent. Sternaulus length: NOT CODED. Speculum ventral limit: not extending ventrally of pleural pit line. Mesometapleural sulcus count: present. Metapleural carina count: present. Transverse line of the metanotum-propodeum vs. antecostal sulcus of the first abdominal tergum: adjacent sublaterally. Lateral propodeal carina count: present. Lateral propodeal carina shape: inverted “Y” (left and right

lateral propodeal are adjacent medially posterior to antecostal sulcus of the first abdominal tergum, and connected to the antecostal sulcus by a median carina representing the median branch of the inverted "Y"). Anteromedian projection of the metanoto-propodeo-metapecto-mesopectal complex count: absent. S1 length vs. shortest width: S1 wider than long. Transverse carina on petiole shape: concave. Distal margin of male S9 shape: NOT CODED. Proximolateral corner of male S9 shape: NOT CODED. Cupula length vs. gonostyle-volsella complex length: NOT CODED. Proximodorsal notch of cupula count: NOT CODED. Proximodorsal notch of cupula shape: NOT CODED. Proximolateral projection of the cupula shape: NOT CODED. Proximodorsal notch of cupula width vs length: NOT CODED. Distodorsal margin of cupula shape: NOT CODED. Dorsomedian conjunctiva of the gonostyle-volsella complex length relative to length of gonostyle-volsella complex: NOT CODED. Dorsomedian conjunctiva of the gonostyle-volsella complex count: NOT CODED. Distal end of dorsomedian conjunctiva of the gonostyle-volsella complex shape: NOT CODED. Parossiculus count (parossiculus and gonostipes fusion): NOT CODED. Apical parossiculal seta number: NOT CODED. Distal projection of the parossiculus count: NOT CODED. Distal projection of the penisvalva count: NOT CODED. Dorsal apodeme of penisvalva count: NOT CODED. Harpe length: NOT CODED. Distodorsal setae of sensillar ring of harpe length vs. harpe width in lateral view: NOT CODED. Distodorsal setae of sensillar ring of harpe orientation: NOT CODED. Sensillar ring area of harpe orientation: NOT CODED. Lateral setae of harpe count: NOT CODED. Lateral setae of harpe orientation: NOT CODED. Distal margin of harpe in lateral view: shape: NOT CODED. Lateral margin of harpe shape: NOT CODED.

Comments

Due to the antennal scrobe that accommodates the scape in almost its entire length, the head is nearly cube shaped in lateral view (Fig. 15B).

Etymology

The species epithet *bucephalus* (Ancient Greek: bou$\kappa\acute{\varepsilon}\varphi\alpha\gamma o\varsigma$ = ox-head) refers to the unique shape of the head that is certainly impacted by the distinct antennal scrobe (asr: Fig. 15B), which is diagnostic for this species.

Material Examined

Holotype female: CASENT 2053589 MADAGASCAR: Province Fianarantsoa,Parc National Ranomafana, radio tower at forest edge, elev 1130m 20 March 3 April 2003 21°15.05'S, 47°24.43'E collector: R. HarinHala California Acad of Sciences malaise, mixed tropical forest MA-02-09B-56 (deposited in CAS).

***Conostigmus clavatus* Mikó and Trietsch sp. nov.**

Figures 10, 11, 12, 13, 14

Diagnosis

Conostigmus clavatus sp. nov. shares the presence of the axillular carina, bulging eyes and medially convex intertorular area (and intertorular carina) with *C. uninasutus* Alekseev 1994 and *C. binasutus* Dessart and Cancemi 1987 and differs from them in the enlarged distal-most female flagellomere (length of F9=length of F6+length of F7+ length of F8, Fig. 13A).

Description Body length: 2325-2500 µm. Color intensity pattern: metasoma lighter than mesosoma and cranium. Color hue pattern: Dark brown except pedicel, proximal 1/5th of scape, fore and middle leg, mandible ochre/yellowish. Occipital carina sculpture: crenulate. Median flange of occipital carina count: present. Submedial flange of occipital carina count: present. Dorsal margin of occipital carina vs. dorsal margin of lateral ocellus in lateral view: occipital carina is ventral to lateral ocellus in lateral view. Preoccipital lunula count: present. Preoccipital carina count: present; absent. Preoccipital carina shape: interrupted dorsally and represented by irregular, not continuous carinae. Preoccipital furrow count: present. Preoccipital furrow anterior end: Preoccipital furrow ends posterior to ocellar triangle. Postocellar carina count: absent. Male ocular ocellar line (OOL): posterior ocellar line (POL): lateral ocellar line (LOL): 2.9-3.6:2.1-2.2:1. Female ocular ocellar line (OOL): posterior ocellar line (POL): lateral ocellar line (LOL): 3.4:2.1-2.2:1.0. Head width vs. interorbital space (HW/IOS) Male: 1.6-1.7.

Head width vs. interorbital space (HW/IOS) Female : 1.6-1.7. Setal pit on vertex size: smaller than diameter of scutes. Transverse frontal carina count: absent. Transverse scutes on frons count: absent. Rugose region on frons count: present; absent. Randomly sized areolae around setal pits on frons count: absent. Antennal scrobe count: absent. Ventromedian setiferous patch and ventrolateral setiferous patch count: absent. Facial pit count: median facial keel present. Supraclypeal depression count: present. Supraclypeal depression structure: absent medially, represented by two grooves laterally of facial pit. Intertorular carina count: present. Intertorular area count: present. Median region of intertorular area shape: convex. Ventral margin of antennal rim vs. dorsal margin of clypeus: not adjacent. Torulo-clypeal carina count: absent. Subtorular carina count: present. Mandibular tooth count: 2. Female flagellomere 1 length vs. pedicel: 0.9. Female ninth flagellomere length: F9=F6+F7+F8. Sensillar patch of the male flagellomere pattern: F5-F9. Length of setae on male flagellomere vs. male flagellomere width: setae shorter than width of flagellomeres. Male flagellomere 1 length vs. male second flagellomere length: 1.2-1.3. Male flagellomere 1 length vs. pedicel length: 2.1-2.4. Ventrolateral invagination of the pronotum count: present. Scutes on posterior region of mesoscutum and dorsal region of mesoscutellum convexity: flat. Notaulus posterior end location: adjacent to transscutal articulation. Median mesoscutal sulcus posterior end: adjacent to transscutal articulation. Scutoscutellar sulcus vs. transscutal articulation: adjacent. Axillular carina count: present. Axillular carina shape: The left and right carina are separated posteromedially. Epicnemium posterior margin shape: anterior discrimenal pit present; epicnemial carina curved. Epicnemial carina count: complete. Sternaulus count: present. Sternaulus length: short, not reaching 1/2 of mesopleuron length at level of sternaulus. Speculum ventral limit: not extending ventrally of pleural pit line. Mesometapleural sulcus count: present. Metapleural carina count: present. Transverse line of the metanotum-propodeum vs. antecostal sulcus of the first abdominal tergum: adjacent sublaterally. Lateral propodeal carina count: present. Lateral propodeal carina shape: NOT CODED. Anteromedian projection of the metanoto-propodeo-metapecto-mesopectal complex count: present. S1 length vs. shortest width: S1 wider than long. Transverse carina on petiole shape: straight. Distal margin of male S9 shape: convex. Proximolateral corner of male S9 shape: acute. Cupula length vs. gonostyle-volsella complex length: cupula less than 1/2 the length of gonostyle-volsella complex in lateral view. Proximodorsal notch of cupula count: present. Proximodorsal notch of cupula shape: arched. Proximolateral projection of the cupula shape: acute. Proximodorsal notch of cupula width vs length: as long as wide. Distodorsal margin of cupula shape: concave. Dorsomedian conjunctiva of the gonostyle-volsella complex length relative to length of gonostyle-volsella complex: dorsomedian conjunctiva extending 2/3 of length of gonostyle-volsella complex in dorsal view. Dorsomedian conjunctiva of the gonostyle-volsella complex count: present. Distal end of dorsomedian conjunctiva of the gonostyle-volsella complex shape: blunt. Parossiculus count (parossiculus and gonostipes fusion): present (not fused with the gonostipes). Apical parossicular seta number: one; two. Distal projection of the parossiculus count: absent. Distal projection of the penisvalva count: absent. Dorsal apodeme of penisvalva count: absent. Harpe length: harpe shorter than gonostipes in lateral view. Distodorsal setae of sensillar ring of harpe length vs. harpe width in lateral view: setae as long or shorter than harpe width. Distodorsal setae of sensillar ring of harpe orientation: distomedially. Sensillar ring area of harpe orientation: medially. Lateral setae of harpe count: present. Lateral setae of harpe orientation: oriented distally. Distal margin of harpe in lateral view: shape: blunt. Lateral margin of harpe shape: widest point of harpe is at its articulation site with gonostyle-volsella complex.

Etymology The species epithet *clavatus* refers to the enlarged apical female flagellomere, resembling a club (F9>F8+F7+F6).

Comments

Conostigmus clavatus, *C. binasutus* and *C. uninasutus* share numerous morphological traits with *Megaspilus* Westwood, 1929 including the presence of bulging eyes, the crenulate and distinct ocular suture, the presence of the axillular carina and the large body size (>2000 μm). Females of all *Conostigmus* species exhibit a distinct clava with 3 rows of ventral, female specific basiconic sensilla (distally gradually widening flagellum). *Megaspilus* female antenna is filiform and lacks ventral basiconic sensilla (pers. obs.).

Material Examined

Holotype male: MADAGASCAR: Province Fianarantsoa, Parc National Ranomafana, Vohiparara at broken bridge, Malaise trap in high altitude rainforest, 22-28.11.2001, R. Harin'Hala , CASENT 2044514 (deposited in CAS). Paratypes (7 males, 4 females): MADAGASCAR: 7 males, 4 females. CASENT 2002179, 2032775, 2044150, 2045085, 2045509, 2045602, 2045755, 2046024, 2046178-2046179, 2053642 (deposited in CAS, MRAC).

***Conostigmus fianarantsoaensis* Mikó and Trietsch sp. nov.**

Figures 18, 19, 20, 21

Diagnosis

Conostigmus fianarantsoensis sp. nov. is most similar to *C. madagascariensis* sp. nov. among Malagasy *Conostigmus* and differs from it by the following characters: mandible with one tooth (mandible is with 2 teeth in *C. madagascariensis*); flagellar setae shorter than the flagellomere width (in *C. madagascariensis*, flagellar setae are distinctly longer than the flagellomere width); blunt proximolateral projection of cupula (acute in *C. madagascariensis*); notched proximodorsal notch of cupula (arched in *C. madagascariensis*); blunt distal end of dorsomedial conjunctiva of gonostyle/volsella complex (acute in C. madagascariensis); and the acute distal margin of harpe in lateral view (blunt in *C. madagascariensis*).

Description

Body length: 1150-2300 µm. Color intensity pattern: metasoma and mandible lighter than mesosoma. Color hue pattern: F3-8, cranium, mandible, metasoma, tegula brown; legs, except brown proximal region of metacoxa and distal region of metafemur, scape, pedicel, F1-4 yellow. Occipital carina sculpture: crenulate. Median flange of occipital carina count: absent. Submedial flange of occipital carina count: absent. Dorsal margin of occipital carina vs. dorsal margin of lateral ocellus in lateral view: occipital carina is ventral to lateral ocellus in lateral view. Preoccipital lunula count: present. Preoccipital carina count: absent. Preoccipital carina shape: NOT CODED. Preoccipital furrow count: present. Preoccipital furrow anterior end: Preoccipital furrow ends posterior to ocellar triangle. Postocellar carina count: absent. Male ocular ocellar line (OOL): posterior ocellar line (POL): lateral ocellar line (LOL): 1.4-1.8:1.5-1.8:1. Female ocular ocellar line (OOL): posterior ocellar line (POL): lateral ocellar line (LOL): 1.7-2.3:1.7-1.8:1.0. Head width vs. interorbital space (HW/IOS) Male: 1.6-1.9. Head width vs. interorbital space (HW/IOS) Female : 2.0-2.2. Setal pit on vertex size: smaller than diameter of scutes. Transverse frontal carina count: absent. Transverse scutes on frons count: absent. Rugose region on frons count: absent. Randomly sized areolae around setal pits on frons count: absent. Antennal scrobe count: absent. Ventromedian setiferous patch and ventrolateral setiferous patch count: absent. Facial pit count: facial pit present. Supraclypeal depression count: present. Supraclypeal depression structure: absent medially, represented by two grooves laterally of facial pit. Intertorular carina count: present. Intertorular area count: present. Median region of intertorular area shape: flat. Ventral margin of antennal rim vs. dorsal margin of clypeus: not adjacent. Torulo-clypeal carina count: present. Subtorular carina count: absent. Mandibular tooth count: 1. Female flagellomere 1 length vs. pedicel: 0.8-1.16. Female ninth flagellomere length: F9 less than F7+F8. Sensillar patch of the male flagellomere pattern: F5-F9. Length of setae on male flagellomere vs. male flagellomere width: setae shorter than width of flagellomeres. Male flagellomere 1 length vs. male second flagellomere length: 1.2-1.4. Male flagellomere 1 length vs. pedicel length: 2.9-3.3. Ventrolateral invagination of the pronotum count: present. Scutes on posterior region of mesoscutum and dorsal region of mesoscutellum convexity: flat. Notaulus posterior end location: adjacent to transscutal articulation. Median mesoscutal sulcus posterior end: adjacent to transscutal articulation. Scutoscutellar sulcus vs. transscutal articulation: adjacent; not adjacent. Axillular carina count: absent. Axillular carina shape: NOT CODED. Epicnemium posterior margin shape: anterior discrimenal pit present; epicnemial carina curved. Epicnemial carina count: interupted medially; complete. Sternaulus count: present. Sternaulus length: short, not reaching 1/2 of mesopleuron length at level of sternaulus. Speculum ventral limit: not extending ventrally of pleural pit line. Mesometapleural sulcus count: present. Metapleural carina count: present. Transverse line of the metanotum-propodeum vs. antecostal sulcus of the first abdominal tergum: adjacent sublaterally. Lateral propodeal carina count: present. Lateral propodeal carina shape: inverted "V" (left and right lateral propodeal carinae are adjacent medially at their intersection with antecostal sulcus of the first abdominal tergum). Anteromedian projection of the

metanoto-propodeo-metapecto-mesopectal complex count: absent. S1 length vs. shortest width: S1 wider than long. Transverse carina on petiole shape: straight. Distal margin of male S9 shape: straight. Proximolateral corner of male S9 shape: blunt. Cupula length vs. gonostyle-volsella complex length: cupula less than 1/2 the length of gonostyle-volsella complex in lateral view. Proximodorsal notch of cupula count: present. Proximodorsal notch of cupula shape: notched. Proximolateral projection of the cupula shape: blunt. Proximodorsal notch of cupula width vs length: wider than long. Distodorsal margin of cupula shape: straight. Dorsomedian conjunctiva of the gonostyle-volsella complex length relative to length of gonostyle-volsella complex: dorsomedian conjunctiva extending 2/3 of length of gonostyle-volsella complex in dorsal view. Dorsomedian conjunctiva of the gonostyle-volsella complex count: present. Distal end of dorsomedian conjunctiva of the gonostyle-volsella complex shape: blunt. Parossiculus count (parossiculus and gonostipes fusion): present (not fused with the gonostipes). Apical parossicular seta number: one. Distal projection of the parossiculus count: absent. Distal projection of the penisvalva count: absent. Dorsal apodeme of penisvalva count: absent. Harpe length: harpe shorter than gonostipes in lateral view. Distodorsal setae of sensillar ring of harpe length vs. harpe width in lateral view: setae as long or shorter than harpe width. Distodorsal setae of sensillar ring of harpe orientation: medially. Sensillar ring area of harpe orientation: medially. Lateral setae of harpe count: present. Lateral setae of harpe orientation: oriented distally. Distal margin of harpe in lateral view: shape: acute. Lateral margin of harpe shape: widest point of harpe is at its articulation site with gonostyle-volsella complex.

Etymology

The species epithet refers to the Fianarantsoa Province of Madagascar, where all specimens of this species were collected.

Comments

This species is very similar to *Conostigmus madagascariensis* sp. nov., and the two might possibly represent a single species.

Material Examined

Holotype male: MADAGASCAR: Ranomafana JIRAMA water works , Malaise trap near river , 16.10-8.11.2001, R. Harin'Hala , CASENT 2053691 (deposited in CAS). Paratypes (17 males, 1 sex unknown, 3 females): MADAGASCAR: 17 males, 1 sex unknown, 3 females. CASENT 2022988, 2044151, 2045601, 2045741, 2045975, 2046177, 2046180, 2053303, 2053306, 2053641, 2053667; IM 2288; PSUC_FEM 79695, 79734, 79737-79738, 79740, 79749, 79756, 79760, 79762 (CAS, MRAC).

***Conostigmus longulus* Dessart, 1997**

Conostigmus longulus : Dessart, 1997 (original description)

Figures 22, 23, 24, 25, 26

Diagnosis

Conostigmus longulus Dessart 1997 shares the presence of a prognathous head (dorsal-most point of occipital carina is dorsal to posterior ocellus in lateral view) and the presence of transverse scutes on the ventral region of frons with *C. babaiax* Dessart 1996, *C. toliaraensis* sp. nov. and *C. pseudobabaiax* sp. nov. *Conostigmus longulus* differs from *C. babaiax*, *C. toliaraensis* sp. nov. and *C. pseudobabaiax* in the presence of an impression surrounding the frontal pit, the absence of white setal patches on the frons, and the presence of the transverse frontal carina. *Conostigmus longulus* differs from other *Conostigmus* species in the distodorsal orientation of the sensillar ring of the harpe (the sensillar ring is oriented distomedially or distoventrally in other *Conostigmus* species).

Description

Body length: 1750-2450 µm. Color intensity pattern: ventral region of cranium is lighter than dorsal region of cranium. Color hue pattern: Legs except proximal region of metacoxa and distal region of metafemur, mouthparts yellow; rest of body ochre; Legs except proximal region of metacoxa and distal 2/3 of metafemur, mouthparts, scape and F1 orange; rest of body brown. Occipital carina sculpture: crenulate. Median flange of occipital carina count: absent. Submedial flange of occipital carina count: absent. Dorsal

margin of occipital carina vs. dorsal margin of lateral ocellus in lateral view: occipital carina is dorsal to lateral ocellus in lateral view. Preoccipital lunula count: NOT CODED. Preoccipital carina count: absent. Preoccipital carina shape: NOT CODED. Preoccipital furrow count: present. Preoccipital furrow anterior end: Preoccipital furrow ends inside ocellar triangle. Postocellar carina count: absent. Male ocular ocellar line (OOL): posterior ocellar line (POL): lateral ocellar line (LOL): 1.1-1.2:1:1. Female ocular ocellar line (OOL): posterior ocellar line (POL): lateral ocellar line (LOL): 1.2-1.3:1.0:1.0. Head width vs. interorbital space (HW/IOS) Male: 2.0-2.5. Head width vs. interorbital space (HW/IOS) Female : 2.3-2.4. Setal pit on vertex size: smaller than diameter of scutes. Transverse frontal carina count: present. Transverse scutes on frons count: present. Rugose region on frons count: absent. Randomly sized areolae around setal pits on frons count: absent. Antennal scrobe count: absent. Ventromedian setiferous patch and ventrolateral setiferous patch count: absent. Facial pit count: facial pit present. Supraclypeal depression count: present. Supraclypeal depression structure: present medially, inverted U-shaped. Intertorular carina count: present. Intertorular area count: present. Median region of intertorular area shape: flat. Ventral margin of antennal rim vs. dorsal margin of clypeus: not adjacent. Torulo-clypeal carina count: absent. Subtorular carina count: absent. Mandibular tooth count: 2. Female flagellomere 1 length vs. pedicel: F1 as long as pedicel (1.0-1.1). Female ninth flagellomere length: F9 less than F7+F8. Sensillar patch of the male flagellomere pattern: F4-F9; F5-F9. Length of setae on male flagellomere vs. male flagellomere width: setae shorter than width of flagellomeres. Male flagellomere 1 length vs. male second flagellomere length: 1.2-1.4. Male flagellomere 1 length vs. pedicel length: 2.4-2.5. Ventrolateral invagination of the pronotum count: present. Scutes on posterior region of mesoscutum and dorsal region of mesoscutellum convexity: flat. Notaulus posterior end location: adjacent to transscutal articulation. Median mesoscutal sulcus posterior end: adjacent to transscutal articulation. Scutoscutellar sulcus vs. transscutal articulation: adjacent. Axillular carina count: absent. Axillular carina shape: NOT CODED. Epicnemium posterior margin shape: anterior discrimenal pit absent; epicnemial carina interrupted medially. Epicnemial carina count: present only laterally. Sternaulus count: absent; present. Sternaulus length: short, not reaching 1/2 of mesopleuron length at level of sternaulus. Speculum ventral limit: not extending ventrally of pleural pit line. Mesometapleural sulcus count: present. Metapleural carina count: present. Transverse line of the metanotum-propodeum vs. antecostal sulcus of the first abdominal tergum: adjacent sublaterally. Lateral propodeal carina count: present. Lateral propodeal carina shape: inverted “Y” (left and right lateral propodeal are adjacent medially posterior to antecostal sulcus of the first abdominal tergum, and connected to the antecostal sulcus by a median carina representing the median branch of the inverted “Y”); straight (left and right lateral propodeal carinae compose a carina that is not broken medially). Anteromedian projection of the metanoto-propodeo-metapecto-mesopectal complex count: absent. S1 length vs. shortest width: S1 wider than long. Transverse carina on petiole shape: concave. Distal margin of male S9 shape: convex. Proximolateral corner of male S9 shape: blunt. Cupula length vs. gonostyle-volsella complex length: cupula less than 1/2 the length of gonostyle-volsella complex in lateral view. Proximodorsal notch of cupula count: present. Proximodorsal notch of cupula shape: arched. Proximolateral projection of the cupula shape: acute. Proximodorsal notch of cupula width vs length: wider than long. Distodorsal margin of cupula shape: straight. Dorsomedian conjunctiva of the gonostyle-volsella complex length relative to length of gonostyle-volsella complex: dorsomedian conjunctiva extending 2/3 of length of gonostyle-volsella complex in dorsal view. Dorsomedian conjunctiva of the gonostyle-volsella complex count: present. Distal end of dorsomedian conjunctiva of the gonostyle-volsella complex shape: acute. Parossiculus count (parossiculus and gonostipes fusion): present (not fused with the gonostipes). Apical parossicular seta number: one. Distal projection of the parossiculus count: absent. Distal projection of the penisvalva count: absent. Dorsal apodeme of penisvalva count: absent. Harpe length: harpe shorter than gonostipes in lateral view. Distodorsal setae of sensillar ring of harpe length vs. harpe width in lateral view: setae two times as long as harpe width. Distodorsal setae of sensillar ring of harpe orientation: distomedially. Sensillar ring area of harpe orientation: dorsomedially. Lateral setae of harpe count: present. Lateral setae of harpe orientation: oriented distally. Distal margin of harpe in lateral view: shape: acute. Lateral margin of harpe shape: widest point of harpe is at its articulation site with gonostyle-volsella complex.

Comments

Males and females are variable in color pattern: in smaller males the coloration is lighter; the legs except the proximal region of hind coxa and distal 2/3 of hind femur, mouthparts, scape and F1 are yellow and

rest of the body is ochre, whereas in larger males the colors of these body parts are orange and brown. In most female specimens, the legs except the proximal region of the hind coxa and the distal 2/3 of hind femur, mouthparts, distal part of scape, pedicel and F1–F4 are yellow and the rest of body is brown, whereas in one specimen (CAS2002193), only the distal 1/5 of scape is yellow and the rest of the antenna is brown. The length of the preoccipital furrow is variable, from reaching the anterior 1/5 of the length of the ocellar triangle (CAS204825) to barely exceeding POL (CAS2053554).
The sternaulus is present and short in larger specimens of *Conostigmus longulus* and absent from smaller specimens. The lateral propodeal carina of *Conostigmus longulus* is straight or Y-shaped and the frontal carina is distinct, sharply defined in larger and indistinct marked by a blunt edge in smaller specimens.

Material Examined
Holotype male: MADAGASCAR: PSUC_FEM 8919 COLL. MUS. Congo Madagascar: Mandraka II-1944 A. Seyrig HOLOTYPUS Holotype Prep. micros-copique n 9508/051 (deposited in MRAC).
Other material (10 males, 6 females): MADAGASCAR: 10 males, 6 females. CASENT 2002193, 2009756, 2040771, 2040900, 2044193, 2046098, 2046100, 2053308, 2053554, 2053688; PSUC_FEM 79732, 79735, 79745, 79748, 79753, 79757 (deposited in CAS, MRAC).

***Conostigmus lucidus* Mikó and Trietsch sp. nov.**

Figures 27, 28, 29, 30

Diagnosis
Conostigmus lucidus sp. nov. differs from other Malagasy *Conostigmus* species in the presence of the long anterior neck of T1 (petiole neck and corresponding S1 are as long as wide in *C. lucidus* and at least about 2× as wide as long in other Malagasy *Conostigmus* species), absence of dorsomedian conjunctiva of the gonostyle/volsella complex and absence of the proximodorsal notch of cupula (both structures are present in other Malagasy *Conostigmus* species). The parossiculus as an independent sclerite is absent (parossiculus and gonostyle fused).
The petiole neck and corresponding first abdominal sternite is also elongated in the Oriental species *Conostigmus ampullaceus* Dessart 1997 where the petiole neck is even longer (sometimes 2× as long as wide) than in *C. lucidus*. The two species differ in numerous distinct characters such as the presence of color contrast between the black head and orange abdomen and the absence of the preoccipital lunula and preoccipital sulcus in *Conostigmus ampullaceus* (all tagmata are uniformly brown and both the preocipital lunula and preocipital suclus are present in *C. lucidus*).

Description
Body length: 2100-2600 µm. Color intensity pattern: front and middle leg lighter than distal half of scape, pedicel and tegula; cranium, distal region of flagellum, mesosoma except legs and petiole neck darker than proximal region of flagellum, hind leg and metasoma posterior to petiole neck and mesosoma d. Color hue pattern: Distal half of scape, pedicel, fore leg and middle leg yellow; proximal part of scape, flagellum, mesosoma except front and middle leg, metasoma brown. Occipital carina sculpture: crenulate. Median flange of occipital carina count: absent. Submedial flange of occipital carina count: absent. Dorsal margin of occipital carina vs. dorsal margin of lateral ocellus in lateral view: occipital carina is ventral to lateral ocellus in lateral view. Preoccipital lunula count: present. Preoccipital carina count: absent. Preoccipital carina shape: NOT CODED. Preoccipital furrow count: present. Preoccipital furrow anterior end: Preoccipital furrow ends posterior to ocellar triangle. Postocellar carina count: present. Male ocular ocellar line (OOL): posterior ocellar line (POL): lateral ocellar line (LOL): 2.2:1.1-1.4:1. Female ocular ocellar line (OOL): posterior ocellar line (POL): lateral ocellar line (LOL): 1.5-2.1:1.2-1.4:1.0. Head width vs. interorbital space (HW/IOS) Male: 2.1. Head width vs. interorbital space (HW/IOS) Female : 2.0-2.1. Setal pit on vertex size: smaller than diameter of scutes. Transverse frontal carina count: absent. Transverse scutes on frons count: absent. Rugose region on frons count: absent. Randomly sized areolae around setal pits on frons count: absent. Antennal scrobe count: absent. Ventromedian setiferous patch and ventrolateral setiferous patch count: absent. Facial pit count: facial pit present. Supraclypeal depression count: present. Supraclypeal depression structure: present medially, inverted U-shaped. Intertorular carina count: present. Intertorular area count: present. Median region of intertorular area

shape: convex. Ventral margin of antennal rim vs. dorsal margin of clypeus: not adjacent. Torulo-clypeal carina count: present. Subtorular carina count: absent. Mandibular tooth count: 2. Female flagellomere 1 length vs. pedicel: 1.0. Female ninth flagellomere length: F9 less than F7+F8. Sensillar patch of the male flagellomere pattern: F5-F9. Length of setae on male flagellomere vs. male flagellomere width: setae shorter than width of flagellomeres. Male flagellomere 1 length vs. male second flagellomere length: 1.4. Male flagellomere 1 length vs. pedicel length: 2.5. Ventrolateral invagination of the pronotum count: present. Scutes on posterior region of mesoscutum and dorsal region of mesoscutellum convexity: flat. Notaulus posterior end location: adjacent to transscutal articulation. Median mesoscutal sulcus posterior end: not adjacent to transscutal articulation (ends anterior to transscutal articulation). Scutoscutellar sulcus vs. transscutal articulation: adjacent. Axillular carina count: absent. Axillular carina shape: NOT CODED. Epicnemium posterior margin shape: anterior discrimenal pit present; epicnemial carina curved. Epicnemial carina count: complete. Sternaulus count: present. Sternaulus length: elongate, exceeding 3/4 of mesopleuron length at level of sternaulus. Speculum ventral limit: not extending ventrally of pleural pit line. Mesometapleural sulcus count: present. Metapleural carina count: present. Transverse line of the metanotum-propodeum vs. antecostal sulcus of the first abdominal tergum: adjacent sublaterally. Lateral propodeal carina count: present. Lateral propodeal carina shape: straight (left and right lateral propodeal carinae compose a carina that is not broken medially). Anteromedian projection of the metanoto-propodeo-metapecto-mesopectal complex count: absent. S1 length vs. shortest width: S1 longer than wide. Transverse carina on petiole shape: straight. Distal margin of male S9 shape: convex. Proximolateral corner of male S9 shape: blunt. Cupula length vs. gonostyle-volsella complex length: cupula less than 1/2 the length of gonostyle-volsella complex in lateral view. Proximodorsal notch of cupula count: absent. Proximodorsal notch of cupula shape: NOT CODED. Proximolateral projection of the cupula shape: NOT CODED. Proximodorsal notch of cupula width vs length: NOT CODED. Distodorsal margin of cupula shape: straight. Dorsomedian conjunctiva of the gonostyle-volsella complex length relative to length of gonostyle-volsella complex: NOT CODED. Dorsomedian conjunctiva of the gonostyle-volsella complex count: absent. Distal end of dorsomedian conjunctiva of the gonostyle-volsella complex shape: NOT CODED. Parossiculus count (parossiculus and gonostipes fusion): absent (fused with the gonostipes). Apical parossiculal seta number: one. Distal projection of the parossiculus count: absent. Distal projection of the penisvalva count: absent. Dorsal apodeme of penisvalva count: absent. Harpe length: harpe shorter than gonostipes in lateral view. Distodorsal setae of sensillar ring of harpe length vs. harpe width in lateral view: setae as long or shorter than harpe width. Distodorsal setae of sensillar ring of harpe orientation: distomedially. Sensillar ring area of harpe orientation: dorsomedially. Lateral setae of harpe count: absent. Lateral setae of harpe orientation: oriented distally. Distal margin of harpe in lateral view: shape: blunt. Lateral margin of harpe shape: widest point of harpe is at its articulation site with gonostyle-volsella complex.

Etymology

The species epithet is derived from the Latin *lucidus* which means “shining”, in reference to the shining appearance of the cuticle due to the weak microsculpture of the large portion of the body.

Material Examined

Holotype male: MADAGASCAR: 3km 41° NE Andranomay, 11.5km 147°SSE Anjozobe, sifted litter in montane rainforest, 3-13.12.2000, Fisher, Griswold et al., CASENT 2001309 (deposited in CAS).
Paratypes (1 male, 6 females): MADAGASCAR: 1 male, 6 females. CASENT 2002181, 2004743, 2004751, 2040895, 2045754, 2046026, 2046176 (deposited in CAS, MRAC).

***Conostigmus macrocupula* Mikó and Trietsch sp. nov.**

Figures 31, 32, 33, 34, 35, 36

Diagnosis

Conostigmus macrocupula sp. nov. differs from other *Conostigmus* species in the elongate cupula, which is as long as the gonostyle volsella complex (the cupula is less than half as long as the gonostyle volsella complex in other *Conostigmus* species).
The only other Ceraphronoidea species with an unusually long cupula is *Dendrocerus phallocrates* Dessart

1987.

Description

Body length: 1270-1300 µm. Color intensity pattern: flagellum, tibiae and tarsi lighter than scape, pedicel, mandible, tegula, coxae and femora. Color hue pattern: Cranium, mesosoma except legs and metasoma except gonostipes and volsella ochre; antenna, legs, mandible, gonostipes and volsella yellow. Occipital carina sculpture: crenulate. Median flange of occipital carina count: absent. Submedial flange of occipital carina count: absent. Dorsal margin of occipital carina vs. dorsal margin of lateral ocellus in lateral view: occipital carina is ventral to lateral ocellus in lateral view. Preoccipital lunula count: present. Preoccipital carina count: absent. Preoccipital carina shape: NOT CODED. Preoccipital furrow count: present. Preoccipital furrow anterior end: Preoccipital furrow ends posterior to ocellar triangle. Postocellar carina count: absent. Male ocular ocellar line (OOL): posterior ocellar line (POL): lateral ocellar line (LOL): 2.0-2.1:1.7-1.8:1. Female ocular ocellar line (OOL): posterior ocellar line (POL): lateral ocellar line (LOL): NOT CODED. Head width vs. interorbital space (HW/IOS) Male: 1.8-2.0. Head width vs. interorbital space (HW/IOS) Female : NOT CODED. Setal pit on vertex size: smaller than diameter of scutes. Transverse frontal carina count: absent. Transverse scutes on frons count: absent. Rugose region on frons count: absent. Randomly sized areolae around setal pits on frons count: absent. Antennal scrobe count: absent. Ventromedian setiferous patch and ventrolateral setiferous patch count: absent. Facial pit count: facial pit present. Supraclypeal depression count: present. Supraclypeal depression structure: absent medially, represented by two grooves laterally of facial pit. Intertorular carina count: present. Intertorular area count: present. Median region of intertorular area shape: flat. Ventral margin of antennal rim vs. dorsal margin of clypeus: not adjacent. Torulo-clypeal carina count: present; absent. Subtorular carina count: absent. Mandibular tooth count: 2. Female flagellomere 1 length vs. pedicel: NOT CODED. Female ninth flagellomere length: F9 less than F7+F8. Sensillar patch of the male flagellomere pattern: F5-F9. Length of setae on male flagellomere vs. male flagellomere width: setae shorter than width of flagellomeres. Male flagellomere 1 length vs. male second flagellomere length: 1.2-1.3. Male flagellomere 1 length vs. pedicel length: 1.2-1.3. Ventrolateral invagination of the pronotum count: present. Scutes on posterior region of mesoscutum and dorsal region of mesoscutellum convexity: flat. Notaulus posterior end location: adjacent to transscutal articulation. Median mesoscutal sulcus posterior end: adjacent to transscutal articulation. Scutoscutellar sulcus vs. transscutal articulation: adjacent. Axillular carina count: absent. Axillular carina shape: NOT CODED. Epicnemium posterior margin shape: anterior discrimenal pit present; epicnemial carina curved. Epicnemial carina count: complete. Sternaulus count: absent. Sternaulus length: NOT CODED. Speculum ventral limit: not extending ventrally of pleural pit line. Mesometapleural sulcus count: absent. Metapleural carina count: present. Transverse line of the metanotum-propodeum vs. antecostal sulcus of the first abdominal tergum: adjacent sublaterally. Lateral propodeal carina count: present. Lateral propodeal carina shape: inverted "Y" (left and right lateral propodeal are adjacent medially posterior to antecostal sulcus of the first abdominal tergum, and connected to the antecostal sulcus by a median carina representing the median branch of the inverted "Y"). Anteromedian projection of the metanoto-propodeo-metapecto-mesopectal complex count: absent. S1 length vs. shortest width: S1 wider than long. Transverse carina on petiole shape: straight. Distal margin of male S9 shape: concave. Proximolateral corner of male S9 shape: blunt. Cupula length vs. gonostyle-volsella complex length: cupula as long as gonostyle-volsella complex in lateral view. Proximodorsal notch of cupula count: present. Proximodorsal notch of cupula shape: arched. Proximolateral projection of the cupula shape: blunt. Proximodorsal notch of cupula width vs length: at least two times as long as wide. Distodorsal margin of cupula shape: straight. Dorsomedian conjunctiva of the gonostyle-volsella complex length relative to length of gonostyle-volsella complex: dorsomedian conjunctiva not extending 2/3 of length of gonostyle-volsella complex in dorsal view. Dorsomedian conjunctiva of the gonostyle-volsella complex count: present. Distal end of dorsomedian conjunctiva of the gonostyle-volsella complex shape: acute. Parossiculus count (parossiculus and gonostipes fusion): present (not fused with the gonostipes). Apical parossiculal seta number: two. Distal projection of the parossiculus count: absent. Distal projection of the penisvalva count: absent. Dorsal apodeme of penisvalva count: absent. Harpe length: harpe as long as gonostipes in lateral view. Distodorsal setae of sensillar ring of harpe length vs. harpe width in lateral view: setae two times as long as harpe width. Distodorsal setae of sensillar ring of harpe orientation: dorsally. Sensillar ring area of harpe orientation: medially. Lateral setae of harpe count: present. Lateral setae of harpe orientation: oriented distally. Distal

margin of harpe in lateral view: shape: blunt. Lateral margin of harpe shape: widest point of harpe is at its articulation site with gonostyle-volsella complex.

Etymology
The species epithet is derived from the Greek macro (large) and the Latin noun cupula (small, inverted cup). The latin name of the species refers to the large cupula that is as long as the gonostyle/volsella complex.

Material Examined
Holotype male: MADAGASCAR: Parc National Ranomafana, Belle Vue at Talatakely, Malaise, secondary tropical forest, 12-19.2.2002, R. Harin'Hala, CASENT 2046023 (deposited in CAS).
Paratypes (7 males): MADAGASCAR: 7 males. CASENT 2046022, 2046025, 2046181, 2053451; PSUC_FEM 79741-79742, 79750 (CAS, MRAC).

***Conostigmus madagascariensis* Mikó and Trietsch sp. nov.**

Figures 37, 38, 39, 40, 41, 42, 43

Diagnosis
Conostigmus madagascariensis sp. nov. is the most similar to *C. fianarantsoaensis* sp. nov. among Malagasy *Conostigmus*. *Conostigmus madagascariensis* differs from *C. fianarantsoaensis* in the presence of two teeth on th mandibles, flagellar setae longer than the flagellomere width (in *C. fianarantsoaensis*, flagellar setae are shorter than flagellomere width), acute proximolateral projection of cupula (blunt in *C. fianarantsoaensis*), arched proximodorsal notch of cupula (notched in *C. fianarantsoaensis*), acute distal end of dorsomedial conjunctiva of gonostyle/volsella complex (blunt in *C. fianarantsoaensis*), and blunt distal margin of harpe in lateral view (acute in *C. fianarantsoaensis*).

Description Body length: 1500-2700 μm. Color intensity pattern: metasoma and mandible lighter than mesosoma. Color hue pattern: Antenna except pedicel, cranium, mesosoma except fore and middle legs and metasoma brown; fore and middle legs, tegula, pedicel, maxillary palp and labial palp yellow; F3-8, cranium, mandible, metasoma, tegula brown; legs, except brown proximal region of metacoxa and distal region of metafemur, scape, pedicel, F1-4 yellow; Antenna except pedicel and scape, cranium, mesosoma except fore and middle legs and distal region of metacoxa, and metasoma brown; fore and middle legs, tegula, pedicel, scape, proximal part of metacoxa, palpus maxillaris, and palpus labialis yellow; Antenna except pedicel and scape, cranium, mesosoma except fore and middle legs and distal region of metacoxa, and metasoma brown; fore and middle legs. tegula, pedicel, scape, maxillary palp, and labial palp yellow ; Antenna except pedicel, cranium, mesosoma except fore and middle legs and distal region of metacoxa, and metasoma brown; fore and middle legs, tegula, pedicel, proximal region of metacoxa, maxillary palp, and labial palp yellow ; Scape, F4-8, cranium, mandible, metasoma, tegula brown; legs, except brown proximal region of metacoxa and distal region of metafemur, pedicel, F1-3 yellow; F1-8, cranium, mandible, metasoma, tegula brown; legs, scape, pedicel yellow . Occipital carina sculpture: crenulate. Median flange of occipital carina count: absent. Submedial flange of occipital carina count: absent. Dorsal margin of occipital carina vs. dorsal margin of lateral ocellus in lateral view: occipital carina is ventral to lateral ocellus in lateral view. Preoccipital lunula count: present. Preoccipital carina count: absent. Preoccipital carina shape: NOT CODED. Preoccipital furrow count: present. Preoccipital furrow anterior end: Preoccipital furrow ends posterior to ocellar triangle. Postocellar carina count: absent. Male ocular ocellar line (OOL): posterior ocellar line (POL): lateral ocellar line (LOL): 1.8-2:1.7-1.8:1. Female ocular ocellar line (OOL): posterior ocellar line (POL): lateral ocellar line (LOL): 1.4:1.6-1.7:1.0. Head width vs. interorbital space (HW/IOS) Male: 1.6-1.9. Head width vs. interorbital space (HW/IOS) Female : 2.3. Setal pit on vertex size: smaller than diameter of scutes. Transverse frontal carina count: absent. Transverse scutes on frons count: absent. Rugose region on frons count: absent. Randomly sized areolae around setal pits on frons count: absent. Antennal scrobe count: absent. Ventromedian setiferous patch and ventrolateral setiferous patch count: absent. Facial pit count: facial pit present. Supraclypeal depression count: present. Supraclypeal depression structure: present medially, inverted U-shaped; absent medially, represented by two grooves laterally of facial pit. Intertorular carina count: present. Intertorular

area count: present. Median region of intertorular area shape: flat. Ventral margin of antennal rim vs. dorsal margin of clypeus: not adjacent. Torulo-clypeal carina count: present. Subtorular carina count: absent. Mandibular tooth count: 2. Female flagellomere 1 length vs. pedicel: 0.8-1.2. Female ninth flagellomere length: F9 less than F7+F8. Sensillar patch of the male flagellomere pattern: F5-F9. Length of setae on male flagellomere vs. male flagellomere width: setae longer than width of flagellomeres. Male flagellomere 1 length vs. male second flagellomere length: 1.2-1.5. Male flagellomere 1 length vs. pedicel length: 4-4.2. Ventrolateral invagination of the pronotum count: present. Scutes on posterior region of mesoscutum and dorsal region of mesoscutellum convexity: flat. Notaulus posterior end location: adjacent to transscutal articulation. Median mesoscutal sulcus posterior end: adjacent to transscutal articulation. Scutoscutellar sulcus vs. transscutal articulation: adjacent. Axillular carina count: absent. Axillular carina shape: NOT CODED. Epicnemium posterior margin shape: anterior discrimenal pit present; epicnemial carina curved. Epicnemial carina count: interupted medially; complete. Sternaulus count: present. Sternaulus length: short, not reaching 1/2 of mesopleuron length at level of sternaulus. Speculum ventral limit: not extending ventrally of pleural pit line. Mesometapleural sulcus count: present. Metapleural carina count: present. Transverse line of the metanotum-propodeum vs. antecostal sulcus of the first abdominal tergum: adjacent sublaterally. Lateral propodeal carina count: present. Lateral propodeal carina shape: inverted "V" (left and right lateral propodeal carinae are adjacent medially at their intersection with antecostal sulcus of the first abdominal tergum); inverted "Y" (left and right lateral propodeal are adjacent medially posterior to antecostal sulcus of the first abdominal tergum, and connected to the antecostal sulcus by a median carina representing the median branch of the inverted "Y"). Anteromedian projection of the metanoto-propodeo-metapecto-mesopectal complex count: absent. S1 length vs. shortest width: S1 wider than long. Transverse carina on petiole shape: straight. Distal margin of male S9 shape: straight. Proximolateral corner of male S9 shape: blunt. Cupula length vs. gonostyle-volsella complex length: cupula less than 1/2 the length of gonostyle-volsella complex in lateral view. Proximodorsal notch of cupula count: present. Proximodorsal notch of cupula shape: arched. Proximolateral projection of the cupula shape: acute. Proximodorsal notch of cupula width vs length: wider than long. Distodorsal margin of cupula shape: straight. Dorsomedian conjunctiva of the gonostyle-volsella complex length relative to length of gonostyle-volsella complex: dorsomedian conjunctiva extending 2/3 of length of gonostyle-volsella complex in dorsal view. Dorsomedian conjunctiva of the gonostyle-volsella complex count: present. Distal end of dorsomedian conjunctiva of the gonostyle-volsella complex shape: acute. Parossiculus count (parossiculus and gonostipes fusion): present (not fused with the gonostipes). Apical parossicular seta number: one. Distal projection of the parossiculus count: absent. Distal projection of the penisvalva count: absent. Dorsal apodeme of penisvalva count: absent. Harpe length: harpe shorter than gonostipes in lateral view. Distodorsal setae of sensillar ring of harpe length vs. harpe width in lateral view: setae longer than harpe width. Distodorsal setae of sensillar ring of harpe orientation: medially. Sensillar ring area of harpe orientation: medially. Lateral setae of harpe count: present. Lateral setae of harpe orientation: oriented distally. Distal margin of harpe in lateral view: shape: blunt. Lateral margin of harpe shape: widest point of harpe is at its articulation site with gonostyle-volsella complex.

Etymology

The species epithet refers to Madagascar where *Conostigmus madagascariensis* is the most commonly collected among *Conostigmus* species.

Comments

The coloration of *Conostigmus madagascariensis* males is variable: specimens CASENT2040905 and CASENT 2046020 have distally yellow hind coxa, and specimens CASENT2040905 and CASENT2022986 have yellow scapes. The coloration of *Conostigmus madagascariensis* females is also variable: F1–8, cranium, mandible, metasoma, tegula brown, legs, scape, pedicel yellow in specimens CASENT2053365, CASENT2053573, CASENT2053574; scape, F4–8, cranium, mandible, metasoma, tegula brown, legs, except brown proximal region of hind coxa and distal region of hind femur, pedicel, F1–4 yellow in specimens CASENT2041648, CASENT2044995.

Most specimens of *Conostigmus madagascariensis* lack postocellar carina. In larger specimens, a very shallow sulcus connecting the posterior margins of lateral ocelli present. In one specimen (CASENT 2044509) the postocellar carina is similar to *Conostigmus lucidus* sp. nov. Other charactersics of *Conostigmus lucidus* are absent from this specimen (*e.g.* petiole neck as long as wide, very weak microsculpture

allover the body, sternaulus longer than half of length of mesopleuron in the level of sternaulus, presence of straigth lateral propodeal carinae).

Material Examined

Holotype male: MADAGASCAR: Province Fianarantsoa, Parc National Ranomafana, radio tower at forest edge, Malaise mixed tropical forest, 12-19.2.2002, R. Harin'Hala , CASENT 2044913 (deposited in CAS).

Paratypes (44 males, 15 females): MADAGASCAR: 44 males, 15 females. CASENT 2000886, 2002178, 2002180, 2002187-2002191, 2004742, 2004744, 2004746-2004750, 2004753-2004754, 2009143-2009144, 2022986-2022987, 2040889-2040894, 2040896-2040899, 2040901, 2040905-2040908, 2041648, 2041940, 2041942, 2041945, 2044507, 2044509, 2044824, 2044895, 2044912, 2044995, 2045756, 2046020, 2053365, 2053393, 2053503, 2053573-2053574; IM 2289; PSUC_FEM 79702, 79759, 79761, 79763, PSUC_79714 (deposited in CAS, MRAC).

***Conostigmus missyhazenae* Mikó and Trietsch sp. nov.**

Figures 44, 45, 46, 47

Diagnosis

Conostigmus missyhazenae sp. nov. differs from other Malagasy *Conostigmus* species in the globular head (almost as long as wide in dorsal view and as high as long in lateral view) and the absence of the preoccipital sulcus.

Description

Body length: 1750-2000 μm. Color intensity pattern: NOT CODED. Color hue pattern: Cranium, mandible, mesosoma excluding front and proximal middle tibia, metasoma, antenna excluding distal scape and pedicel brown; distal scape, pedicel, protibia and proximal mesotibia ochre. Occipital carina sculpture: smooth. Median flange of occipital carina count: absent. Submedial flange of occipital carina count: absent. Dorsal margin of occipital carina vs. dorsal margin of lateral ocellus in lateral view: occipital carina is ventral to lateral ocellus in lateral view. Preoccipital lunula count: absent. Preoccipital carina count: absent. Preoccipital carina shape: NOT CODED. Preoccipital furrow count: absent. Preoccipital furrow anterior end: NOT CODED. Postocellar carina count: absent. Male ocular ocellar line (OOL): posterior ocellar line (POL): lateral ocellar line (LOL): 1.1-1.2:1.6-1.8:1. Female ocular ocellar line (OOL): posterior ocellar line (POL): lateral ocellar line (LOL): 1.0-1.1:1.4:1.0. Head width vs. interorbital space (HW/IOS) Male: 1.8-1.9. Head width vs. interorbital space (HW/IOS) Female : 2.4. Setal pit on vertex size: smaller than diameter of scutes. Transverse frontal carina count: absent. Transverse scutes on frons count: absent. Rugose region on frons count: absent. Randomly sized areolae around setal pits on frons count: absent. Antennal scrobe count: absent. Ventromedian setiferous patch and ventrolateral setiferous patch count: absent. Facial pit count: facial pit present. Supraclypeal depression count: present. Supraclypeal depression structure: present medially, inverted U-shaped. Intertorular carina count: present. Intertorular area count: present. Median region of intertorular area shape: flat. Ventral margin of antennal rim vs. dorsal margin of clypeus: not adjacent. Torulo-clypeal carina count: present. Subtorular carina count: absent. Mandibular tooth count: 2. Female flagellomere 1 length vs. pedicel: 0.9-1.0. Female ninth flagellomere length: F9 less than F7+F8. Sensillar patch of the male flagellomere pattern: F5-F9. Length of setae on male flagellomere vs. male flagellomere width: setae shorter than width of flagellomeres. Male flagellomere 1 length vs. male second flagellomere length: 1.1-1.2. Male flagellomere 1 length vs. pedicel length: 3.2-4.0. Ventrolateral invagination of the pronotum count: present. Scutes on posterior region of mesoscutum and dorsal region of mesoscutellum convexity: flat. Notaulus posterior end location: adjacent to transscutal articulation. Median mesoscutal sulcus posterior end: adjacent to transscutal articulation. Scutoscutellar sulcus vs. transscutal articulation: adjacent. Axillular carina count: absent. Axillular carina shape: NOT CODED. Epicnemium posterior margin shape: anterior discrimenal pit present; epicnemial carina curved. Epicnemial carina count: complete. Sternaulus count: present. Sternaulus length: short, not reaching 1/2 of mesopleuron length at level of sternaulus. Speculum ventral limit: not extending ventrally of pleural pit line. Mesometapleural sulcus count: present. Metapleural carina count: present. Transverse line of the metanotum-propodeum vs.

antecostal sulcus of the first abdominal tergum: adjacent sublaterally. Lateral propodeal carina count: present. Lateral propodeal carina shape: inverted "Y" (left and right lateral propodeal are adjacent medially posterior to antecostal sulcus of the first abdominal tergum, and connected to the antecostal sulcus by a median carina representing the median branch of the inverted "Y"). Anteromedian projection of the metanoto-propodeo-metapecto-mesopectal complex count: absent. S1 length vs. shortest width: S1 wider than long. Transverse carina on petiole shape: concave. Distal margin of male S9 shape: convex. Proximolateral corner of male S9 shape: blunt. Cupula length vs. gonostyle-volsella complex length: cupula less than 1/2 the length of gonostyle-volsella complex in lateral view. Proximodorsal notch of cupula count: present. Proximodorsal notch of cupula shape: arched. Proximolateral projection of the cupula shape: acute. Proximodorsal notch of cupula width vs length: wider than long. Distodorsal margin of cupula shape: straight. Dorsomedian conjunctiva of the gonostyle-volsella complex length relative to length of gonostyle-volsella complex: dorsomedian conjunctiva extending 2/3 of length of gonostyle-volsella complex in dorsal view. Dorsomedian conjunctiva of the gonostyle-volsella complex count: present. Distal end of dorsomedian conjunctiva of the gonostyle-volsella complex shape: acute. Parossiculus count (parossiculus and gonostipes fusion): present (not fused with the gonostipes). Apical parossicular seta number: one. Distal projection of the parossiculus count: absent. Distal projection of the penisvalva count: absent. Dorsal apodeme of penisvalva count: absent. Harpe length: harpe shorter than gonostipes in lateral view. Distodorsal setae of sensillar ring of harpe length vs. harpe width in lateral view: setae as long or shorter than harpe width. Distodorsal setae of sensillar ring of harpe orientation: distomedially. Sensillar ring area of harpe orientation: medially. Lateral setae of harpe count: present. Lateral setae of harpe orientation: oriented distoventrally. Distal margin of harpe in lateral view: shape: blunt. Lateral margin of harpe shape: widest point of harpe is in its proximal 1/3rd.

Etymology The species epithet honors Missy Hazen, research technologist at The Huck Institute of the Life Sciences, Pennsylvania State University, who facilitated the microscopy of these and other specimens.

Material Examined Holotype male: MADAGASCAR: Parc National Ranomafana, Belle Vue at Talatakely, Malaise, secondary tropical forest, 12-19.2.2002, R. Harin'Hala CASENT 2046019 (deposited in CAS). Paratypes (2 males, 2 females): MADAGASCAR: 2 males, 2 females. CASENT 2002183, 2004752; PSUC_FEM 79731, 79747 (CAS).

***Conostigmus pseudobabaiax* Mikó and Trietsch sp. nov.**

Figures 48, 49, 50, 51, 52

Diagnosis
Conostigmus pseudobabaiax sp. nov. shares the presence of a prognathous head (dorsal-most point of occipital carina is dorsal to posterior ocellus in lateral view) and the presence of transverse scutes on the ventral region of frons with *C. babaiax* Dessart 1996, *C. toliaraensis* sp. nov. and *Conostigmus longulus* Dessart 1997. *Conostigmus pseudobabaixC. babaiax*, and *C. toliaraensis* sp. nov. differ from other *Conostigmus* species by the presence of ventromedian and ventrolateral white, setiferous patches on the frons. *Conostigmus pseudobabaiax* and *C. toliaraensis* differ from *Conostigmus babaiax* in OOL longer than LOL (in *Conostigmus babaiax* OOL is shorter than LOL). *Conostigmus toliaraensis* can be readily differentiated from *C. pseudobabaiax* by the following phenotypes: first female flagellomere 0.9× the length of pedicel (1.4× as long in *C. pseudobabaiax*); male flagellomere 1 1.1× as long as second male flagellomere (1.3–1.4× as long in *C. pseudobabaiax*); scutes are strongly convex (flat in *C. pseudobabaiax*); proximodorsal notch of cupula as long as wide and harpe as long as gonostyle/volsella complex in lateral view (proximodorsal notch of cupula almost 2× as wide as long; harpe 0.7× length of gonostyle/volsella complex in *C. pseudobabaiax*).

Description
Body length: 2450-3125 µm. Color intensity pattern: ventral region of cranium is lighter than dorsal region of cranium. Color hue pattern: Distal part of scape, pedicel, F1-3 ochre; legs except proximal metacoxa yellow; rest of body brown. Occipital carina sculpture: crenulate. Median flange of occipital carina count: absent. Submedial flange of occipital carina count: absent. Dorsal margin of occipital carina

vs. dorsal margin of lateral ocellus in lateral view: occipital carina is dorsal to lateral ocellus in lateral view. Preoccipital lunula count: NOT CODED. Preoccipital carina count: absent. Preoccipital carina shape: NOT CODED. Preoccipital furrow count: present. Preoccipital furrow anterior end: Preoccipital furrow ends inside ocellar triangle. Postocellar carina count: absent. Male ocular ocellar line (OOL): posterior ocellar line (POL): lateral ocellar line (LOL): 1.2-1.3:1:1. Female ocular ocellar line (OOL): posterior ocellar line (POL): lateral ocellar line (LOL): 1.4:1.0-1.2:1.0. Head width vs. interorbital space (HW/IOS) Male: 2.0-2.2. Head width vs. interorbital space (HW/IOS) Female : 2.3-2.6. Setal pit on vertex size: smaller than diameter of scutes. Transverse frontal carina count: absent. Transverse scutes on frons count: present. Rugose region on frons count: absent. Randomly sized areolae around setal pits on frons count: absent. Antennal scrobe count: absent. Ventromedian setiferous patch and ventrolateral setiferous patch count: present. Facial pit count: no external corresponding structure present. Supra-clypeal depression count: absent. Supraclypeal depression structure: NOT CODED. Intertorular carina count: present. Intertorular area count: present. Median region of intertorular area shape: flat. Ventral margin of antennal rim vs. dorsal margin of clypeus: not adjacent. Torulo-clypeal carina count: present. Subtorular carina count: absent. Mandibular tooth count: 2. Female flagellomere 1 length vs. pedicel: 1.4. Female ninth flagellomere length: F9 less than F7+F8. Sensillar patch of the male flagellomere pattern: F4-F9. Length of setae on male flagellomere vs. male flagellomere width: setae shorter than width of flagellomeres. Male flagellomere 1 length vs. male second flagellomere length: 1.3-1.4. Male flagellomere 1 length vs. pedicel length: 3.0-3.2. Ventrolateral invagination of the pronotum count: present. Scutes on posterior region of mesoscutum and dorsal region of mesoscutellum convexity: flat. Notaulus posterior end location: adjacent to transscutal articulation. Median mesoscutal sulcus posterior end: not adjacent to transscutal articulation (ends anterior to transscutal articulation). Scutoscutellar sulcus vs. transscutal articulation: adjacent. Axillular carina count: absent. Axillular carina shape: NOT CODED. Epicnemium posterior margin shape: anterior discrimenal pit absent; epicnemial carina inter-rupted medially. Epicnemial carina count: present only laterally. Sternaulus count: present. Sternaulus length: short, not reaching 1/2 of mesopleuron length at level of sternaulus. Speculum ventral limit: not extending ventrally of pleural pit line. Mesometapleural sulcus count: present. Metapleural carina count: present. Transverse line of the metanotum-propodeum vs. antecostal sulcus of the first abdominal tergum: adjacent sublaterally. Lateral propodeal carina count: present. Lateral propodeal carina shape: straight (left and right lateral propodeal carinae compose a carina that is not broken medially). Anteromedian projection of the metanoto-propodeo-metapecto-mesopectal complex count: absent. S1 length vs. shortest width: S1 wider than long. Transverse carina on petiole shape: concave. Distal margin of male S9 shape: convex. Proximolateral corner of male S9 shape: blunt. Cupula length vs. gonostyle-volsella complex length: cupula less than 1/2 the length of gonostyle-volsella complex in lateral view. Proximodorsal notch of cupula count: present. Proximodorsal notch of cupula shape: arched. Proximolateral projection of the cupula shape: blunt. Proximodorsal notch of cupula width vs length: wider than long. Distodorsal margin of cupula shape: straight. Dorsomedian conjunctiva of the gonostyle-volsella complex length relative to length of gonostyle-volsella complex: dorsomedian conjunctiva extending 2/3 of length of gonostyle-volsella complex in dorsal view. Dorsomedian conjunctiva of the gonostyle-volsella complex count: present. Distal end of dorsomedian conjunctiva of the gonostyle-volsella complex shape: acute. Parossiculus count (parossiculus and gonostipes fusion): present (not fused with the gonostipes). Apical parossicular seta number: one. Distal projection of the parossiculus count: absent. Distal projection of the penisvalva count: absent. Dorsal apodeme of penisvalva count: absent. Harpe length: harpe shorter than gonostipes in lateral view. Distodorsal setae of sensillar ring of harpe length vs. harpe width in lateral view: setae as long or shorter than harpe width. Distodorsal setae of sensillar ring of harpe orientation: distomedially. Sensillar ring area of harpe orientation: medially. Lateral setae of harpe count: present. Lateral setae of harpe orientation: oriented distally. Distal margin of harpe in lateral view: shape: blunt. Lateral margin of harpe shape: widest point of harpe is at its articulation site with gonostyle-volsella complex.

Etymology From the Greek *pseudo-* (=false) and the specific name *babaiax*, indicating a close resemblance of *Conostigmus pseudobabaiax* and *C. babaiax*.

Material Examined Holotype male: MADAGASCAR: Ranomafana JIRAMA water works , Malaise trap near river , 16.10-8.11.2001, R. Harin'Hala, CASENT 2053690 (deposited in CAS).

Paratypes (5 males, 6 females): MADAGASCAR: 5 males, 6 females. CASENT 2006450-2006451, 2032774, 2041943, 2046097, 2046151, 2053381-2053382, 2053425, CASENT_2040937; PSUC_FEM 79736 (deposited in CAS, MRAC).

***Conostigmus toliaraensis* Mikó and Trietsch sp. nov.**

Figures 53, 54, 55, 56, 57

Diagnosis

Conostigmus toliaraensis sp. nov. shares the presence of a prognathous head (dorsal-most point of occipital carina is dorsal to posterior ocellus in lateral view) and the presence of transverse scutes on the ventral region of frons with *C. babaiax* Dessart 1996, *C. pseudobabaiax* sp. nov. and *Conostigmus longulus* Dessart 1997. *Conostigmus toliaraensisC. babaiax*, and *C. pseudobabaiax* sp. nov. differ from other *Conostigmus* species by the presence of ventromedian and ventrolateral white, setiferous patches on the frons. *Conostigmus pseudobabaiax* and *C. toliaraensis* differ from *Conostigmus babaiax* in OOL longer than LOL (in *Conostigmus babaiax* OOL is shorter than LOL). *Conostigmus toliaraensis* can be readily differentiated from *C. pseudobabaiax* by the following phenotypes: first female flagellomere 0.9× the length of pedicel (1.4× as long in *C. pseudobabaiax*); male flagellomere 1 1.1× as long as second male flagellomere (1.3–1.4× as long in *C. pseudobabaiax*); scutes are strongly convex (flat in *C. pseudobabaiax*); proximodorsal notch of cupula as long as wide and harpe as long as gonostyle/volsella complex in lateral view (proximodorsal notch of cupula almost 2× as wide as long; harpe 0.7× length of gonostyle/volsella complex in *C. pseudobabaiax*).

Description

Body length: 2000-3450 µm. Color intensity pattern: ventral region of cranium is lighter than dorsal region of cranium. Color hue pattern: Distal part of scape, pedicel, F1-3 ochre; legs except proximal metacoxa yellow; rest of body brown; Scape, hind leg except metacoxa ochre; fore and hind legs, distal metacoxa yellow; rest of body brown. Occipital carina sculpture: crenulate. Median flange of occipital carina count: absent. Submedial flange of occipital carina count: absent. Dorsal margin of occipital carina vs. dorsal margin of lateral ocellus in lateral view: occipital carina is dorsal to lateral ocellus in lateral view. Preoccipital lunula count: NOT CODED. Preoccipital carina count: absent. Preoccipital carina shape: NOT CODED. Preoccipital furrow count: present. Preoccipital furrow anterior end: Preoccipital furrow ends inside ocellar triangle. Postocellar carina count: absent. Male ocular ocellar line (OOL): posterior ocellar line (POL): lateral ocellar line (LOL): 1.3-1.5:1:1. Female ocular ocellar line (OOL): posterior ocellar line (POL): lateral ocellar line (LOL): 1.2-1.3:1.0:1.0. Head width vs. interorbital space (HW/IOS) Male: 2.0-2.2. Head width vs. interorbital space (HW/IOS) Female : 2.3-2.7. Setal pit on vertex size: smaller than diameter of scutes. Transverse frontal carina count: absent. Transverse scutes on frons count: present. Rugose region on frons count: absent. Randomly sized areolae around setal pits on frons count: absent. Antennal scrobe count: absent. Ventromedian setiferous patch and ventrolateral setiferous patch count: present. Facial pit count: no external corresponding structure present. Supraclypeal depression count: absent. Supraclypeal depression structure: NOT CODED. Intertorular carina count: present. Intertorular area count: present. Median region of intertorular area shape: flat. Ventral margin of antennal rim vs. dorsal margin of clypeus: not adjacent. Torulo-clypeal carina count: absent. Subtorular carina count: absent. Mandibular tooth count: 2. Female flagellomere 1 length vs. pedicel: 0.9. Female ninth flagellomere length: F9 less than F7+F8. Sensillar patch of the male flagellomere pattern: F4-F9; F5-F9. Length of setae on male flagellomere vs. male flagellomere width: setae shorter than width of flagellomeres. Male flagellomere 1 length vs. male second flagellomere length: 1.0-1.1; 1.1. Male flagellomere 1flagellomere 1 length vs. pedicel length: 2.5-3.0. Ventrolateral invagination of the pronotum count: present. Scutes on posterior region of mesoscutum and dorsal region of mesoscutellum convexity: convex. Notaulus posterior end location: adjacent to transscutal articulation. Median mesoscutal sulcus posterior end: not adjacent to transscutal articulation (ends anterior to transscutal articulation). Scutoscutellar sulcus vs. transscutal articulation: adjacent. Axillular carina count: absent. Axillular carina shape: NOT CODED. Epicnemium posterior margin shape: anterior discrimenal pit absent; epicnemial carina interrupted medially. Epicnemial carina count: present only laterally. Sternaulus count: present. Sternaulus length: short, not reaching 1/2 of mesopleuron length at

level of sternaulus. Speculum ventral limit: not extending ventrally of pleural pit line. Mesometapleural sulcus count: present. Metapleural carina count: present. Transverse line of the metanotum-propodeum vs. antecostal sulcus of the first abdominal tergum: adjacent sublaterally. Lateral propodeal carina count: present. Lateral propodeal carina shape: inverted "Y" (left and right lateral propodeal are adjacent medially posterior to antecostal sulcus of the first abdominal tergum, and connected to the antecostal sulcus by a median carina representing the median branch of the inverted "Y"); straight (left and right lateral propodeal carinae compose a carina that is not broken medially). Anteromedian projection of the metanoto-propodeo-metapecto-mesopectal complex count: absent. S1 length vs. shortest width: S1 wider than long. Transverse carina on petiole shape: concave. Distal margin of male S9 shape: convex. Proximolateral corner of male S9 shape: blunt. Cupula length vs. gonostyle-volsella complex length: cupula less than 1/2 the length of gonostyle-volsella complex in lateral view. Proximodorsal notch of cupula count: present. Proximodorsal notch of cupula shape: arched. Proximolateral projection of the cupula shape: blunt. Proximodorsal notch of cupula width vs length: as long as wide. Distodorsal margin of cupula shape: straight. Dorsomedian conjunctiva of the gonostyle-volsella complex length relative to length of gonostyle-volsella complex: dorsomedian conjunctiva extending 2/3 of length of gonostyle-volsella complex in dorsal view. Dorsomedian conjunctiva of the gonostyle-volsella complex count: present. Distal end of dorsomedian conjunctiva of the gonostyle-volsella complex shape: acute. Parossiculus count (parossiculus and gonostipes fusion): present (not fused with the gonostipes). Apical parossicular seta number: one. Distal projection of the parossiculus count: absent. Distal projection of the penisvalva count: absent. Dorsal apodeme of penisvalva count: absent. Harpe length: harpe as long as gonostipes in lateral view. Distodorsal setae of sensillar ring of harpe length vs. harpe width in lateral view: setae as long or shorter than harpe width. Distodorsal setae of sensillar ring of harpe orientation: distomedially. Sensillar ring area of harpe orientation: medially. Lateral setae of harpe count: present. Lateral setae of harpe orientation: oriented distally. Distal margin of harpe in lateral view: shape: blunt. Lateral margin of harpe shape: widest point of harpe is at its articulation site with gonostyle-volsella complex.

Comments

The length of the preoccipital furrow is variable in *Conostigmus toliaraensis* Dessart 1997, from reaching the median ocellus (CAS2053309) to barely exceeding POL (CAS2040934). Two specimens from Foret Classee have narrower heads and bodies (distinct in HW/IOS ratio). Since the rest of the specimens are from Forret d'Ankazotsihitafototra, these two specimens might represent a different subspecies or species. The fact that there are only a few minute differences in the male genitalia morphology between *Conostigmus toliaraensis* and *C. pseudobabaiax* is unique, since male genitalia characters are traditionally used for species separation in Megaspilidae and in some cases provide the only diagnostic tool.

Etymology From the Greek *pseudo-* (=false) and the specific name *babaiax*, indicating a close resemblance of *Conostigmus pseudobabaiax* and *C. babaiax*.

Material Examined Holotype male: CASENT 2053309 MADAGASCAR: Toliara Prov: Res. Speciale d'Ambohijanahary: Foret d' Ankazotsihitafototra: 35.2km; NW Ambaravaranala; 1050m; 18°16'00"S, 45°24'24"E; 13-17.i.2003; MT; MISC BLF7019; Fisher, Griswold, et al. California Academy of Sciences. Yellow pan trap- in montane rainforest. (deposited in CAS).

Paratypes (9 females): MADAGASCAR: 9 females. CASENT 2009754, 2040934-2040936, 2040983, 2041206, 2053310-2053311, 2053452 (CAS).(deposited in CAS MRAC).

Identification key for Malagasy *Conostigmus* Dahlbom

1. **a.** Antennomeres gradually widening apically (Figs 6B, 8B, 13A, females) **2**
aa. Antennomeres not widening apically (Fig. 13B, males) **12**

2. **a.** Scutes on ventral region of frons transverse (vrf: Figs 1A, 16B, 22B, 48A) .... **3** **aa.** Scutes on ventral region of frons not transverse (Figs 7A, 10A, 18A) **6**

3. **a.** White setal patches on frons absent (Figs 22A, B)
b. Depression surrounding frontal pit present (dep: Figs 22A, B)
c. Transverse frontal carina present (tfc: Figs 22A, B) ..... ***Conostigmus longulus*** Dessart 1997

aa. White setal patches on frons present (msp, ssp: Figs 4A, 48A)
bb. Depression surrounding frontal pit absent (Figs 4A, 48A))
cc. Transverse frontal carina absent (Figs 4A, 48A) **4**

4. aa. LOL longer than OOL (Fig. 6A)
Conostigmus babaiax Dessart 1997
bb. OOL shorter than LOL (Figs 48) **5**

5. a. Flagellomere 1 length 0.9× pedicel length (Fig. 53A)
b. Scutes on frons and mesonotum strongly convex (Figs 55A, B, 51A) ***Conostigmus toliaraaensis*** Mikó and Trietsch sp. nov.

aa. Flagellomere 1 1.4× as long as pedicel (Fig. 49A)
bb. Scutes on frons and mesonotum flat (Figs 50A, B, 51B) . ***Conostigmus pseudobabaiax*** Mikó and Trietsch sp. nov.

6. a. Flagellomere 9 as long as sum of lengths of flagellomeres 6–8 (Fig. 13A)
b. Rugous region on frons present (Figs 10A, B)
c. Subtorular carina present (stc: Fig. 10C)
d. Median and submedial flanges of occipital carina present (mfc, sfc: Figs 11A, 12B)
e. Axillular carina present, carinae not adjacent posteriorly (not composing a U-shaped carina surrounding disc of mesoscutellum) (axc: Figs 11B, 12A, B) ...***Conostigmus clavatus*** Mikó and Trietsch sp. nov.

aa. Flagellomere 9 shorter than sum of lengths of flagellomere 7 and flagellomere 8 (Figs6B, 8B)
bb. Rugous region on frons absent (Figs 3A, 7A, 16B)
cc. Subtorular carina absent (Figs 18A, B, 37A, B)
dd. Median and submedial flanges of occipital carina absent (Figs 7B, 8A)
ee. Axillular carina absent (Figs 5A, 15A, 19B) or axillular carinae adjacent posteriorly (composing a U-shaped carina surrounding disc of mesoscutellum) (usc: Figs 8A, 9A, B) **7**

7. a. Preoccipital carina present (poc: Figs 7B, 11A, 12B)
b. Anteromedian projection of the metanoto-propodeo-metapecto-mesopectal complex present (app: Fig. 8A)
c. Randomly sized areolae around setal basis on frons present (aro: Fig. 7A)
d. Axillular carinae adjacent posteriorly (composing a U-shaped carina surrounding disc of mesoscutellum) (usc: Figs 8A, 9A, B) ..... ***Conostigmus ballescoracas*** Dessart 1997

aa. Preoccipital carina absent (Figs 5A, 15A, 25A, B)
bb. Anteromedian projection of the metanoto-propodeo-metapecto-mesopectal complex absent (Figs 5A, 15A, 25A, B)
cc. Randomly sized areolae around setal basis on frons absent (Figs 4A, 16B, 18A)
dd. Axillular carinae absent (Figs 5A, 15A, 19B) **8**

8. a. Anterior neck of T1 (and corresponding S1) as long as wide (Fig. 28B)
b. Median mesoscutal line marked by a row of punctures (mml: Fig. 28B)
c. Sternaulus elongate (exceeding 3/4 of mesopleuron length measured at level of sternaulus)(ste: Figs 29A, B)
d. Postocellar carina present (pcc: Figs 28B, 29B) .. ***Conostigmus lucidus*** Mikó and Trietsch sp. nov.

aa. Anterior neck of T1 (and corresponding S1) much wider than long (9B, 16A, 25B)
bb. Median mesoscutal line marked by a groove (mml: Figs 5A, B, 9A, B, 12 A, B)
cc. Sternaulus short, not reaching 1/2 of mesopleuron length measured at level of sternaulus (ste: Figs 6B, 19A, 24B)
dd. Postocellar carina absent (Figs 5A, 15A, 25A, 42A, B) **9**

9. a. Antennal scrobe present (asr: Figs 15B, 16B)
b. Depressions around setal bases on dorsal region of cranium and mesonotum larger than scutes (Fig. 15A) ..... ***Conostigmus bucephalus*** Mikó and Trietsch sp. nov.

aa. Antennal scrobe absent (Figs 4A, 7A, 10A, B)
bb. Depressions around setal bases on cranium and mesonotum smaller than scutes **10**

10. a. Head globular, almost as long as wide in dorsal view and as high as long in lateral view (Figs 46A, B)
b. OOL almost as long as LOL (Fig. 46A)
c. Preoccipital sulcus absent (Fig. 46A) . ***Conostigmus missyhazenae*** Mikó and Trietsch sp. nov.

aa. Head transverse, distinctly wider than long in dorsal view
bb. OOL about 2× as long as LOL (Figs 41A, B)
cc. Preoccipital sulcus present (pos: Figs 41A, B, 39 A, B) **11**

11. a. Mandible with one tooth (Figs 18A, B) ***Conostigmus fianarantsoaensis*** Mikó and Trietsch sp. nov.

aa. Mandible with two teeth (Figs 37A, B) ***Conostigmus madagascariensis*** Mikó and Trietsch sp. nov.

12. a. Scutes on ventral region of frons transverse (vrf: Figs 1A, 16B, 22B, 48A) **13**

aa. Scutes on ventral region of frons not transverse (Figs 7A, 10A, 18A) **15**

13. a. White setal patches on frons absent (Figs 22A, B)
b. Depression surrounding frontal pit present (dep: Figs 22A, B)
c. Transverse frontal carina present (tfc: Figs 22A, B)
d. Setal ring area of the harpe oriented dorsomedially (hrp: Figs 26A, B)
e.Dorsomedial setae of harpal setal ring elongate, apical ends adjacent medially, 2–3× as long as harpe width in lateral view (dhs: Fig. 26B) ..... ***Conostigmus longulus*** Dessart 1997

aa. White setal patches on frons present (msp, ssp: Figs 4A, 48A)
bb. Depression surrounding frontal pit absent (Figs 4A, 48A))
cc. Transverse frontal carina absent (Figs 4A, 48A)
dd. Setal ring area of the harpe oriented medially (hrp: Fig. 57B)
ee. Dorsomedial setae of harpal setal ring short, apical ends not adjacent medially, shorter than harpe width in lateral view (dhs: Fig. 57B) **14**

14. a. Flagellomere 1 1.1× as long as second flagellomere (Fig. 53B)
b. Scutes on frons and mesonotum strongly convex (Fig. 51A)
c. Proximodorsal notch of cupula as long as wide (pdc: Fig. 57B)
d. Harpe as long as gonostyle-volsella complex in lateral view (hrp, gvs: Fig. 57B) ***Conostigmus toliaraensis*** Mikó and Trietsch sp. nov.

aa. Flagellomere 1 1.3–1.4× as long as second flagellomere (Fig. 49B)
bb. Scutes on frons and mesonotum flat (Fig. 51B)
cc. Proximodorsal notch of cupula almost 2X as wide as long (pdc: Fig. 51B)
ee. Harpe 0.7 length of gonostyle/volsella complex in lateral view (hrp, gvs: Fig. 51B) ***Conostigmus pseudobabaiax*** Mikó and Trietsch sp. nov.

15. a. Subtorular carina present (stc: Fig. 10C)
b. Axillular carina present (axc: Figs 11B, 12A, B)
c. Median and submedial flanges of occipital carina present (mfc, sfc: Figs 11A, 12B)
d. Rugulose sculpture on frons present (Figs 10A, B)
e. OOL/LOL>3.3 (Fig. 10B)
f. Interorbital space wide (HW/IOS=1.63–1.66)
g. Distodorsal margin of cupula concave medially (ddm: Fig. 14B)
h. Eyes bulging (Figs 10, 11A, 12B); (Fig. 10B) ***Conostigmus clavatus*** Mikó and Trietsch sp. nov.

aa. Subtorular carina absent (stc: Fig. 10C)
bb. Axillular carina absent (axc: Figs 11B, 12A, B)
cc. Median and submedial flanges of occipital carina absent (mfc, sfc: Figs 11A, 12B)
dd. Rugulose sculpture on frons absent (Figs 10A, B)
ee. OOL/LOL<3.3 (Fig. 10B)

ff. Interorbital space narrow (HW/IOS>1.8)
gg. Distodorsal margin of cupula straight medially
hh. Eyes not bulging (Figs 10, 11A, 12B) **16**

16. a. Anterior neck of T1 (and corresponding S1) as long as wide (Fig. 28B)
b. Median mesoscutal line marked by a row of punctures (mml: Fig. 28B)
c. Sternaulus elongate (exceeding ¾ of mesopleuron length measured at level of sternaulus; ste: Figs 29A, B)
d. Postocellar carina present (pcc: Figs 28B, 29B)
e. Dorsomedian conjunctiva of the gonostyle/volsella complex absent (Fig. 30C)
f. Proximodorsal notch of cupula absent (Fig. 30C)
g. Parossiculus absent (parossiculus and gonostyle fused, Fig. 30C) . ***Conostigmus lucidus*** Mikó and Trietsch sp. nov.

aa. Anterior neck of T1 (and corresponding S1) much wider than long (9B, 16A, 25B)
bb. Median mesoscutal line marked by a groove (mml: Figs 5A, B, 9A, B, 12 A, B)
cc. Sternaulus short, not reaching ½ of mesopleuron length measured at level of sternaulus (ste: Figs 6B, 19A, 24B)
dd. Postocellar carina absent (Figs 5A, 15A, 25A, 42A, B)
ee. Dorsomedian conjunctiva of the gonostyle/volsella complex present (dc: Figs 21C, 43A)
ff. Proximodorsal notch of cupula present (pdc: Fig. 21B)
gg. Parossiculus present (parossiculus and gonostyle not fused, Fig. 1A) **17**

17. a. Preoccipital carina present (poc: Figs 7B,)
b. Anteromedian projection of the metanoto-propodeo-metapecto-mesopectal complex present (app: Fig. 8A)
c. Randomly sized areolae around setal bases on frons present (aro: Fig. 7A)
d. Axillular carinae adjacent posteriorly (composing a U-shaped carina surrounding posteriorly and laterally mesoscutellar disc) (usc: Figs 8A, 9A, B) .... ***Conostigmus ballescoracas*** Dessart 1997

aa. Preoccipital carina absent (Figs 5A, 15A, 25A, B)
bb. Anteromedian projection of the metanoto-propodeo-metapecto-mesopectal complex absent (Figs 5A, 15A, 25A, B)
cc. Randomly sized areolae around setal bases on frons absent (Figs 4A, 16B, 18A)
dd. Axillular carinae absent (Figs 5A, 15A, 19B) **18**

18. a. Head globular, almost as long as wide in dorsal view and as high as long in lateral view (Figs 46A, B)
b. OOL almost as long as LOL (Fig. 46A)
c. Preoccipital sulcus absent (Fig. 46A)
d. Proximal region of lateral margins of harpe diverging distally and widest point of harpe is in its proximal ⅓rd (hrp: Figs 47 B, C) ..... ***Conostigmus missyhazenae*** Mikó and Trietsch sp. nov.

aa. Head transverse, distinctly wider than long in dorsal view
bb. OOL about 2× as long as LOL (Figs 41A, B)
cc. Preoccipital sulcus present (pos: Figs 41A, B, 39 A, B)
dd. Lateral margins of harpe gradually converging distally, widest point of harpe is at its articulation site with gonostyle-volsella complex (Figs 30A, 36A, 52A) **19**

19. a. Cupula as long as gonostyle-volsella complex (cup: Fig. 36A)
b. Distal 3–4 setae in dorsal region of sensillar ring of harpe oriented distodorsally (Figs 36A–C)
c. Distal margin of S9 concave
d. Distal end of dorsomedial conjunctiva of gonostyle-volsella complex not extending ½ of length of gonostyle-volsella complex (dc: Fig. 36C)
e. Parossiculus with two parossiculal setae (pss: Fig. 36D) ***Conostigmus macrocupula*** Mikó and Trietsch sp. nov.

aa. Cupula at least ½ of gonostyle (Figs 21A, B)
bb. Setae of sensillar ring of harpe oriented distomedially (Figs 21, 43)
cc. Distal margin of S9 convex

dd. Distal end of dorsomedial conjunctiva of gonostyle-volsella complex extending ⅔ of length of gonostyle-volsella complex (dc: Fig. 43A)
e. Parossiculus with one parossicular seta (pss: Fig. 43) **20**

20. a. Mandible with one tooth (Figs 18A, B)
b. Setae on antenna shorter than or as long as width of flagellomeres (Fig. 40A)
c. Proximolateral projection of cupula blunt (Fig. 21A)
d. Proximodorsal notch of cupula notched (pdc: Fig. 21C)
e. Distal end of dorsomedial conjunctiva of gonostyle/volsella complex blunt (dc: Fig. 21C)
f. Distal margin of harpe in lateral view acute (hrp: Fig. 21C) .. ***Conostigmus fianarantsoaensis*** Mikó and Trietsch sp. nov.

aa. Mandible with two teeth (Figs 37A, B)
bb. Setae on antenna longer than width of flagellomeres (Fig. 20A)
cc. Proximolateral projection of cupula acute (ppc: Fig. 43B)
dd. Proximodorsal notch of cupula arched (pdc: Fig. 43)
e. Distal end of dorsomedial conjunctiva of gonostyle-volsella complex acute (dc: Fig. 43A)
f. Distal margin of harpe in lateral view blunt (hrp: Fig. 43C) .. ***Conostigmus madagascariensis*** Mikó and Trietsch sp. nov.

DISCUSSION

Latitudinal diversity gradient and Malagasy *Conostigmus*

Including our data, almost an order of magnitude more *Conostigmus* species have been described from the Holarctic (n=125) than from the Afrotropical region (n=13) (Johnson and Musetti, 2004; Dessart, 1997). This biodiversity pattern suggests that *Conostigmus* joins other taxa known to be exceptions to the typical latitudinal diversity gradient (LDG): mollusks (Valdovinos et al., 2003), nematodes (Lambshead et al., 2000), fig wasps (Agaonidae; Hawkins and Compton, 1992), galling insects (Price et al., 1998), bees (Anthophila; Michener, 1979), sawflies ("Symphyta"; Kouki et al., 1994), Ichneumonidae (Gauld, 1986; Owen and Owen, 1974), Braconidae (Quicke and Kruft, 1995), some Lepidoptera (Holloway, 1987), psyllids and aphids (Dixon et al., 1987; Eastop, 1977, 1978).

Noyes (1989) survey of two similarly-sized countries supports the validity of reverse LDG in Ceraphronoidea. Standardized sampling of the megaspilids of Sulawesi and Great Britain revealed a much higher diversity in the temperate (69 spp.) than in the tropical (9 spp.) region, as determined by Paul Dessart.

Deviation from the LDG in Ceraphronoidea has been only superficially examined, however, and could result from sampling bias. The only taxonomic revision of *Conostigmus* species was published by Dessart (1997). He treated the faunas of Africa, Asia, and Australia and examined 145 specimens compared to the many hundreds if not thousands of specimens examined for Palearctic species. Of the 36 species, nineteen are known exclusively by holotypes, eight by the holotype and one paratype, and only one species (*Conostigmus canariensis*) was based on more than 10 specimens.

The present revision focuses solely on Malagasy *Conostigmus* and is based on observations of 159 specimens representing 12 species, more than five times as many as the earlier recorded *Conostigmus* species from Madagascar (Dessart, 1997). This species number is still just a small fragment of the known Palaearctic *Conostigmus* species (n=97; Johnson and Musetti, 2004) and one fourth of the number of species recorded from the Atlantic Archipelago (n=44; Broad and Livermore, 2014), which is almost half the size of Madagascar (315,159 km² vs. 587,041km²). Considering that Madagascar is a biodiversity hotspot (Myers et al., 2000), our study lends support to the hypothesis that Megaspilidae show a reverse latitudinal biodiversity gradient.

The single layer epithelium and body size polyphenism

Insects are epidermal organisms (Locke, 1998) and the single-layered epidermis is responsible for their tremendous phenotypic diversity. Epidermal cells produce the cuticle, the acellular exoskeleton that is the subject of most morphological descriptions in insect systematics (Deans et al., 2012). For instance, in the present paper we exclusively used cuticle-related phenotypes. The dominance of cuticular characters in insect systematics descriptions is easy to explain: besides the remnants of some skeletal muscles, the cuticle is perhaps the only component of an insect body that can be accurately studied

even on an improperly fixed specimen. This resilient replica of the pupal epidermis can be studied on specimens that are millions of years old (Carpenter, 1992).

The epidermis arises exclusively and solely from imaginal disks. The growth of imaginal disks, and thus the final cell number and cell size of the epidermis, is regulated in collaboration by insulin and ecdysone (Nijhout and Grunert, 2010; Nijhout et al., 2007; Nijhout and Callier, 2015) that are controlled mostly by environmental factors, such as temperature, oxygen level and nutrition. Oxygen concentration and temperature mostly influence body size through cell growth (Callier and Nijhout, 2014; Heinrich et al., 2011; Harrison and Haddad, 2011; Peck and Maddrell, 2005; Azevedo et al., 2002; Partridge et al., 1994) while nutrition level seems to impact cell number through regulating proliferation (Emlen et al., 2007; Liu et al., 2015).

Ceraphronoidea exhibit substantial body size polyphenism, which varies by almost a factor of two in some species (Mikó et al., 2013; Fergusson, 1980; Liebscher, 1972). This tendency is followed by Malagasy *Conostigmus*, for example the IOS (interorbital distance, an anatomical line between the medial eye margins that reflects body size) reveals a two-fold difference in *C. longulus* (138–263 μm). Body size polyphenism is usually induced by variability in host body size in polyphagous and nest size in gregarious parasitic Hymenoptera (Quicke, 1997; Nalepa and Grisell, 1993; Medal and Smith, 2015). Numerous ceraphronoid species are known to parasitize hosts with variable body size (Fergusson, 1980; Gilkeson et al., 1993) and gregariousness is not uncommon (Cooper and Dessart, 1975; Starý, 1977; Liebscher, 1972; Mackauer and Chow, 2015; Takada, 1973). Mackauer and Chow (2015) A clear relationship between ceraphronoid body mass and nest size was recently shown in the facultative gregarious *Dendrocerus carpenteri*, where the body mass of a single solitary specimen did not differ from the combined body mass of two gregarious specimens Mackauer and Chow (2015).

Information on *Conostigmus* biology is very limited, but body size of their hosts (Syrphidae and boreid mecopterans) certainly allows the development of multiple parasitoids specimens (Dessart, 1980; Cooper and Dessart, 1975; Weems and Howard, 1954; Kamal, 1926; Ulber et al., 2010; Panis, 2008). These data suggest that differences in ceraphronoid body size is nutrition dependent thus body size polyphenism is most likely related to differences in cell number.

Wing trichomes (`http://purl.obolibrary.org/obo/HAO_0002454`) have a one to one match to epidermal cells (Dobzhansky, 1929; Stevenson et al., 1995; Partridge et al., 1994; Heinrich et al., 2011) and they were traditionaly used in comparative evo-devo studies to estimate cell density and size in different *Drosophila* mutant specimens (Stern and Emlen, 1999; Emlen et al., 2007; Nijhout and Callier, 2015).

Sculptural elements of the cuticle likewise correspond to the patterns and geometry of epidermal cells (Wigglesworth, 1973; Locke, 1959, 1967) and they have never been explored as a potential source for understanding cellular processes in the developing imaginal disks.

The nature of scutes

In Malagasy *Conostigmus* species, the head and the mesosoma is covered with repetitive, usually hexagonal and isodiametric, 6.6–25 μm wide elements, referred as scutes (Cals, 1974; Moretto et al., 2015) or sculpticells (Allen and Ball, 1979). Arthropod taxa often exhibit scutes (Meyer, 1842; Cals, 1974; Krell, 1994) that are considered as ancestral sculpture elements in Insecta (Hinton, 1970). The surface morphology of scutes (convex vs concave; Figs 51A, 51B) and the depth of the impressions separating them (Figs 50, 31A, B) are important for separating Malagasy *Conostigmus species* while differences in their superficial density (Figs 24, 25A, B; they are less dense in smaller specimens) is perhaps the most obvious intraspecific trait.

Due to their hexagonal shape and size, scutes have long been speculated to reflect the surface of epidermal cells (Kölliker, 1856; Warren, 1903). Fusco et al. (2000) studied the correspondence between scutes and epidermal cells in subsequent instars of lithobiomorph centipedes and demonstrated a one to one match between the cells and scutes. Hinton (1970); Cals (1973, 1974); Blaney and Chapman (1969) likewise found correspondences between the number of epidermal cell nuclei in mature adults and scutes in different insect groups, but Blaney and Chapman (1969) found 1–2 percent less epidermal cells than scutes and explained this discrepancy by ecdysial cell death based on the presence of some degraded cell nuclei. One-to-one correspondence between scutes and epidermal cells is also supported by the fact that elongate scutes correspond to elongate epidermal cells (Hinton, 1970).

Locke (1959, 1967) and Wigglesworth (1973) performed detailed histological and developmental

studies to reveal cellular origin of stellate folding, ripple patterns, dome-like plaques, and setal pits and revealed that these structures are the product of multiple epidermal cells. Unfortunately, the relationships between scutes and epidermal cells have never been proved by similarly detailed examinations.

Bigger cells or more cells?

Although the relationship between scutes and epidermal cells have been broadly acknowledged in insect systematics (Ball, 1985; Allen and Ball, 1979; Burks et al., 2013; Krell, 1994), no one has used this knowledge to understand body size polyphenism. According to our findings, scute size is independent of body size (*i.e.* the epithelium of smaller specimens is built by proportionally less scutes than that in larger specimens). The number of scutes along the IOS (interorbital space, shortest distance between compound eyes) of a smaller specimen is half the number of scutes along the same line in a specimen with an IOS two times as long (Figs 31A, B).

It follows that there is no difference in epidermal cell size of the smaller and the larger specimens and therefore cell number differences must contribute exclusively to body size polyphenism in Malagasy *Conostigmus longulus* Dessert 1997 specimens. Based on our collective understanding of underlying developmental processes, the size difference in *Conostigmus longulus* is likely related to nutritional differences that likely result from the complexities of polyphagy and gregariousness.

We observed a substantial intraindividual variation in scute morphology: scutes and cell size on the frons are smaller than that on the mesoscutellum. This variation might reflect the difference in the growth of the head and wing imaginal disks contributing to allometric changes.

Intraspecific differences in body size often impact species diagnoses. Statements, such as "smaller specimens can be very difficult, if not impossible, to identify correctly because the morphology of typical specimens is not expressed" (Al Khatib et al., 2014, page 809) and "in smaller specimens, the characters are subdued" (Smith, 2012, page 215) are common in taxonomic descriptions and often refer cuticular specializations, such as carinae or grooves. Despite the importance of allometric reductions, developmental causes of these phenomena have never been revealed. In *Conostigmus longulus* the transverse carina of the frons is less expressed in smaller specimens (tfc: Figs 22 A, B), encumbering their identification. The carina is the product of the concerted action of 52 epidermal cells (26 columns in 2 rows) in small specimens and 156 cells (52 columns in 3 rows) in a large specimens (Figs 22 A, B) suggesting that allometric reduction of cuticular specializations might be related to cell number and that more epidermal cells are able to produced more conspicuous structures. In this respect, the impact of epidermal cell density to the distinctness of cuticular specialization might be similar to the impact of pixel density to the resolution of digital images; one can see more details on an image with 1200 dpi than on one with 256 dpi resolution.

CONCLUSIONS

Our data reveal that Megaspilidae show a reverse latitudinal biodiversity gradient, but we acknowledge that *Conostigmus* in the temperate zone remains poorly understood (e.g., types of half the described Holarctic species are missing (Johnson and Musetti, 2004)). Species concepts are also based strictly on morphological data, which, for some taxa, can mask true species-level diversity (Smith et al., 2008).

The correspondence between scutes and epidermal cells has already been proved by developmental studies in centipedes (Moretto et al., 2015), but we need to validate this relationship in insects. To understand spatial relationships between cellular and subcellular components of the epithelium is now easier to achieve with the advent of contemporary 3D reconstruction techniques such as confocal laser scanning microscopy or serial block face scanning electron microscopy. Ceraphronoidea would be especially feasible model for this kind of examination since the head and the mesosoma are almost uniformly covered with scutes, and it is relatively easy to establish sustainable colonies of multiple species (Araj et al., 2006; Chow and Mackauer, 1999). *Dendrocerus carpenteri* is facultatively gregarious(Mackauer and Chow, 2015) with nest size varying between 1 and 3 larvae making this taxon feasible even for simultaneous analyses of nutrition, oxygen level and temperature dependence of epidermal development.

Being able to understand cellular processes in the developing epithelium of adult insects by reading sculptural elements can provide invaluable information about the influence of environmental factors on allometric differentiation. Sculpture is not only one of the most important traits for insect classification, it also conserves the history of developmental processes in the single cell thick epithelium accountable for

the tremendous morphological diversity in arthropods. Sculpture also remains available as a source of biological information long after a specimen has been collected or preserved as a fossil.

Therefore we believe that sculpture, a witness to developmental and evolutionary history of arthropods, could serve as a messenger between morphology based classical arthropod taxonomy and the 21st century insect ecology, evolutionary biology, and cell and developmental biology.

ACKNOWLEDGMENTS

We thank Brian Fisher, Charles Griswold, and Darryll Ubick, California Academy of Sciences, San Francisco for making this material available for study, Missy Hazen (Penn State Huck Institute of the Life Sciences, Microscopy and Cytometry Facility) for her assistance in Confocal Laser Scanning Microscopy and James Balhoff for his help in generating semantic statements in owl. Stéphane Hanot, Akice-Marie Buset and Van den Spiegel D. kindly sent us type specimens of the species deposited in Tervuren (Royal Museum of Central Africa, Belgium). This material is based upon work supported by the U. S. National Science Foundation, under Grant Numbers DBI-0850223, DEB-0956049, DBI-1356381, DEB-1353252 and grant No. DEB-0072713 to BL. Fisher and CE Griswold and DEB-0344731 to B.L. Fisher and P.S. Ward. Fieldwork that provided the basis for this work could not have been completed without the gracious support of the Malagasy people. Any opinions, findings, and conclusions our recommendations expressed in this material are those of the author(s) and do not necessarily reflect the views of the National Science Foundation.

REFERENCES

Al Khatib, F., Fusu, L., Cruaud, A., Gibson, G., Borowiec, N., Rasplus, J.-Y., Ris, N., and Delvare, G. (2014). An integrative approach to species discrimination in the *Eupelmus urozonus* complex (Hymenoptera, Eupelmidae), with the description of 11 new species from the Western Palaearctic. *Systematic Entomology*, 39(4):806–862.

Allen, R. T. and Ball, G. E. (1979). Synopsis of Mexican taxa of the *Loxandrus* series (Coleoptera: Carabidae: Pterostichini). *Transactions of the American Entomological Society (1890-)*, 105(4):481–575.

Araj, S. A., Wratten, S. D., Lister, A. J., and Buckley, H. L. (2006). Floral nectar affects longevity of the aphid parasitoid *Aphidius ervi* and its hyperparasitoid *Dendrocerus aphidum*. *New Zealand Plant Protection*, 59:178.

Azevedo, R. B. R., French, V., and Partridge, L. (2002). Temperature modulates epidermal cell size in *Drosophila melanogaster*. *Journal of Insect Physiology*, 48:231–237.

Balhoff, J. P., Mikó, I., Yoder, M. J., Mullins, P. L., and Deans, A. R. (2013). A semantic model for species description applied to the ensign wasps (Hymenoptera: Evaniidae) of New Caledonia. *Systematic Biology*, 62(5):639–659.

Ball, G. E. (1985). Characteristics and evolution of elytral sculpture in the tribe Galeritini (Coleoptera: Carabidae). *Questiones Entomologicae*, 21:349–367.

Bennett, A. W. and Sullivan, D. J. (1978). Defensive behavior against tertiary parasitism by the larva of *Dendrocerus carpenteri* an aphid hyperparasitoid. *Journal of the New York Entomological Society*, pages 153–160.

Blaney, W. M. and Chapman, R. F. (1969). The anatomy and histology of the maxillary palp of *Schistocerca gregaria* (Orthoptera, Acrididae). *Journal of Zoology*, 157(4):509–535.

Broad, G. R. and Livermore, L. (2014). Checklist of british and irish hymenoptera - ceraphronoidea. *Biodiversity Data Journal*, 2:e1167.

Burks, K. N., Miko, I., and Deans, A. R. (2016). *Dendrocerus mexicali* Megaspilidae): Novel antennal morphology, first description of female, and expansion of known range into the U.S. *ZooKeys*, 569, 569:53–69.

Burks, R., Masner, L., Johnson, N., and Austin, A. (2013). Systematics of the parasitic wasp genus *Oxyscelio* Kieffer (Hymenoptera, Platygastridae s.l.), Part I: Indo-Malayan and Palearctic fauna. *ZooKeys*, 292:1–263.

Callier, V. and Nijhout, F. (2014). Plasticity of insect body size in response to oxygen: integrating molecular and physiological mechanisms. *Current Opinion in Insect Science*, 1:59–65.

1545 Cals, P. (1973). Polarité antéro-postérieure du tégument des Arthropodes. Apport du microscope
1546 électronique à balayage dans l'analyse des structure cuticulaires à l'échelle cellulaire. *Comptes*
1547 *rendus de l'Académie des sciences, Série D*, 277:1021–1024.
1548 Cals, P. (1974). Mise en évidence, par le microscope électronique à balayage, de champs mor-
1549 phogénétiques polarisés, exprimés par les cellules épidermiques normales dans l'appendice locomoteur
1550 des Arthopodes : *Tylos latreilli* (Audoin) (Crustacé, Isopode) et *Periplaneta americana* (L.) (Insecte,
1551 Dictyoptère). *Comptes rendus de l'Académie des sciences Paris*, 279D:663–666.
1552 Carpenter, F. M. (1992). *Superclass Hexopoda.*, volume Arthropoda 4 of *Treatise on Invertebrate*
1553 *Paleontology, Part R.* The Geological Society of America, Boulder CO.
1554 Chow, A. and Mackauer, M. (1999). Host handling and specificity of the hyperparasitoid wasp, *Den-*
1555 *drocerus carpenteri* (Curtis) (Hym., Megaspilidae): importance of host age and species. *Journal of*
1556 *Applied Entomology*, 123(2):83–91.
1557 Cooper, K. W. and Dessart, P. (1975). Adult, larva and biology of *Conostigmus quadratogenalis* Dessart
1558 & Cooper, sp.n., (Hym., Ceraphronoidea), parasite of *Boreus* (Mecoptera) in California. *Bulletin et*
1559 *Annales de la Société Royale Belge d'Entomologie*, 111:37–53.
1560 Core Team, R. (2015). *R: A Language and Environment for Statistical Computing*. R Foundation for
1561 Statistical Computing, Vienna, Austria.
1562 Deans, A. R., Miko, I., Wipfler, B., and Friedrich, F. (2012). Evolutionary phenomics and the emerging
1563 enlightenment of arthropod systematics. *Invertebrate Systematics*, 26(3):323–330.
1564 Dessart, P. (1980). Redescription de *Conostigmus triangularis* (Thomson, 1858) comb. nov. (Hym.
1565 Ceraphronoidea Megaspilidae). *Bulletin et Annales de la Société Royale Belge d'Entomologie*, 116:19–
1566 28.
1567 Dessart, P. (1997). Les Megaspilinae ni europeens, ni americains. 1. Le genre *Conostigmus* Dahlbom,
1568 1858 (Hym. Ceraphronoidea Megaspilidae). *Memoires de la Société Royale Belge d'Entomologie*,
1569 37:3–144.
1570 Dessart, P. and Gärdenfors (1985). *Dendrocerus paradoxus* n. sp. et *D. ulmicola* n. sp. (Hym. Cer-
1571 aphronoidea Megaspilidae), deux nouveaux hyperparasites palearctiques de pucerons. *Bulletin et*
1572 *Annales de la Société Royale Belge d'Entomologie*, 121:197–211.
1573 Dixon, A. F. G., Kindlmann, P., Lepš, J., and Holman, J. (1987). Why there are so few species of aphids,
1574 especially in the tropics. *The American Naturalist*, 129(4):580–592.
1575 Dobzhansky, T. (1929). The influence of the quantity and quality of chromosomal material on the size of
1576 the cells in *Drosophila melanogaster*. *Development Genes and Evolution*, 115(3):363–379.
1577 Eastop, V. (1977). Worldwide importance of virus vectors. In Harris, K. F. and Maramorosch, K., editors,
1578 *Aphids as Virus Vectors*, pages 4–47. Academic Press, New York, San Francisco, London.
1579 Eastop, V. (1978). Diversity of the Sternorrhyncha within major climatic zones. In Mound, L. and Waloff,
1580 N., editors, *Diversity of Insect Faunas. Symposium of the Royal Entomological Society*, volume 9,
1581 pages 71–78.
1582 Emlen, D. J., Lavine, L. C., and Ewen-Campen, B. (2007). On the origin and evolutionary diversification
1583 of beetle horns. *Proceedings of the National Academy of Sciences*, 104(suppl 1):8661–8668.
1584 Ernst, A., Mikó, I., and Deans, A. R. (2013). Morphology and function of the ovipositor mechanism in
1585 Ceraphronoidea (Hymenoptera, Apocrita). *Journal of Hymenoptera Research*, 33:25–61.
1586 Fergusson, N. D. M. (1980). A revision of the British species of *Dendrocerus* Ratzeburg (Hymenoptera:
1587 Ceraphronoidea) with a review of their biology as aphid hyperparasites. *Bulletin of the British Museum*
1588 *(Natural History), Entomology Series*, 41(4):255–314.
1589 Fusco, G., Brena, C., and Minelli, A. (2000). Cellular processes in the growth of lithobomorph centipeds
1590 (Chilopoda: Lithobiomorpha). A cuticular view. *Zoologischer Anzeiger - A Journal of Comparative*
1591 *Zoology*, 239:91–102.
1592 Gauld, I. D. (1986). Latitudinal gradients in ichneumonid species-richness in Australia. *Ecological*
1593 *Entomology*, 11(2):155–161.
1594 Gilkeson, L. A., McLean, J. P., and Dessart, P. (1993). *Aphanogmus fulmeki* Ashmead (Hymenoptera:
1595 Ceraphronidae), a parasitoid of *Aphidoletes aphidimyza* Rondani (Diptera: Cecidomyiidae). *The*
1596 *Canadian Entomologist*, 125(01):161–162.
1597 Harrison, J. F. and Haddad, G. G. (2011). Effects of oxygen on growth and size: synthesis of molecular,
1598 organismal, and evolutionary studies with *Drosophila melanogaster*. *Annual Review of Physiology*,
1599 73:95–113.

Haviland, M. D. (1920). Memoirs: On the Bionomics and Development of *Lygocerus testaceimanus*, Kieffer, and *Lygocerus cameroni*, Kieffer (Proctotrypoidea-Ceraphronidae), Parasites of Aphidius (Braconidae). *Quarterly Journal of Microscopical Science*, 2(257):101–127.

Hawkins, B. A. and Compton, S. G. (1992). African fig wasp communities: Undersaturation and latitudinal gradients in species richness. *Journal of Animal Ecology*, 61(2):361–372.

Heinrich, E. C., Farzin, M., Klok, C. J., and Harrison, J. F. (2011). The effect of developmental stage on the sensitivity of cell and body size to hypoxia in *Drosophila melanogaster*. *The Journal of Experimental Biology*, 214(9):1419–1427.

Heraty, J., Ronquist, F., Carpenter, J. M., Hawks, D., Schulmeister, S., Dowling, A. P., Murray, D., Munro, J., Wheeler, W. C., Schiff, N., et al. (2011). Evolution of the hymenopteran megaradiation. *Molecular phylogenetics and evolution*, 60(1):73–88.

Hinton, H. E. (1970). Some little known surface structures. *Symposium of the Royal Entomological Society of London*, 5:41–58.

Holloway, J. D. (1987). Macrolepidoptera diversity in the Indo-Australian tropics: geographic, biotopic and taxonomic variations. *Biological Journal of the Linnean Society*, 30(4):325–341.

Johnson, N. F. and Musetti, L. (2004). Catalog of the systematic literature of the superfamily Ceraphronoidea (Hymenoptera). *Contributions of the American Entomological Institute*, 33:1–149.

Kamal, M. (1926). Four new species of parasites from aphidiophagous Syrphidae (Hymenoptera). *The Canadian Entomologist*, 58(11):283–286.

Kamal, M. (1939). Biological studies on some Hymenopterous parasites of aphidophagous Syrphidae. *Bulletin. Ministry of Agriculture, Egypt. Technical and Scientific Service. Entomology Section*, 207:1–111.

Kouki, J., Niemelä, P., and Viitasaari, M. (1994). Reversed latitudinal gradient in species richness of sawflies (Hymenoptera, Symphyta). *Annales Zoologici Fennici*, 31(1):83–88.

Krell, F.-T. (1994). Phylogenetic and taxonomic consideration on the variability of cuticular surface micromorphology within one species, *Aphodius* (*Nialus*) *varians* Duftschmid (Insecta: Coleoptera: Scarabaeidae: Aphodiinae). *Revue Suisse de Zoologie*, 101:265–287.

Kölliker, A. (1856). Untersuchungen zur vergleichenden Gewebelehre, angestellt in Nizza im Herbste 1856. *Verhandlungen Physikalisch-Medizinische Gesellschaft Würzburg*, 8:1–128.

Lambshead, P., Tietjen, J., Ferrero, T., and Jensen, P. (2000). Latitudinal diversity gradients in the deep sea with special reference to North Atlantic nematodes. *Journal of Marine Ecology Progressive Series*, 194:159–167.

Liebscher, S. (1972). *Zur Taxonomie und Biologie von Dendrocerus-Arten (Hymenoptera, Ceraphronoidea: Megaspilidae) im Hyperparasitenkreis der Lachnidae (Homoptera, Aphidoidea) auf Pinus und Larix*. PhD thesis, Technical University of Dresden, Dresden.

Liu, C.-Y., Zhao, W.-L., Wang, J.-X., and Zhao, X.-F. (2015). Cyclin-dependent kinase regulatory subunit 1 promotes cell proliferation by insulin regulation. *Cell Cycle*, 14(19):3045–3057.

Locke, M. (1959). The cuticular pattern in an insect, *Rhodnius prolixus* St\a al. *Journal of Experimental Biology*, 36(3):459–477.

Locke, M. (1967). The development of patterns in the integument of insects. *Advances in morphogenesis*, 6:33–88.

Locke, M. (1998). Epidermis. In Harrison, F. W. and Locke, M., editors, *Insecta*, volume 11A of *Microscopic Anatomy of Invertebrates*, pages 75–138. Wiley-Liss Inc., New York.

Mackauer, M. and Chow, A. (2015). Facultative gregarious development in a solitary parasitoid wasp, *Dendrocerus carpenteri*: larvae may share nutritional resources. *Entomologia Experimentalis et Applicata*, 157(2):170–180.

Mann, H. B. and Whitney, D. R. (1947). On a test of whether one of two random variables is stochastically larger than the other. *The Annals of Mathematical Statistics*, 18(1):50–60.

Medal, J. and Smith, T. (2015). Reversible polyphenism in *Trissolcus japonicus* (Hymenoptera: Platygastridae) induced by stink bug egg size. *Journal of Entomological Science*, 50(4):363–366.

Meyer, H. (1842). Über den Bau der Hornschale der Käfer. *Archiv für Anatomie, Physiologie und Wissenschaftliche Medicin.*, 1842:12–16.

Michener, C. D. (1979). Biogeography of the bees. *Annals of the Missouri Botanical Garden*, 66(3):277–347.

Mikó, I., Copeland, R. S., Balhoff, J. P., Yoder, M. J., and Deans, A. R. (2014). Folding wings like a

cockroach: a review of transverse wing folding ensign wasps Hymenoptera: Evaniidae: *Afrevania* and *Trissevania*). *PLoS ONE*, 9(5):e94056.

Mikó, I. and Deans, A. R. (2013). What is fluorescing? *Hamuli*, 4:19–22.

Mikó, I., Masner, L., Johannes, E., Yoder, M. J., and Deans, A. R. (2013). Male terminalia of Ceraphronoidea: morphological diversity in an otherwise monotonous taxon. *Insect Systematics & Evolution*, 44(3-4):261–347.

Mikó, I., Yoder, M., and Deans, A. (2011). Order Hymenoptera, family Megaspilidae Genus *Dendrocerus*. In van Harten, A., editor, *Arthropod fauna of the UAE*, volume 4, pages 353–374.

Mikó, I., Yoder, M. J., Balhoff, J. P., and Deans, A. (2015). Generating semantic phenotypes. 00003 DOI:10.6084/m9.figshare.1314904.v1.

Moretto, M., Minelli, A., and Fusco, G. (2015). Cell size versus body size in geophilomorph centipedes. *The Science of Nature*, 102(3-4).

Myers, N., Mittermeier, R. A., Mittermeier, C. G., da Fonseca, G. A. B., and Kent, J. (2000). Biodiversity hotspots for conservation priorities. *Nature*, 403(6772):853–858.

Nalepa, C. and Grisell, E. (1993). Host seed size and adult size, Emergence, and morphology of *Megastigmus acuelatus nigroflavus* (Hymenoptera: Rorymidae). *Environmental entomology*, 22(6):1313–1317.

Nijhout, H. F. and Callier, V. (2015). Developmental mechanisms of body size and wing-body scaling in insects. *Annual Review of Entomology*, 60(1):141–156.

Nijhout, H. F. and Grunert, L. W. (2010). The Cellular and Physiological Mechanism of Wing-Body Scaling in *Manduca sexta*. *Science*, 330(6011):1693–1695.

Nijhout, H. F., Smith, W. A., Schachar, I., Subramanian, S., Tobler, A., and Grunert, L. W. (2007). The control of growth and differentiation of the wing imaginal disks of *Manduca sexta*. *Developmental Biology*, 302(2):569–576.

Noyes, J. S. (1989). The diversity of Hymenoptera in the tropics with special reference to Parasitica in Sulawesi. *Ecological Entomology*, 14(2):197–207.

Osborne, J. W. and Overbay, A. (2008). Best Practices in Data Cleaning. In *Best Practices in Quantitative Methods*, pages 205–213. SAGE.

Owen, D. F. and Owen, J. (1974). Species diversity in temperate and tropical Ichneumonidae. *Nature*, 249(5457):583–584.

Panis, A. (2008). *Conostigmus dimidiatus* Thomson new to France (Hymenoptera, Megaspilidae). *Nouvelle Revue d'Entomologie*, 24(4):321–328.

Partridge, L., Barrie, K., Fowler, K., and French, V. (1994). Evolution and development of body size and cell size in *Drosophila melanogaster* in response to temperature. *Evolution*, 48:1269–1276.

Peck, L. S. and Maddrell, S. H. (2005). Limitation of size by hypoxia in the fruit fly *Drosophila melanogaster*. *Journal of Experimental Zoology Part A: Comparative Experimental Biology*, 303A(11):968–975.

Popovici, O., Mikó, I., Seltmann, K., and Deans, A. R. (2014). The maxillo-labial complex of *Sparasion* (Hymenoptera, Platygastroidea). *Journal of Hymenoptera Research*, 37:77–111.

Price, P. W., Fernandes, G. W., Lara, A. C. F., Brawn, J., Barrios, H., Wright, M. G., Ribeiro, S. P., and Rothcliff, N. (1998). Global patterns in local number of insect galling species. *Journal of Biogeography*, 25(3):581–591.

Quicke, D. L. J. (1997). *Parasitic Wasps*. Springer, London ; New York, 2 edition edition.

Quicke, D. L. J. and Kruft, R. A. (1995). Latitudinal gradients in North American braconid wasp species richness and biology. *Journal of Hymenoptera Research*, 4:194–203.

Smith, M. A., Rodriguez, J. J., Whitfield, J. B., Deans, A. R., Janzen, D. H., Hallwachs, W., and Hebert, P. D. (2008). Extreme diversity of tropical parasitoid wasps exposed by iterative integration of natural history, DNA barcoding, morphology, and collections. *Proceedings of the National Academy of Sciences USA*, 105(34):12359–12364.

Smith, N. J. (2012). Addition of two new species and a previously unknown female to the ammoplanine complex, and a species of Pulverro Pate, 1937 is entered into synonymy (Hymenoptera: Crabronidae). *Pan-Pacific Entomologist*, 88(2):212–221.

Starý, P. (1977). *Dendrocerus* hyperparasites of aphids in Czechoslovakia (Hymenoptera, Ceraphronoide). *Acta entomoloigca Bohemoslovaca*, 74:1–9.

Stern, D. L. and Emlen, D. J. (1999). The developmental basis for allometry in insects. *Development*, 126(6):1091–1101.

1710 Stevenson, R. D., Hill, M. F., and Bryant, P. J. (1995). Organ and Cell Allometry in Hawaiian *Drosophila*:
1711 How to Make a Big Fly. *Proceedings: Biological Sciences*, 259(1355):105–110.
1712 Sullivan, D. J. and Völkl, W. (1999). Hyperparasitism: multitrophic ecology and behavior. *Annual review*
1713 *of entomology*, 44:291–315.
1714 Takada, H. (1973). Studies on aphid hyperparasites of Japan, I. Aphid hyperparasites of the genus
1715 *Dendrocerus* Ratzeburg occurring in Japan (Hymenoptera: Ceraphronidae). *Insecta Matsumurana*,
1716 2:1–37.
1717 Ulber, B., Williams, I. H., Klukowski, Z., Luik, A., and Nilsson, C. (2010). Parasitoids of Oilseed Rape
1718 Pests in Europe: Key Species for Conservation Biocontrol. In Williams, I. H., editor, *Biocontrol-Based*
1719 *Integrated Management of Oilseed Rape Pests*, pages 45–76. Springer Netherlands.
1720 Valdovinos, C., Navarrete, S., and Marquet, P. (2003). Mollusk species diversity in the Southeastern
1721 Pacific: why are there more species towards the pole? *Ecography*, 26:139–144.
1722 Vilhelmsen, L., Miko, I., and Krogmann, L. (2010). Beyond the wasp-waist: structural diversity and
1723 phylogenetic significance of the mesosoma in apocritan wasps (insecta: Hymenoptera). *Zoological*
1724 *Journal of the Linnean Society*, 159(1):22–194.
1725 Warren, E. (1903). A Preliminary Attempt to Ascertain the Relationship Between the Size of Cell and the
1726 Size of Body in Daphnia Magna Straus. *Biometrika*, 2:255.
1727 Weems, J. and Howard, V. (1954). Natural enemies and insecticides that are detrimental to beneficial
1728 Syrphidae. *The Ohio Journal of Science*, 54(1):45–54.
1729 Wigglesworth, V. B. (1973). The role of the epidermal cells in moulding the surface pattern of the cuticle
1730 in *Rhodnius* (Hemiptera). *Journal of cell science*, 12(3):683–705. 00030.
1731 Withycombe, C. (1924). Note on the economic value of the Neuroptera, with special reference to the
1732 Coniopterygidae. *Annals of Applied Biology*, 11:112–125. 00000.

Figure 4. Brightfield image showing the lateral habitus of *Conostigmus babaiax* Dessart 1997.

Figure 5. Brightfield image showing the head and mesosoma of *Conostigmus babaiax* Dessart 1997. A. Lateral view. B. Dorsal view.

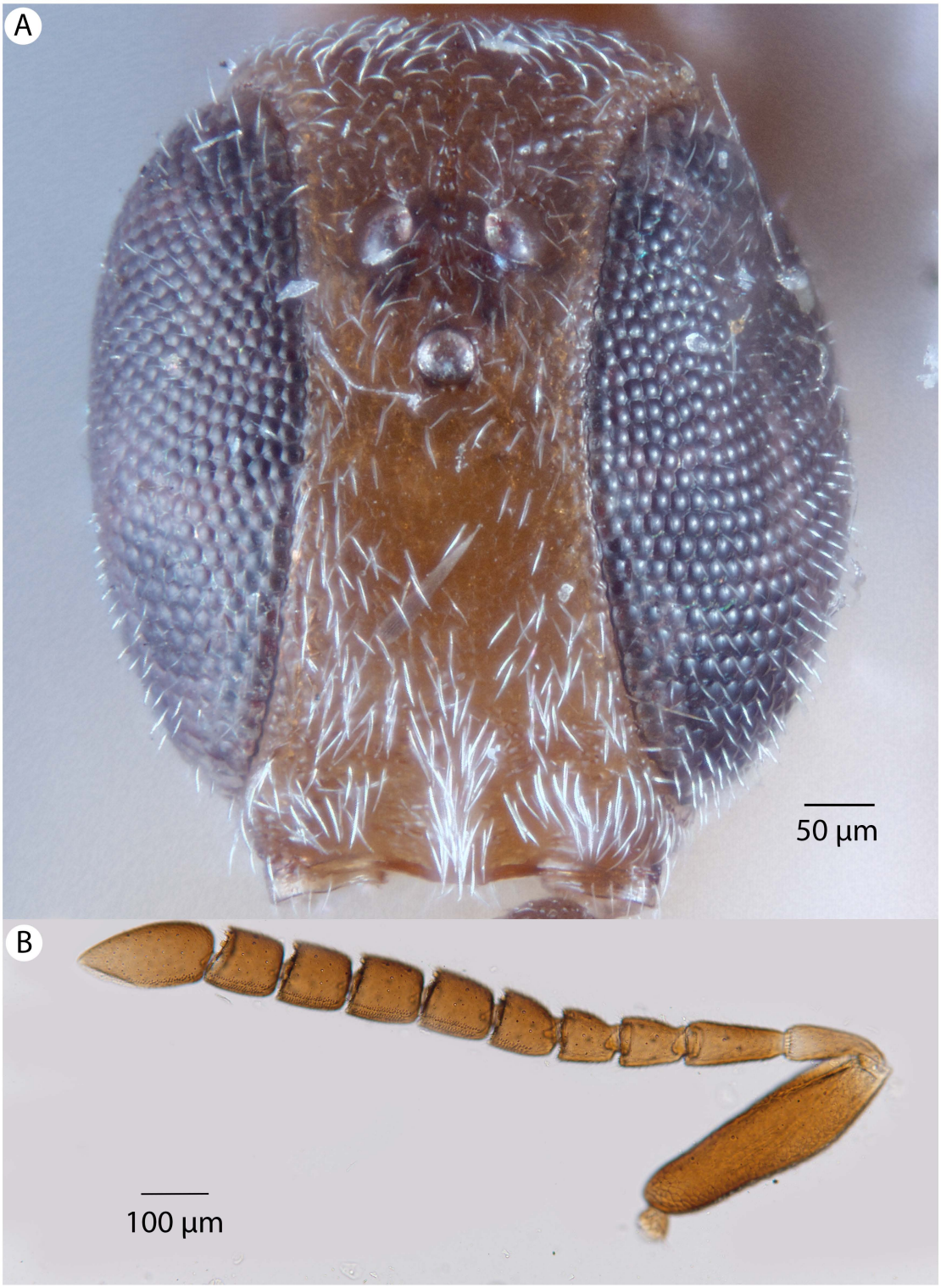

Figure 6. Brightfield image showing the head and female antenna of *Conostigmus babaiax* Dessart 1997. A. Head, anterior view. B. Female antenna.

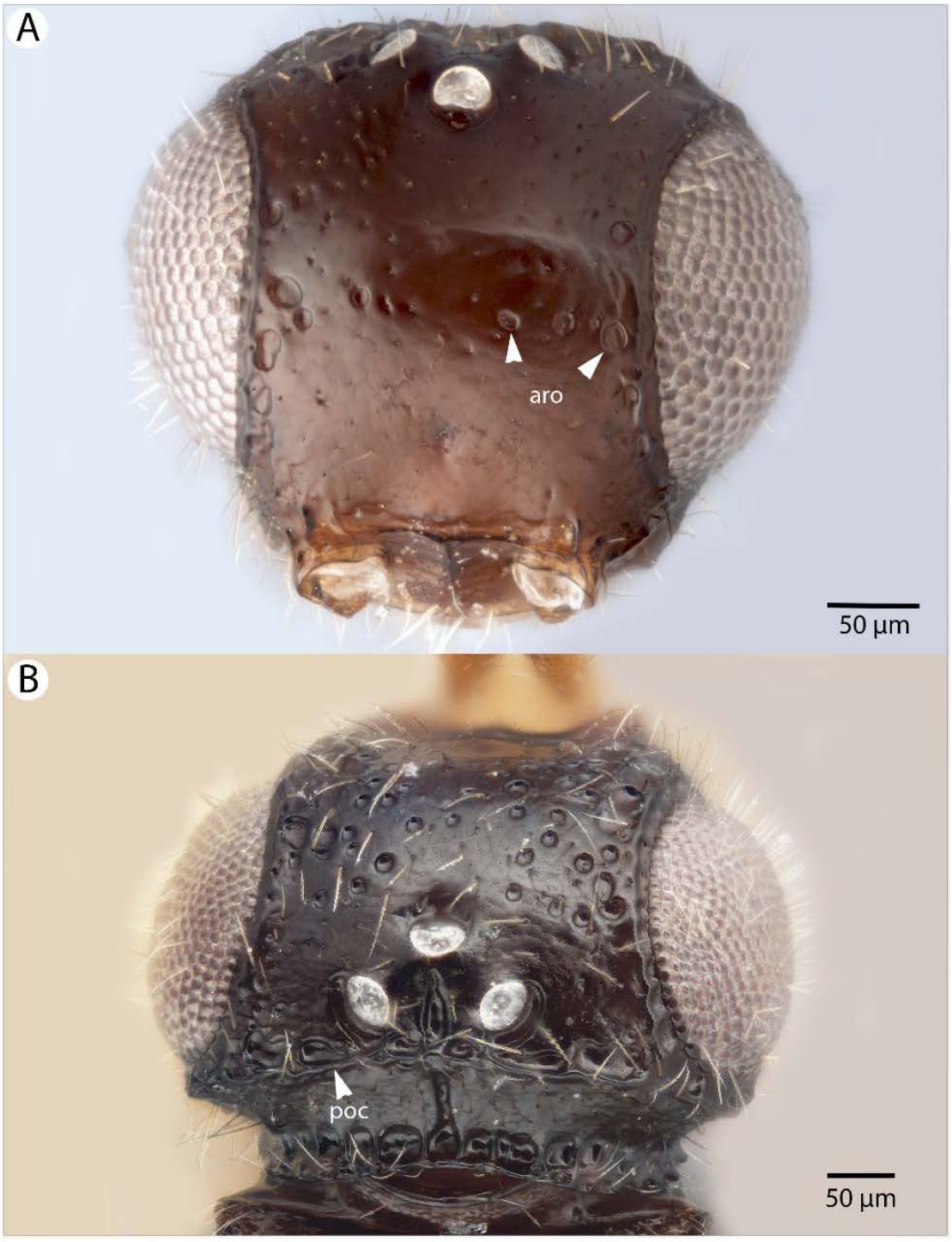

Figure 7. Brightfield image showing the head of *Conostigmus ballescoracas* Dessart 1997. A. Anterior view. B. Dorsal view (ar= randomly sized areolae around setal basis, poc=preoccipital carina).

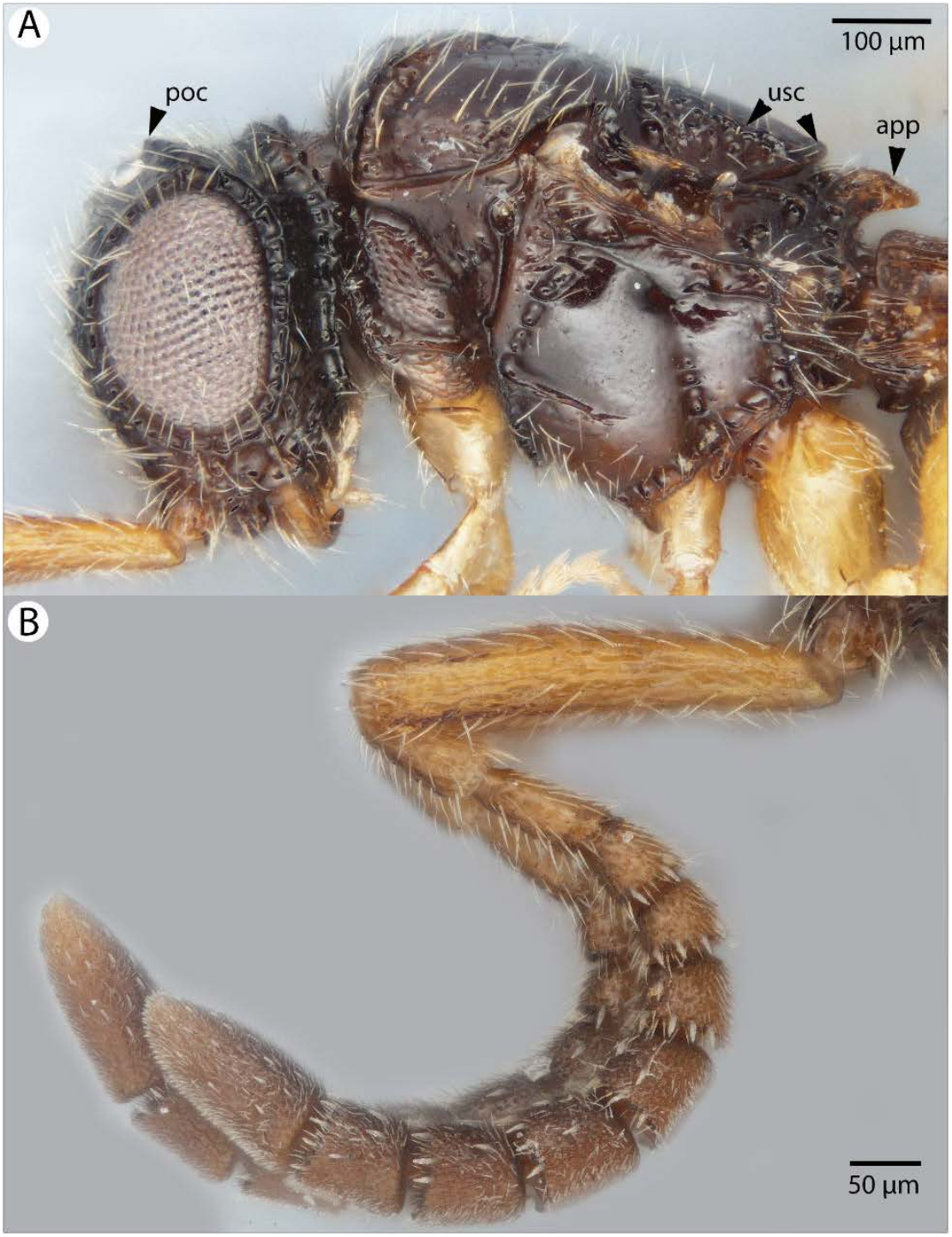

Figure 8. Brightfield image of *Conostigmus ballescoracas* Dessart 1997. A. Head and mesosoma lateral view. B. Female antenna lateral view (poc= preoccipital carina, app= anteromedian projection of the metanoto-propodeo-metapecto-mesopectal complex, usc= u-shaped carina surrounding posteriorly and laterally the disc of the mesoscutellum).

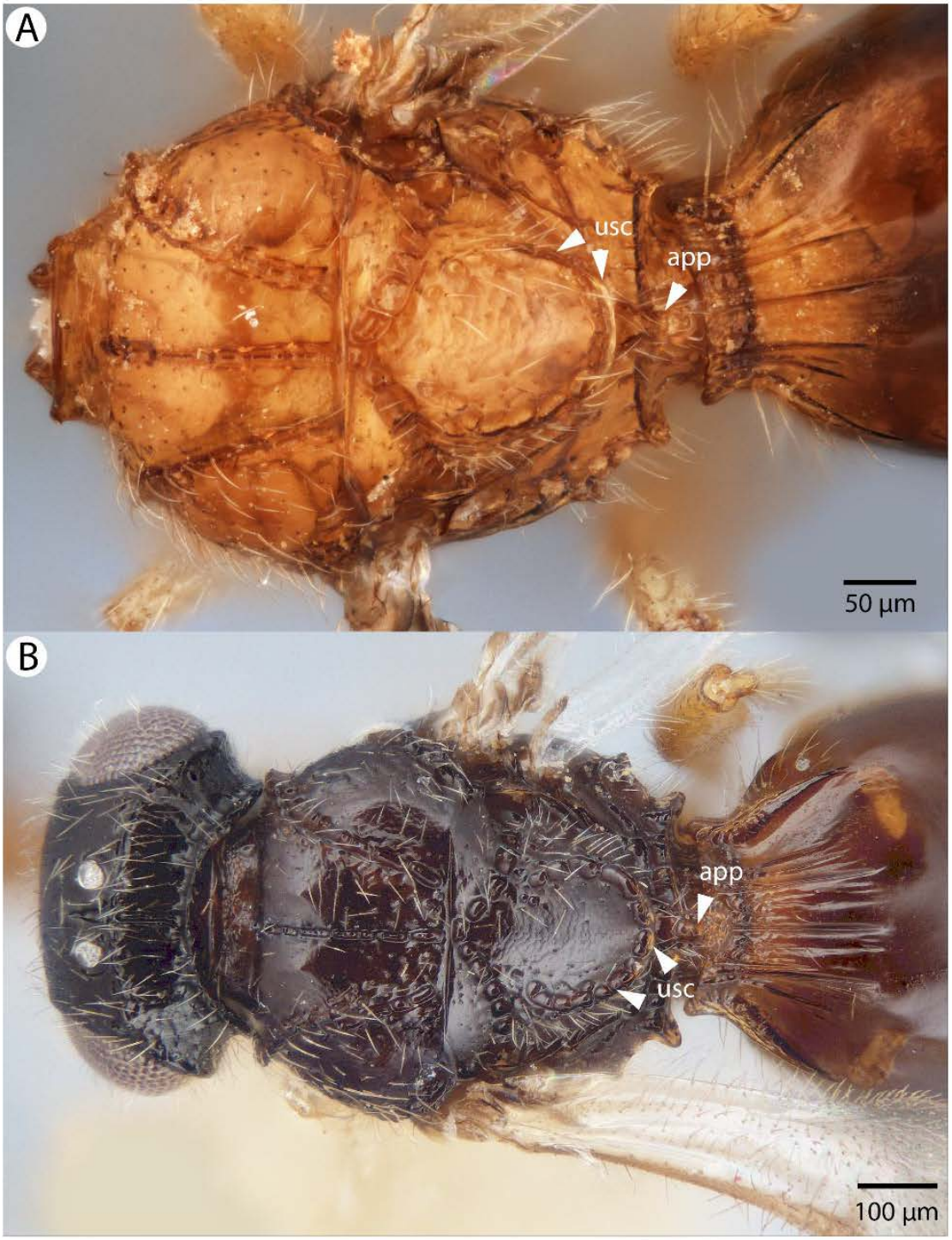

Figure 9. Brightfield image of *Conostigmus ballescoracas* Dessart 1997. A. Mesosoma and anterior metasoma, dorsal view. B. Head, mesosoma and anterior metasoma, dorsal view (app= anteromedian projection of the metanoto-propodeo-metapecto-mesopectal complex, usc= u-shaped carina surrounding posteriorly and laterally the disc of the mesoscutellum).

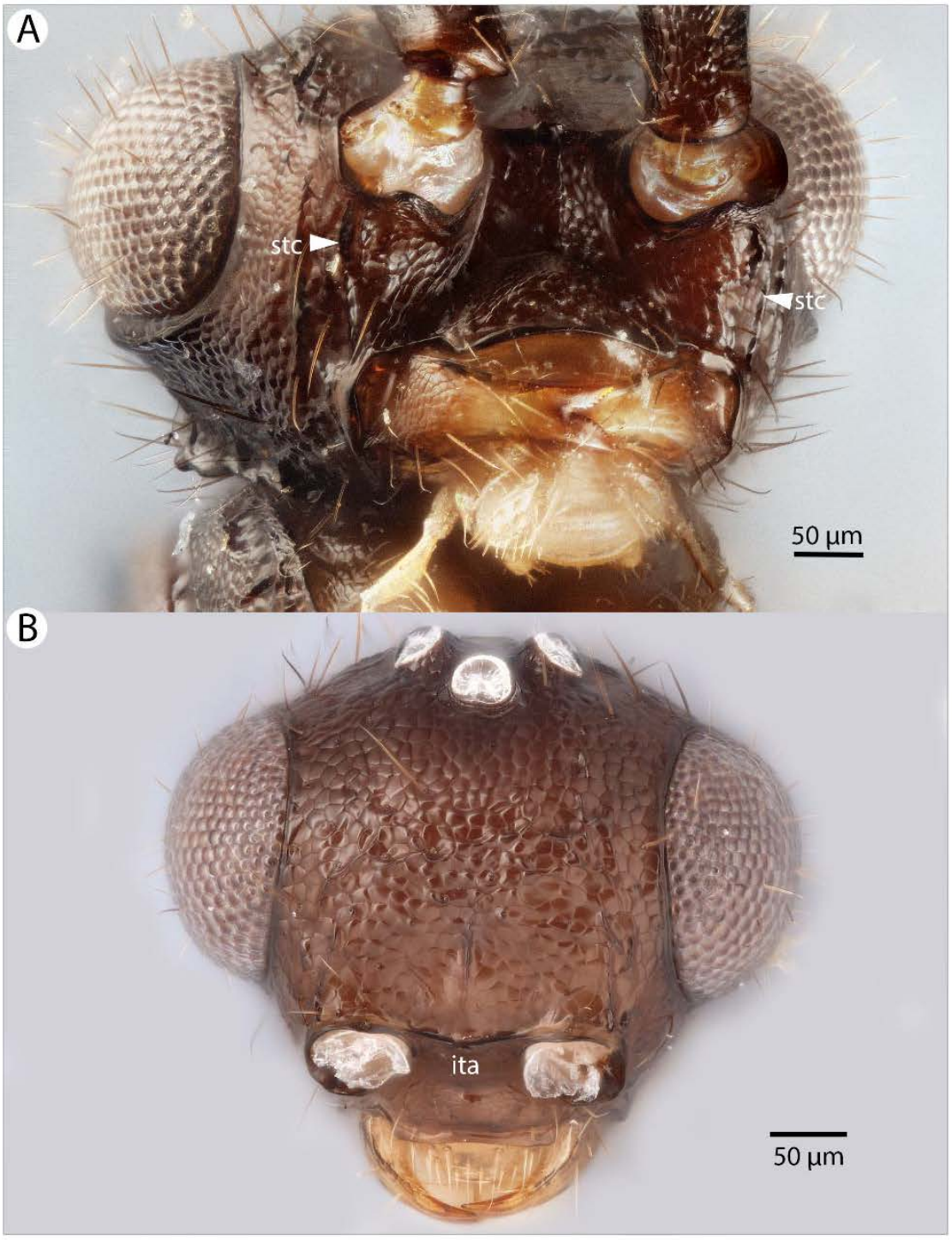

Figure 10. Brightfield image showing the head of *Conostigmus clavatus* Dessart 1997. A. Ventral view. B. Anterior view (stc= subtorular carina, ita=intertorular area).

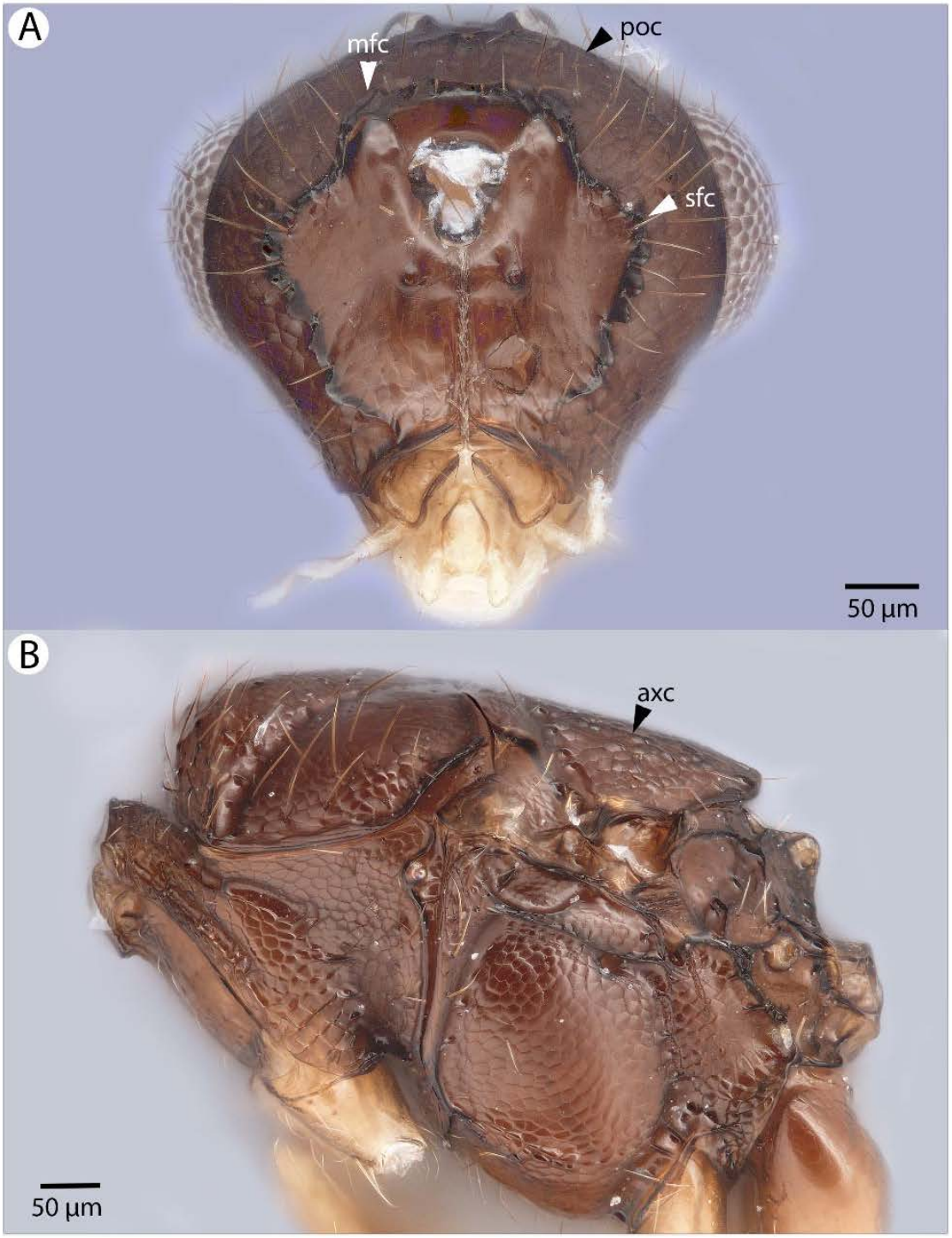

Figure 11. Brightfield image showing the head and mesosoma of *Conostigmus clavatus* Dessart 1997. A. Head, posterior view. B. Mesosoma, lateral view (poc= preoccipital carina, axc= axillular carina, mfc= median flange of occipital carina, sfc= submedial flange of occipital carina).

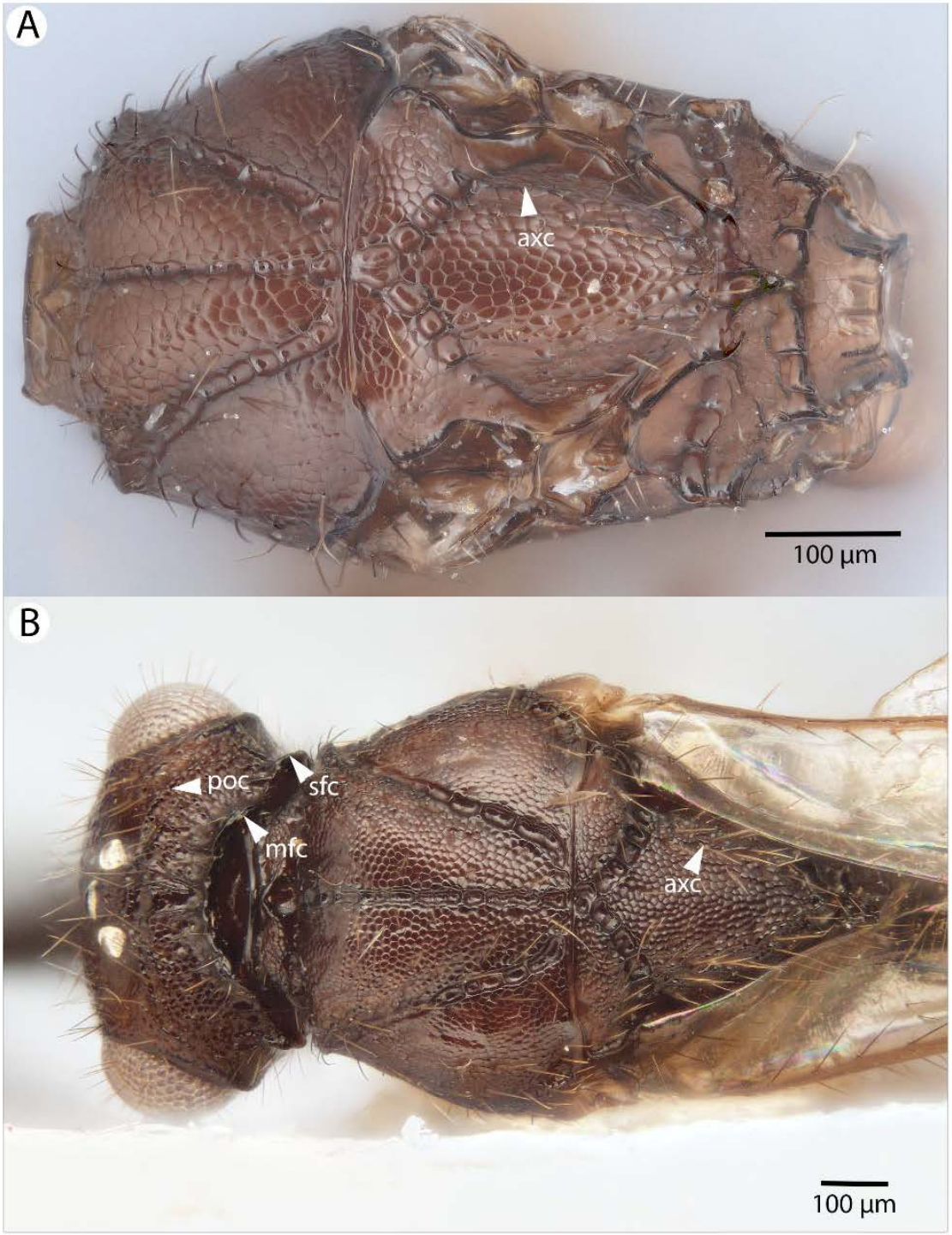

Figure 12. Brightfield image showing the head and mesosoma of *Conostigmus clavatus* Dessart 1997. A. Mesomoma, dorsal view. B. Head and mesosoma, dorsal view (poc= preoccipital carina, axc= axillular carina, mfc= median flange of occipital carina, sfc= submedial flange of occipital carina).

Figure 13. Brightfield image showing the antenna of *Conostigmus clavatus* Dessart 1997. A. Female. B. Male.

Figure 14. CLSM volume rendered micrographs showing the male genitalia of *Conostigmus clavatus* Mikó and Trietsch sp. nov. A. Ventral view B. Dorsal view (ddm=distodorsal margin of cupula, pdc=proximodorsal notch of cupula).

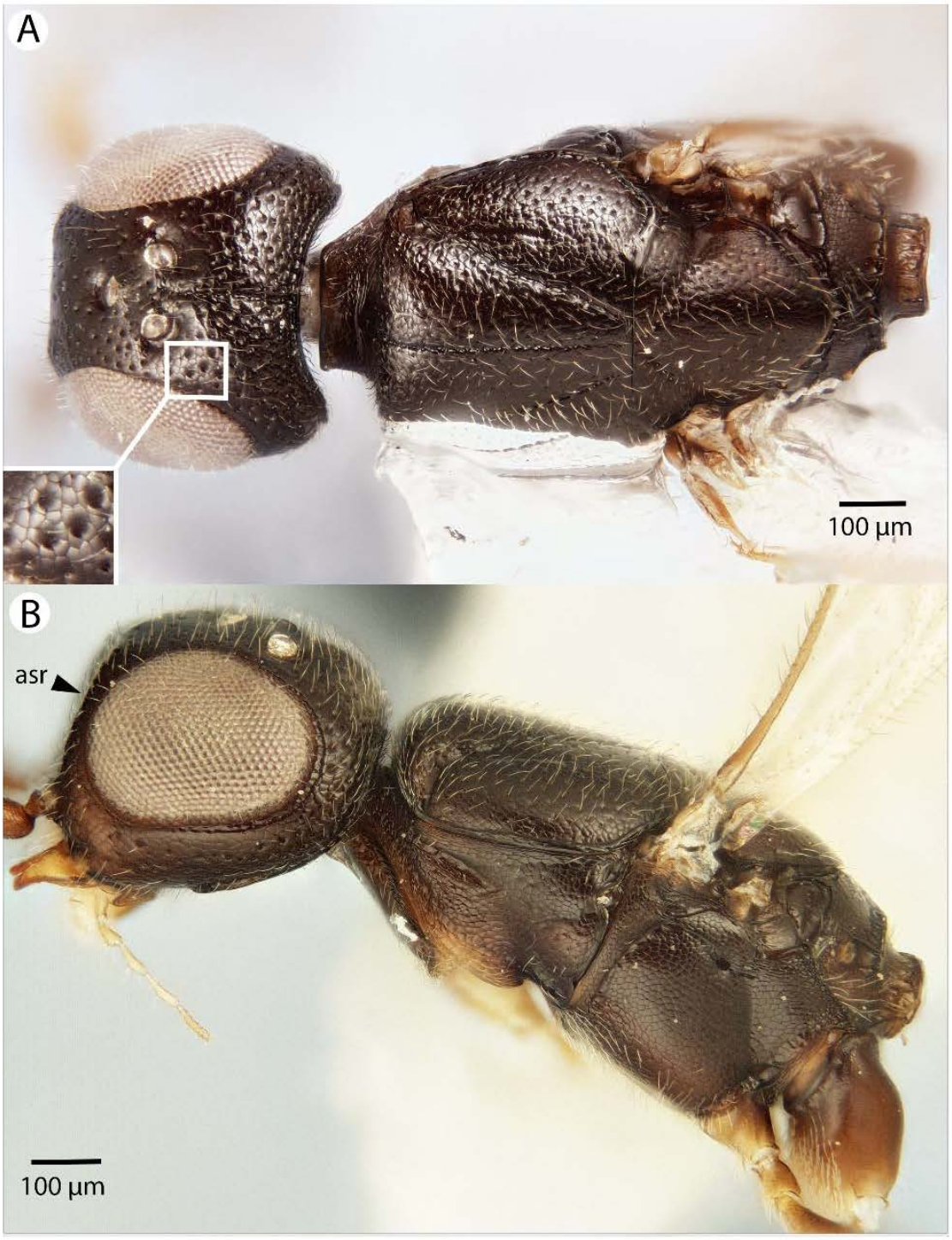

Figure 15. Brightfield image showing the head and mesosoma of *Conostigmus bucephalus* Mikó and Trietsch sp. nov. A. Dorsal view. B. Lateral view.

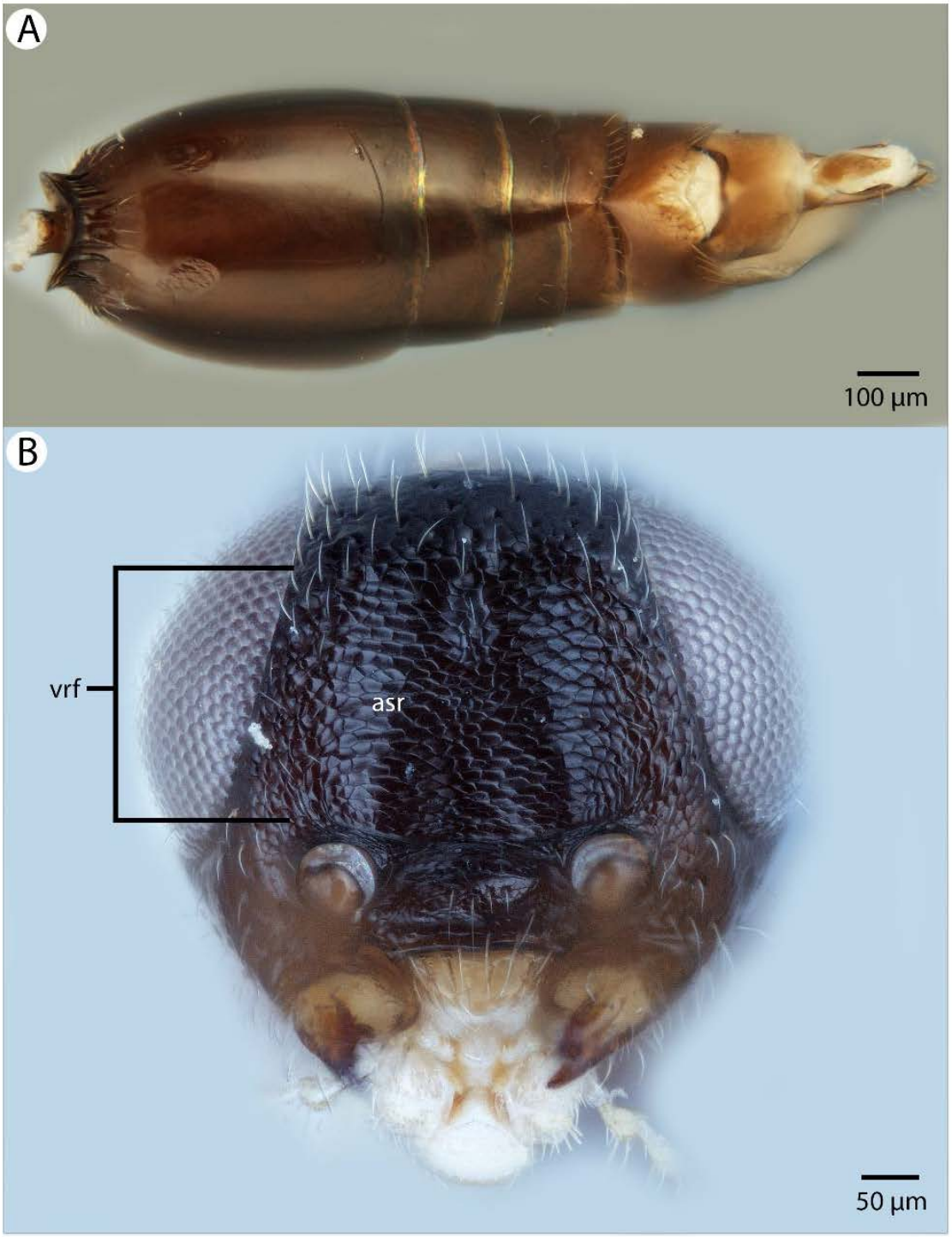

Figure 16. Brightfield image showing the head and metasoma of *Conostigmus bucephalus* Mikó and Trietsch sp. nov. A. Metasoma, dorsal view. B. Head, anterior view (vrf= ventral region on frons, asr= antennal scrobe).

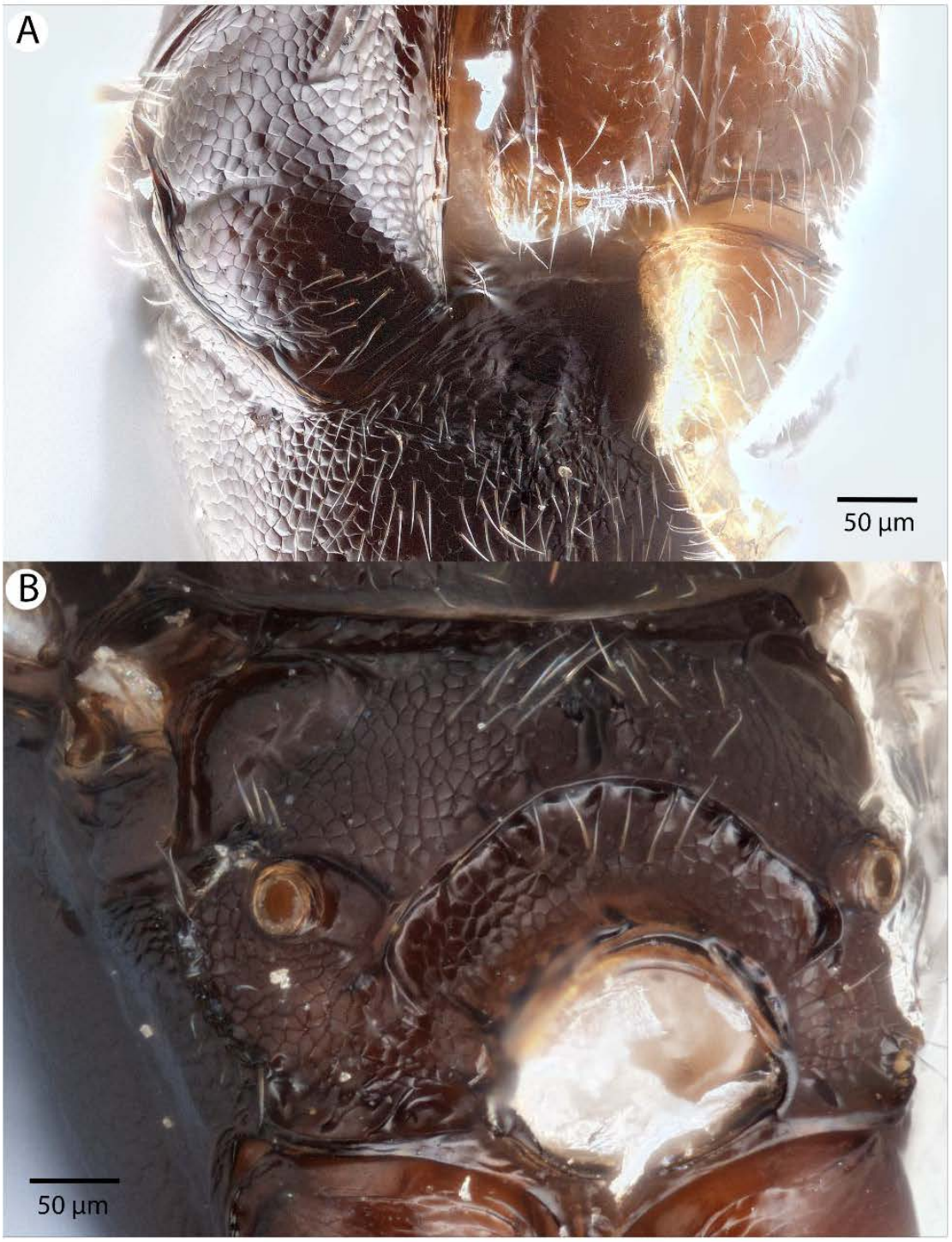

Figure 17. Brightfield image showing the mesosoma of *Conostigmus bucephalus* Mik6 and Trietsch sp. nov. A. Pronotum, part of propleuron and part of mesopectus, anterolateral view. B. Part of mesomoma, posterior view (vrf= ventral region on frons with transverse scutes, asr= antennal scrobe).

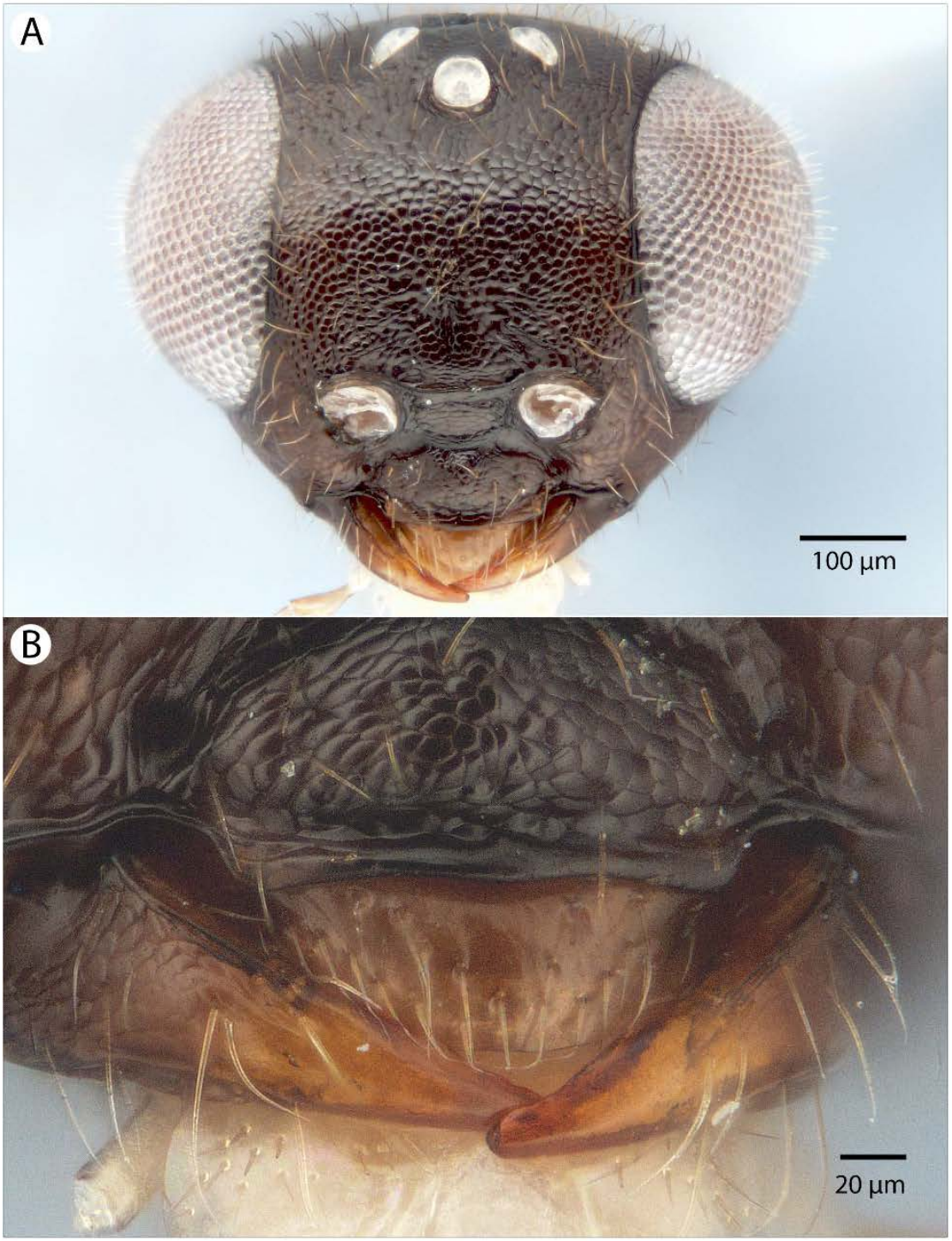

Figure 18. Brightfield image showing the head of *Conostigmus madagascariensis* Mikó and Trietsch sp. nov. A. Head, anterior view. B. Mandible, labrum and clypeus, anteroventral view.

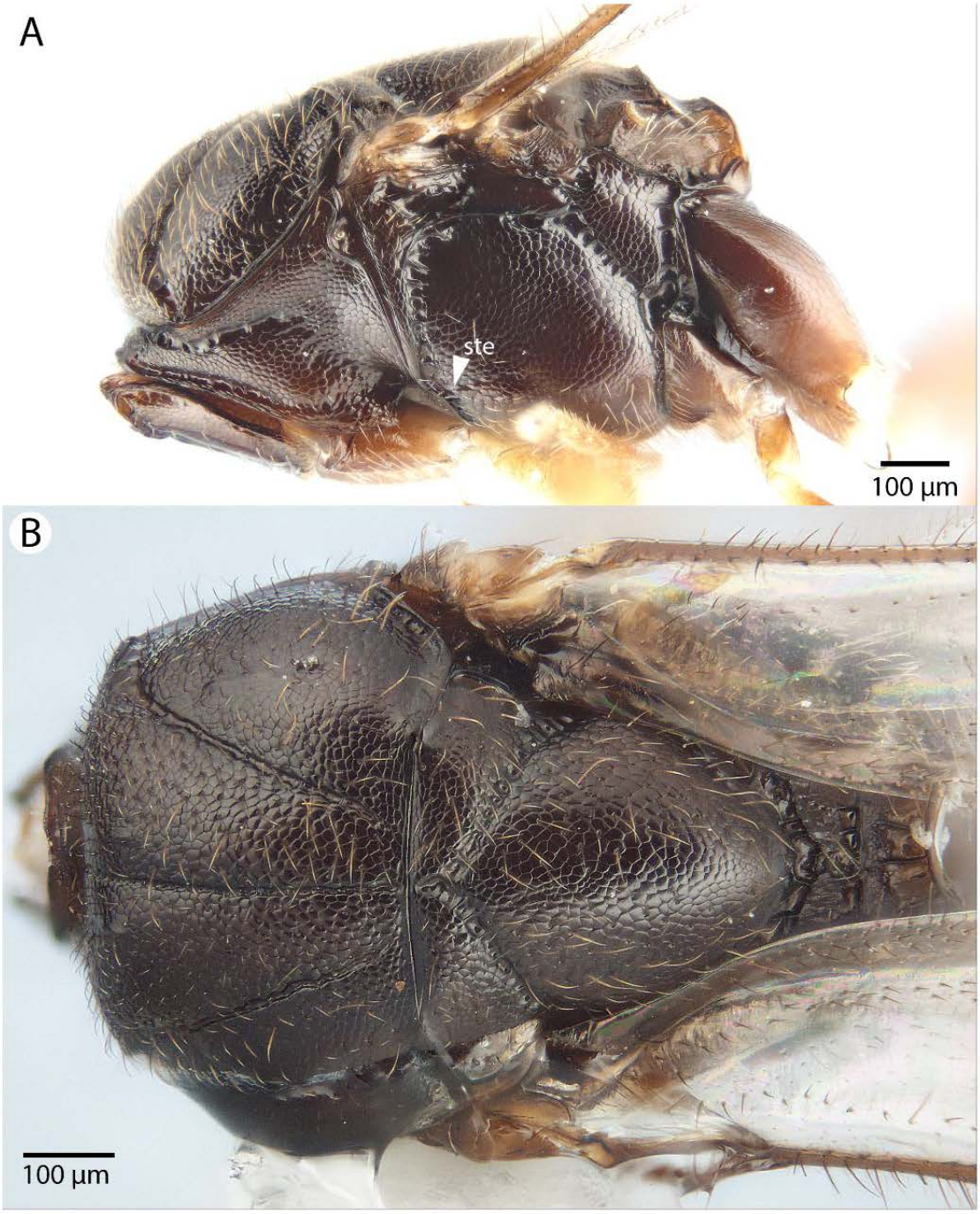

Figure 19. Brightfield image showing the mesosoma of *Conostigmus madagascariensis* Mikó and Trietsch sp. nov. A. mesosoma, lateral view. B. Mesosoma, dorsal view (ste= sternaulus).

Figure 20. Brightfield image showing the antenna of *Conostigmus madagascariensis* Mikó and Trietsch sp. nov. A. Male. B. Female.

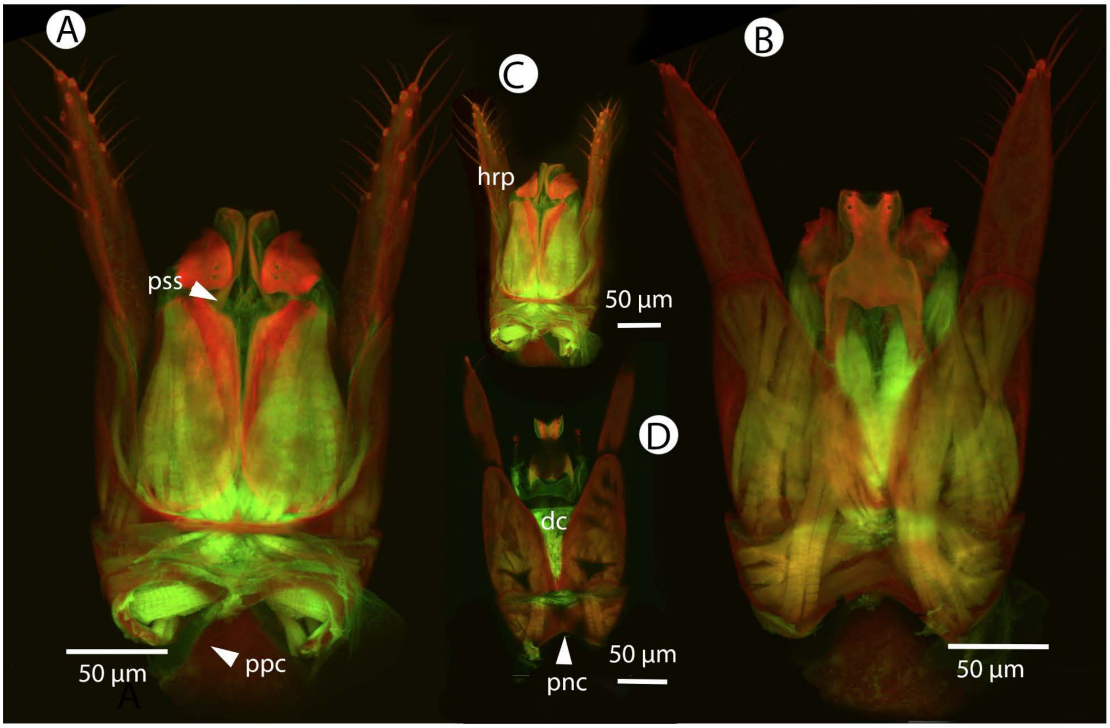

Figure 21. CLSM volume rendered micrographs showing the male genitalia of *Conostigmus fianarantsoaensis* Mikó and Trietsch sp. nov. A. Ventral view. B. Dorsal view. C. Lateroventral view. D. Dorsal view partially rendered (ppc= proximolateral projection of cupula, pdc=proximodorsal notch of cupula, hrp= harpe, dc= Dorsomedian conjunctiva of the gonostyle/volsella complex, aps= apical parossicular seta).

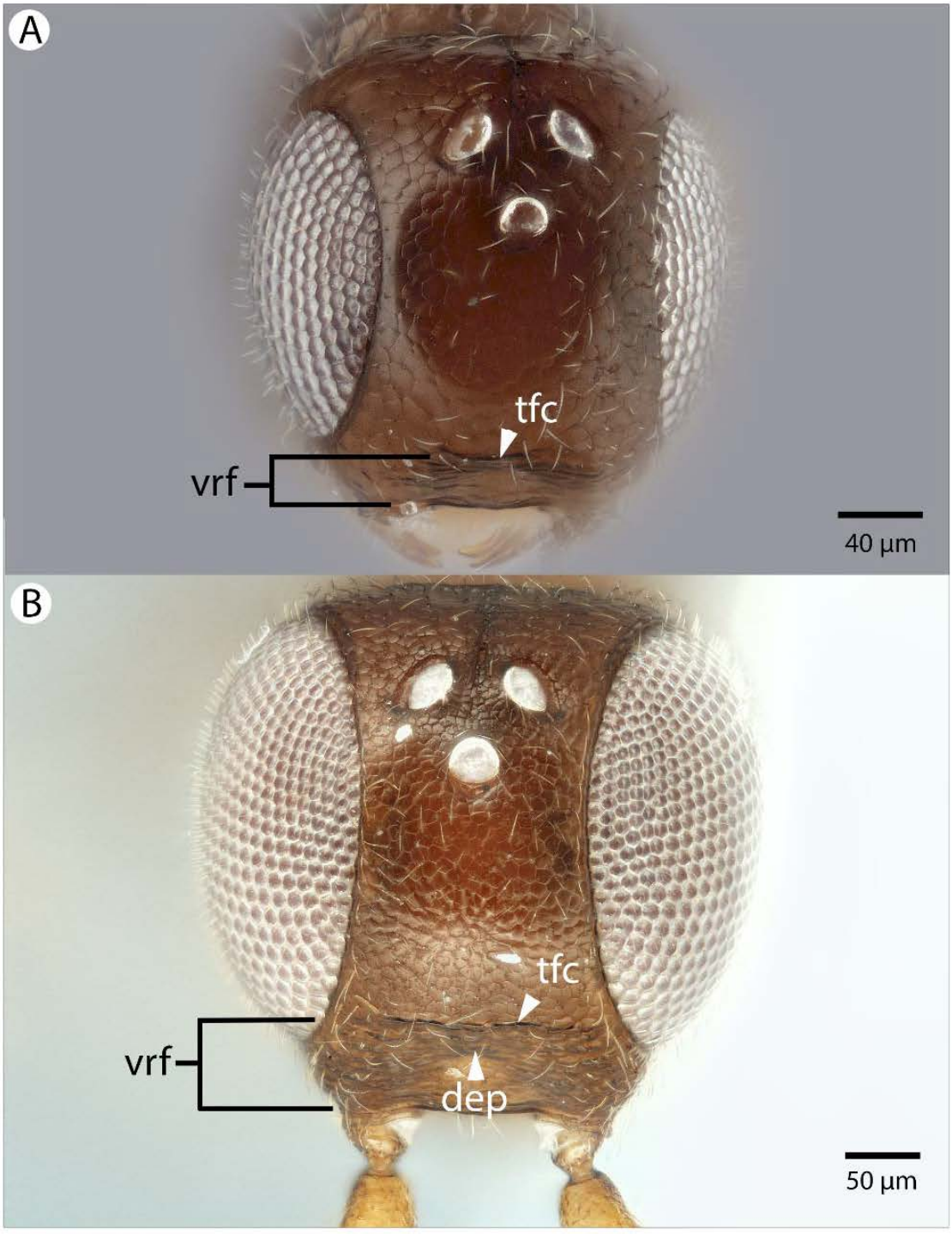

Figure 22. Brightfield image showing the head of *Conostigmus longulus* Dessart 1997, anterior view A. Smaller specimen. B. Larger specimen (tfc=transverse frontal carina, vrf=ventral region of frons, dep=depression surrounding frontal pit).

Figure 23. Brightfield image showing the antenna of *Conostigmus longulus* Dessart 1997, lateral view A. Female. B. Male.

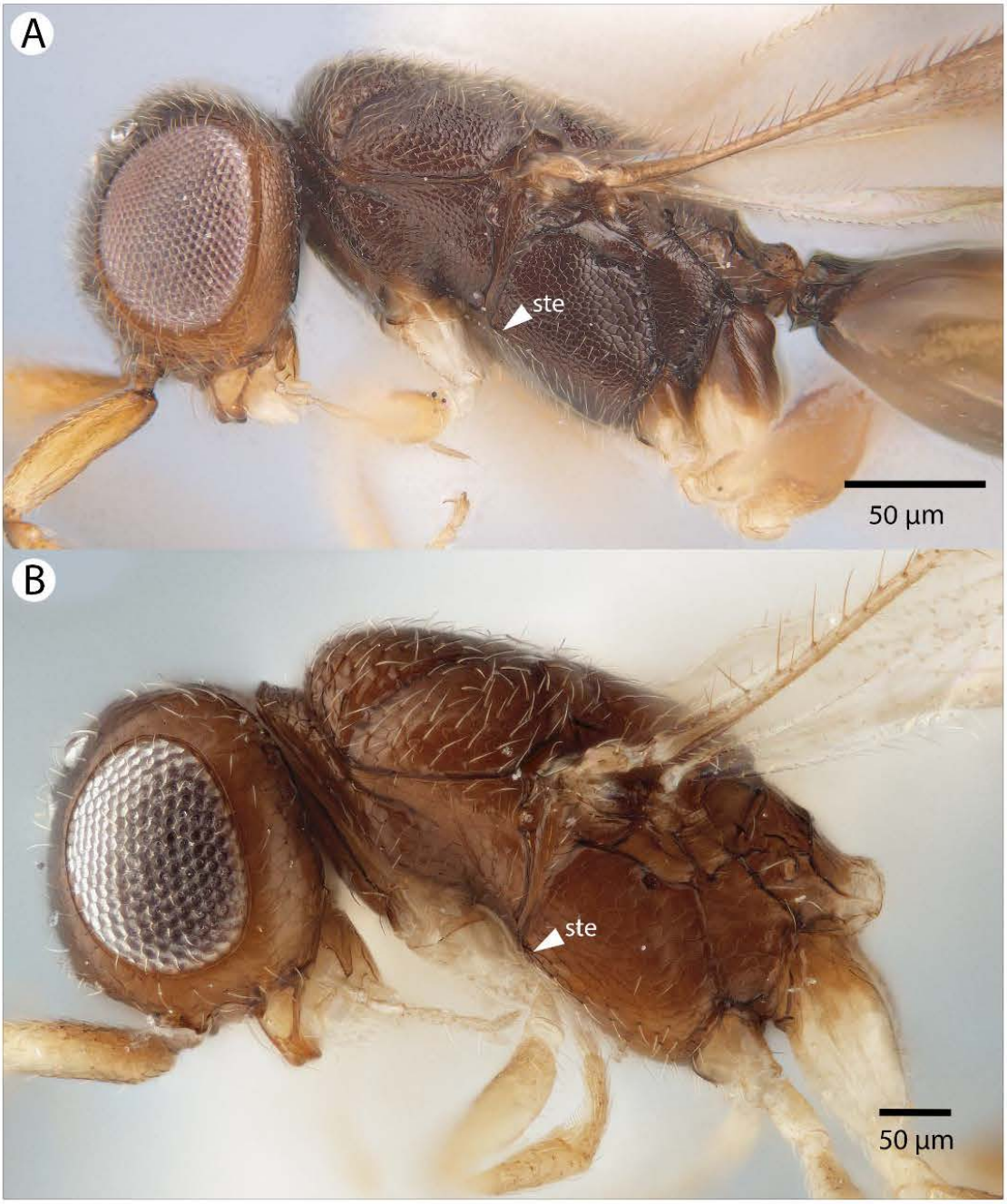

Figure 24. Brightfield image showing the head and mesosoma of *Conostigmus longulus* Dessart 1997, anterior view A. Larger specimen. B. Smaller specimen.

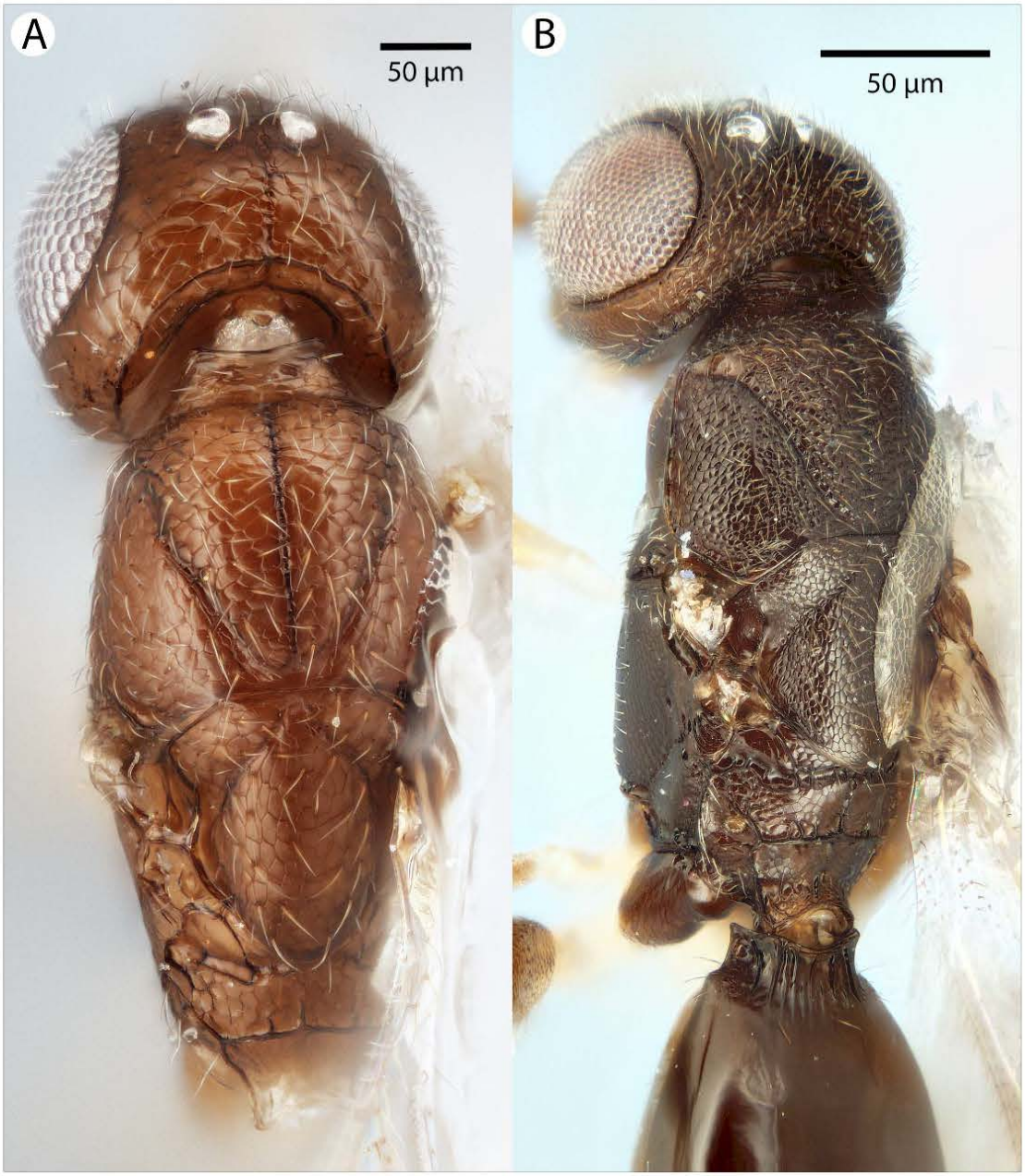

Figure 25. Brightfield image showing the head and mesosoma of *Conostigmus longulus* Dessart 1997, anterior view A. Larger specimen. B. Smaller specimen.

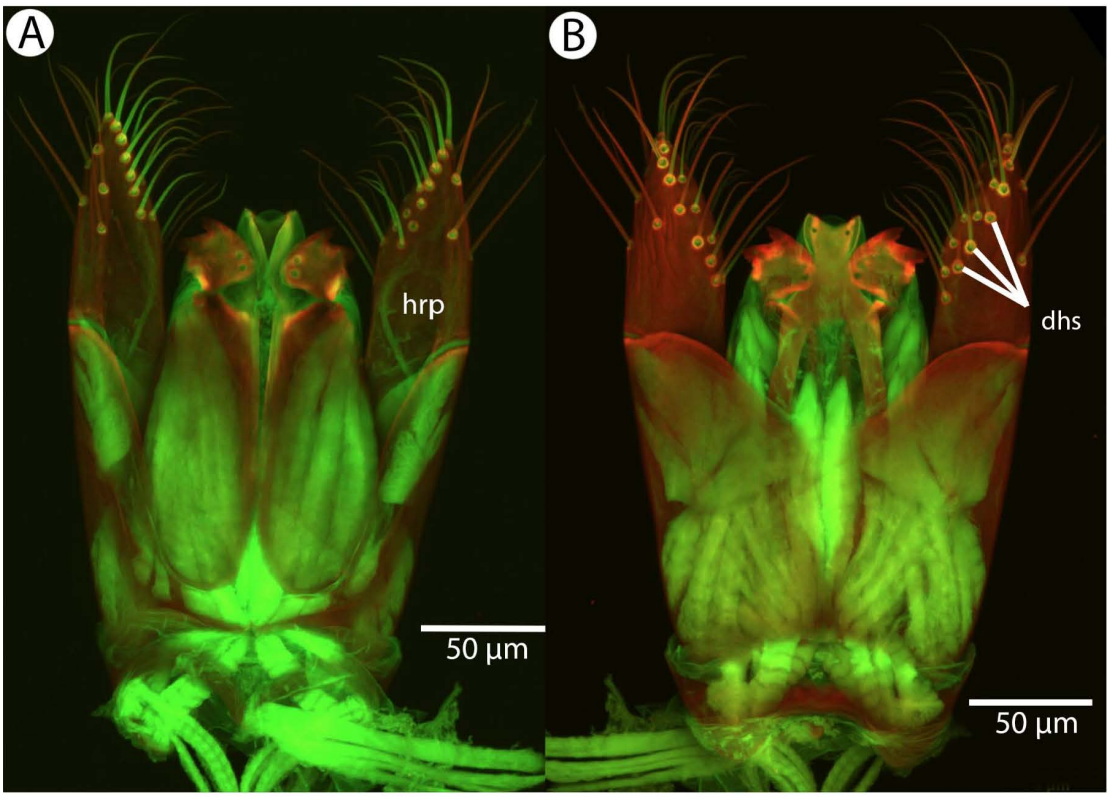

Figure 26. CLSM volume rendered micrographs showing the male genitalia of *Conostigmus longulus* Dessart 1997. A. Ventral view. B. Dorsal view (hrp=harpe, dhs=dorsomedial setae of harpal setal ring).

Figure 27. Brightfield image showing the antenna of *Conostigmus lucidus* Mikó and Trietsch sp. nov., lateral view. A. Female. B. Male.

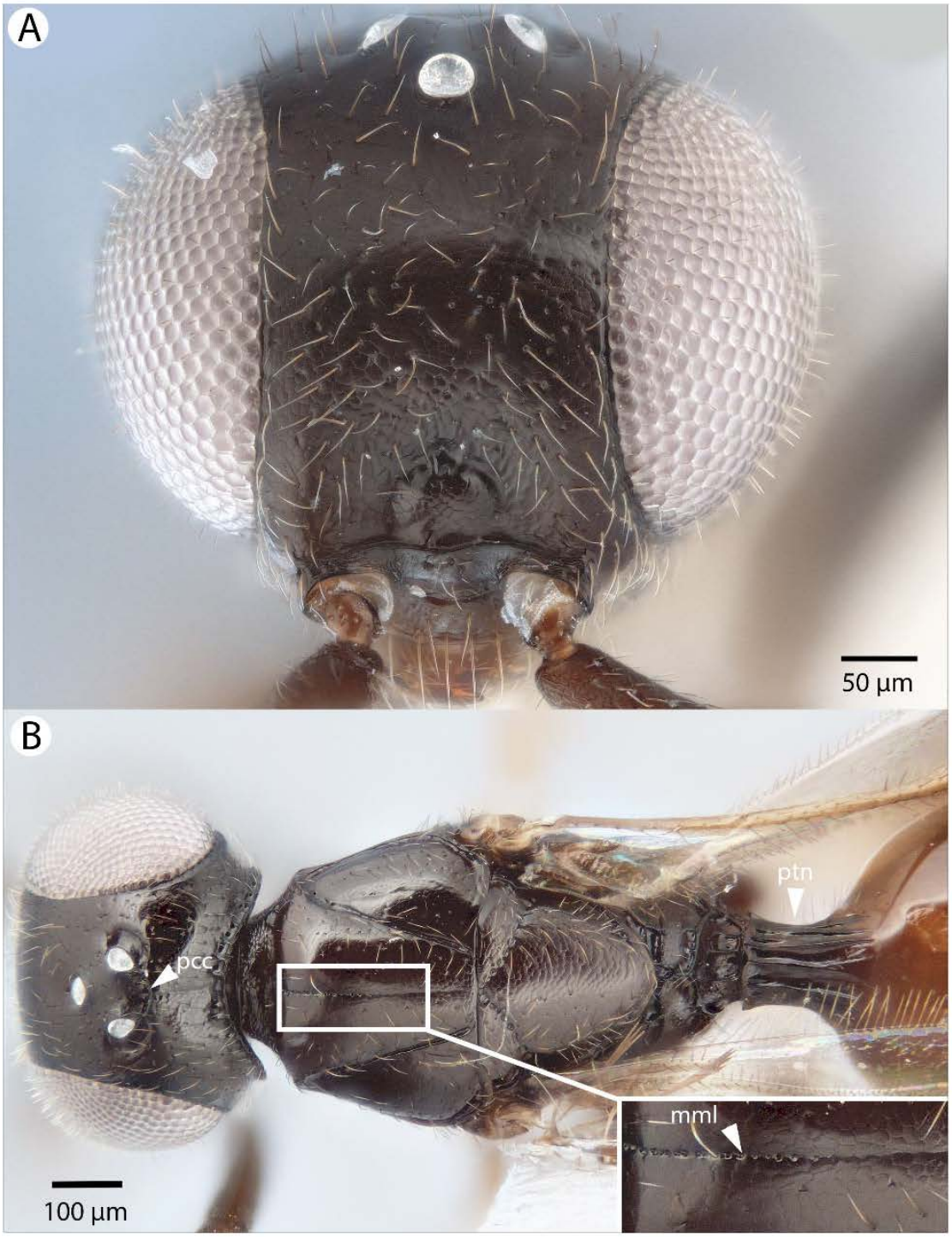

Figure 28. Brightfield image showing the head and mesosoma of *Conostigmus lucidus* Mik6 and Trietsch sp. nov. A. Head, anterior view. B. Head and mesosoma, dorsal view (mml= median mesoscutal line).

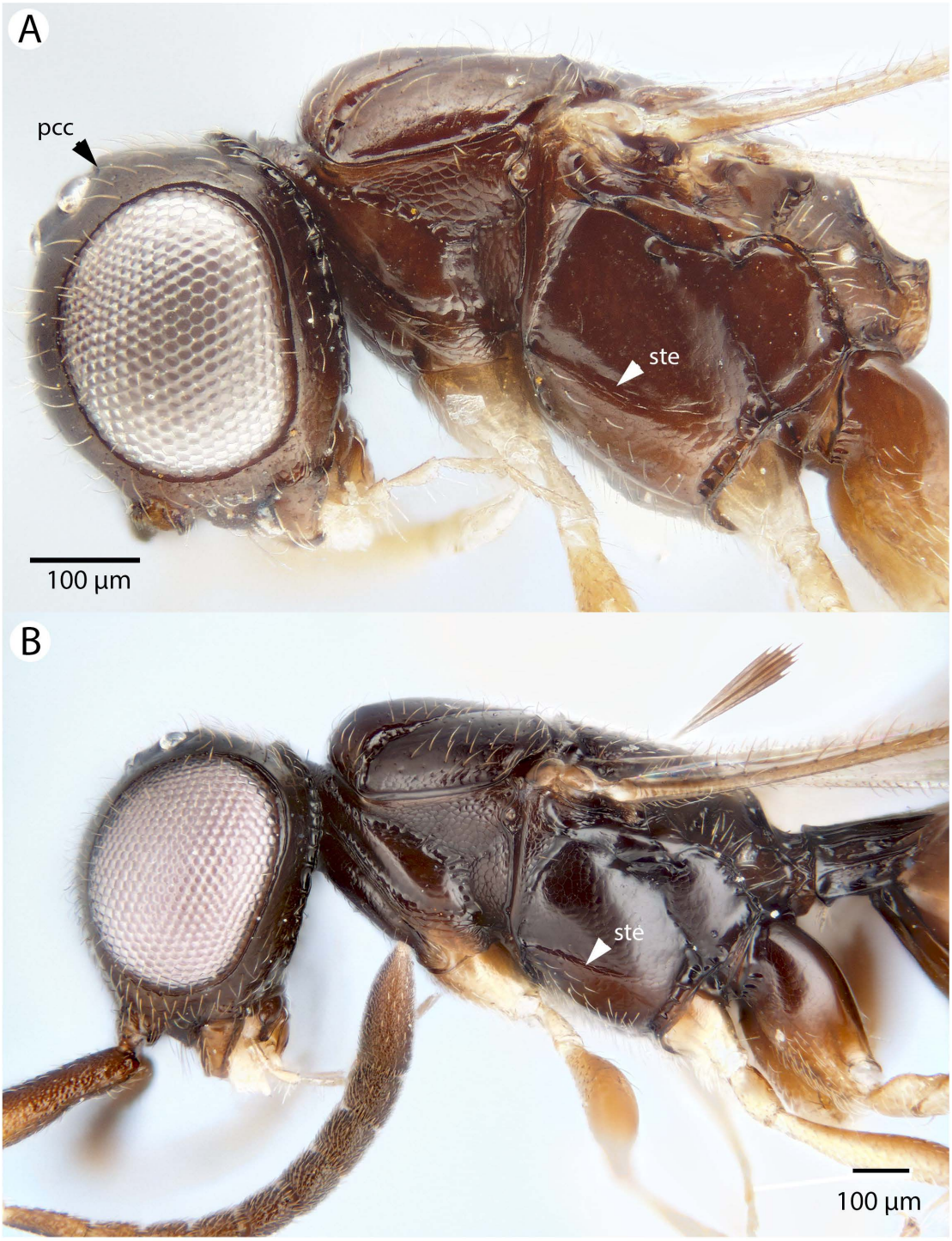

Figure 29. Brightfield image showing the head and mesosoma of *Conostigmus lucidus* Mikó and Trietsch sp. nov., lateral view. A. Smaller specimen. B. Larger specimen (ste= sternaulus).

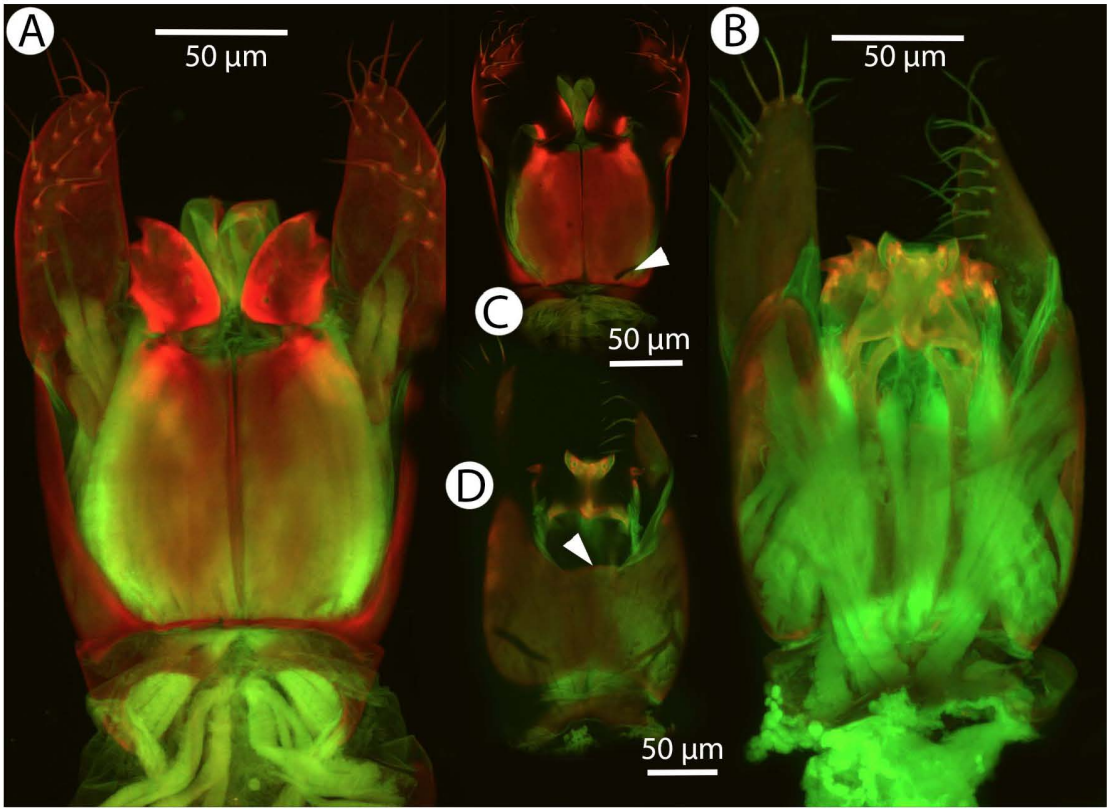

Figure 30. CLSM volume rendered micrographs showing the male genitalia of *Conostigmus lucidus* Mikó and Trietsch sp. nov. A. Ventral view. B. Dorsal view. C. Ventral view, partially rendered. D. Dorsal view, partially rendered. (Arrow on C. showing bridge connecting parossiculus with gonostyle, on D. showing lack of dorsomedian conjectiva of gonostyle/volsella complex).

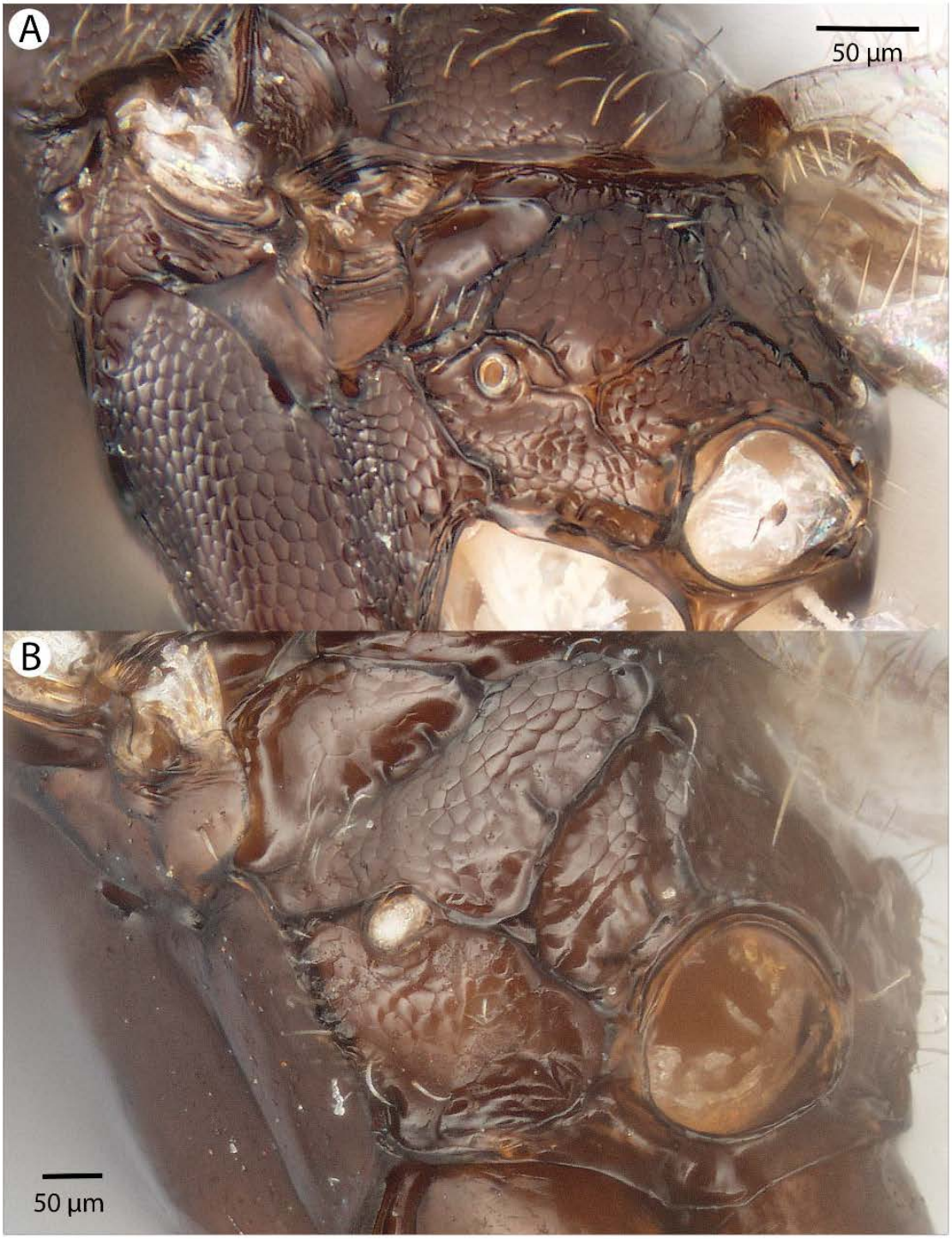

Figure 31. Brightfield image showing the mesosoma of *Conostigmus* species, posterolateral view. A. *Conostigmus missyhazenae* Mikó and Trietsch sp. nov. B. *Conostigmus lucidus* Mikó and Trietsch sp. nov.

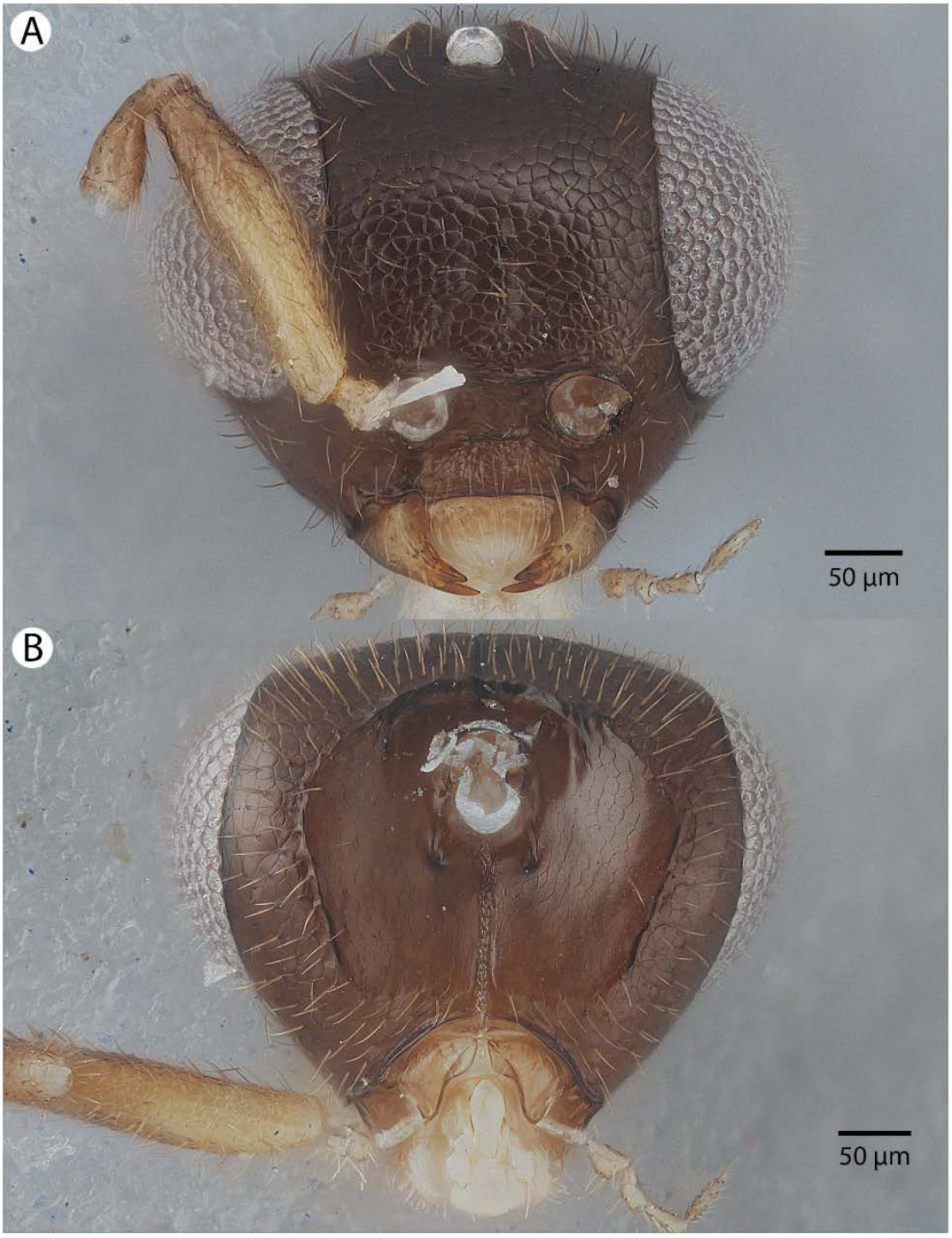

Figure 32. Brightfield image showing the head of *Conostigmus macrocupula* Mikó and Trietsch sp. nov. A. Anterior view. B. Posterior view.

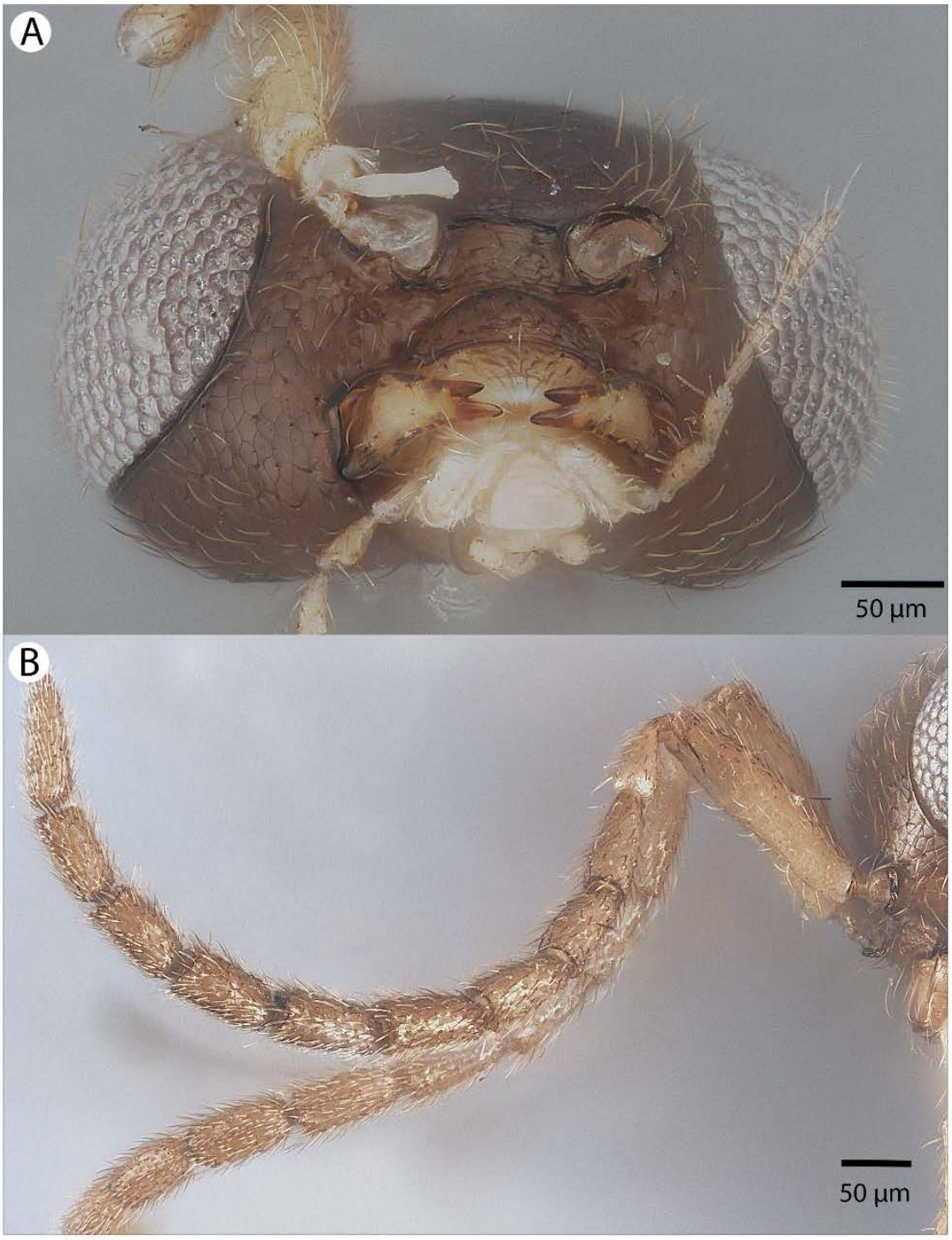

Figure 33. Brightfield image showing the head and antenna of *Conostigmus macrocupula* Mikó and Trietsch sp. nov. A. Head, ventral view. B. Antenna, lateral view.

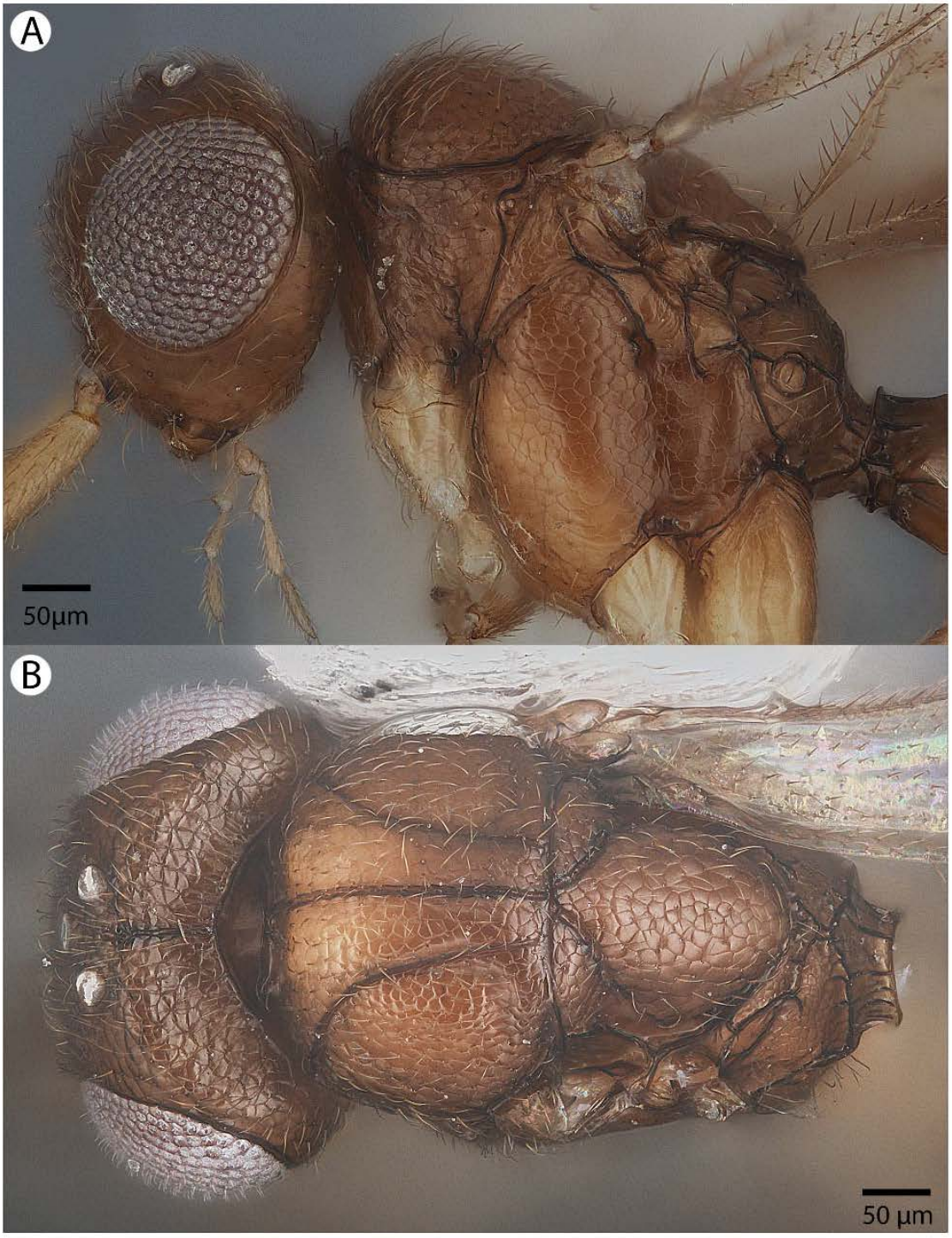

Figure 34. Brightfield image showing the head and mesosoma of *Conostigmus macrocupula* Mikó and Trietsch sp. nov. A. Lateral ventral view. B. Dorsal view.

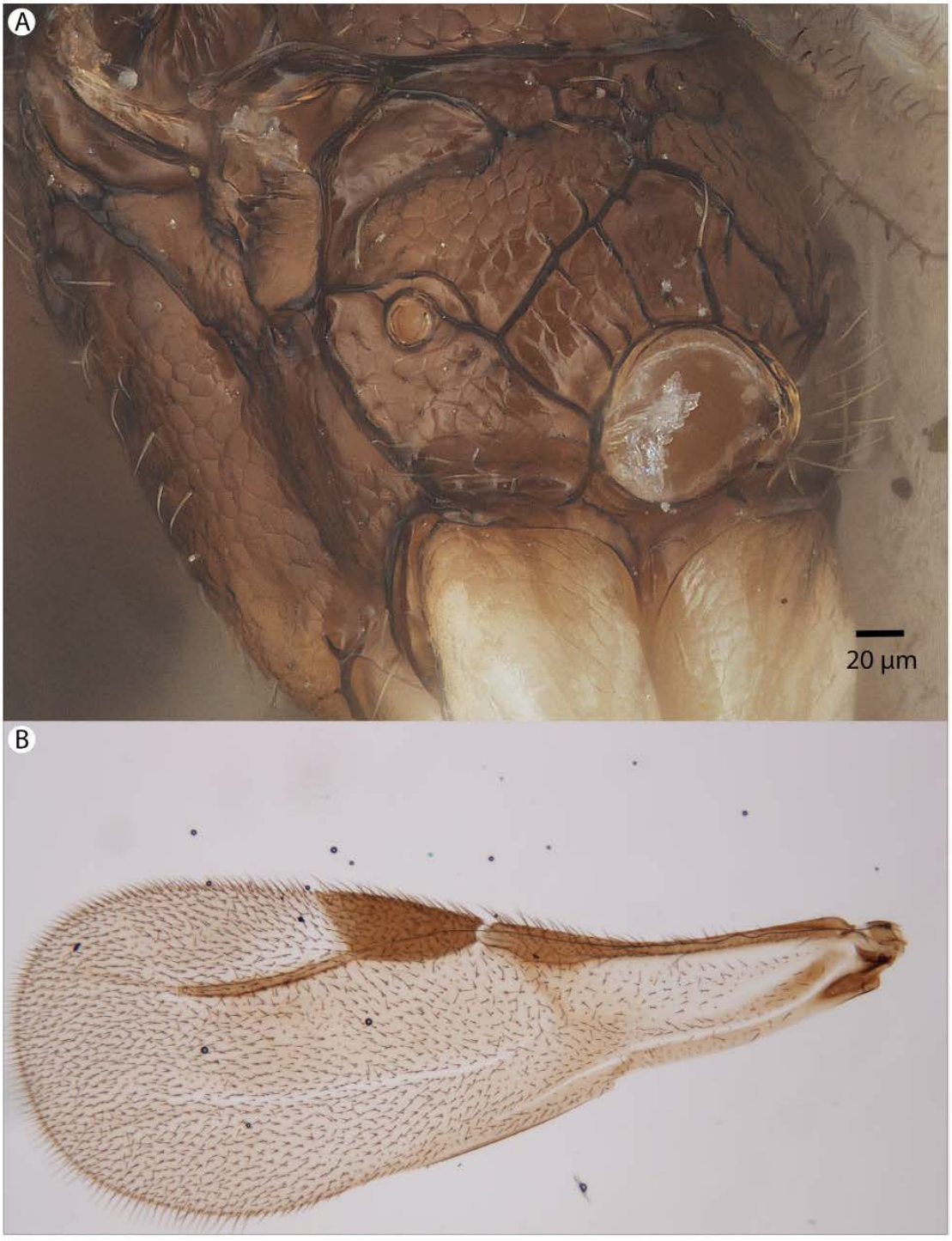

Figure 35. Brightfield image showing the mesosoma and wing of *Conostigmus macrocupula* Mikó and Trietsch sp. nov. A. Mesosoma, posterolateral view. B. Fore wing.

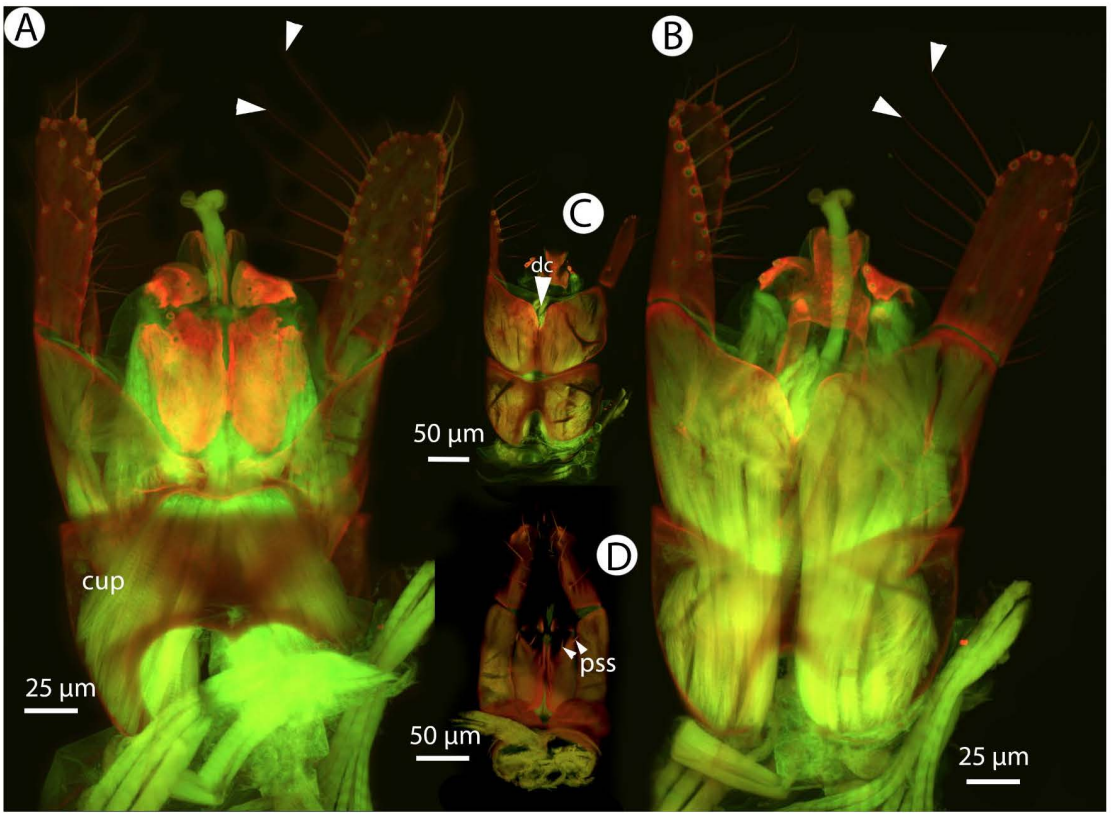

Figure 36. CLSM volume rendered micrographs showing the male genitalia of *Conostigmus macrocupula* Mió and Trietsch sp. nov. A. Ventral view. B. Dorsal view (cup= cupula, pss= parosiculal setae, dc= dorsomedial conjunctiva of gonostyle/volsella complex).

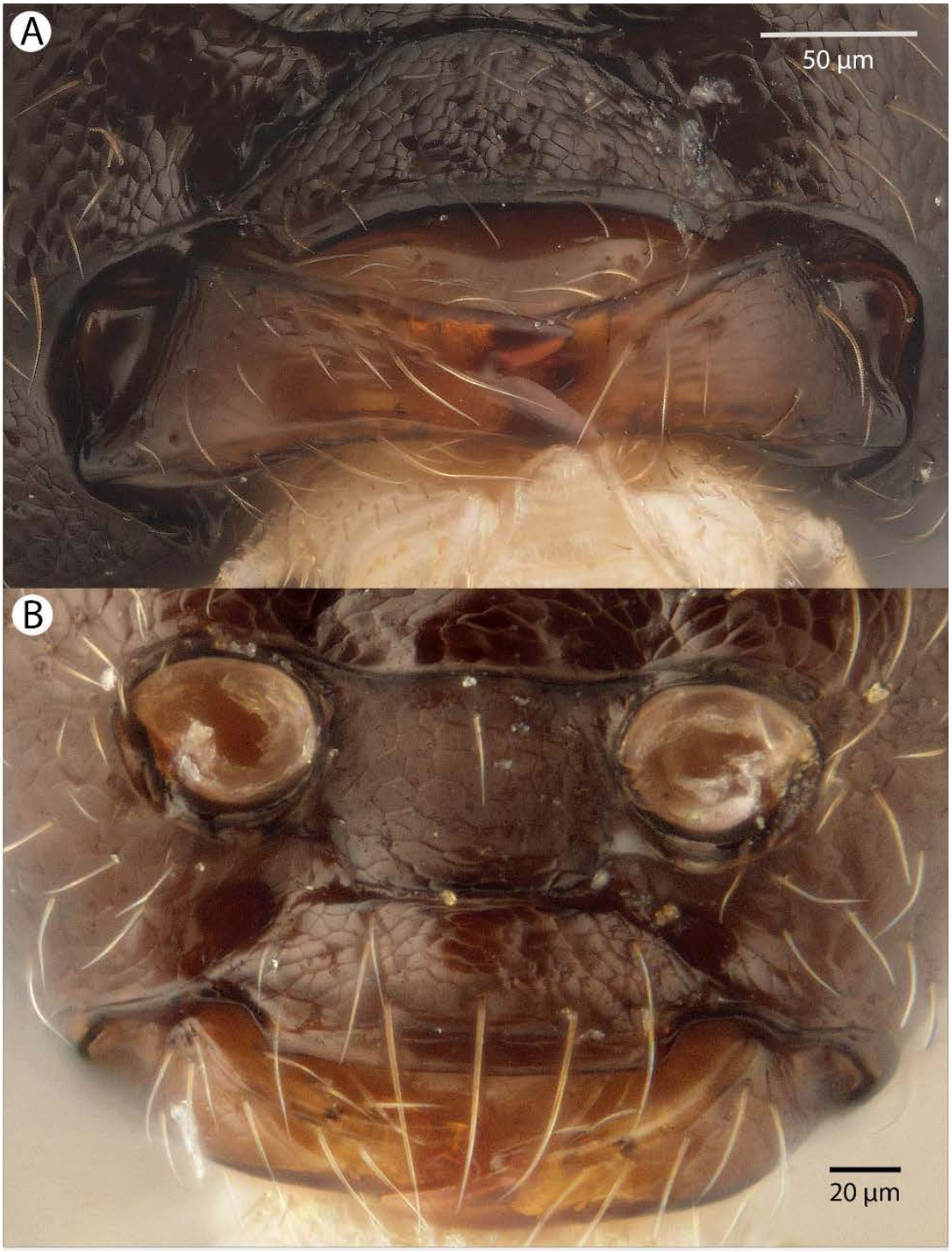

Figure 37. Brightfield image showing the intraspecific variability in mandible structure of *Conostigmus madagascariensis* Mikó and Trietsch sp. nov.

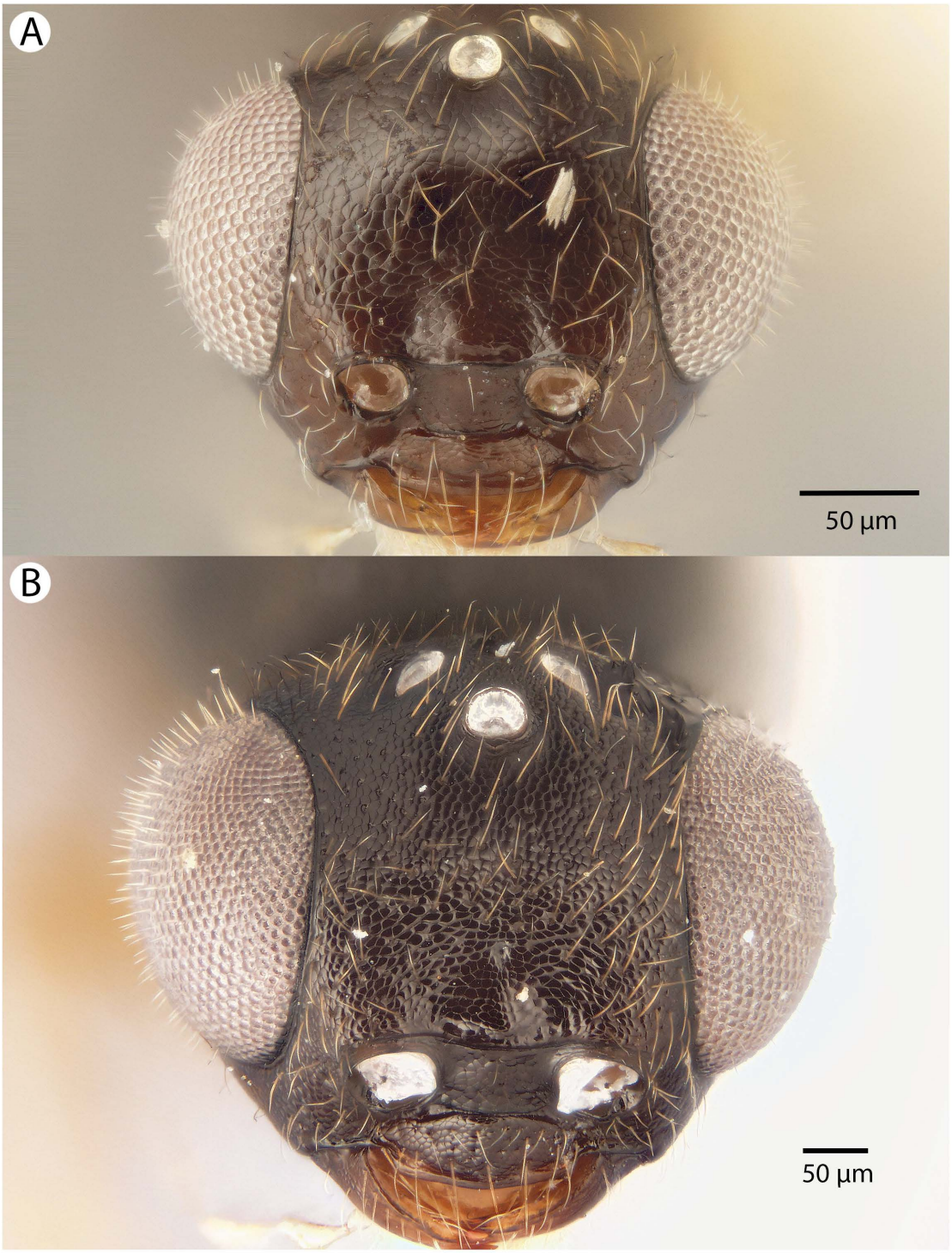

Figure 38. Brightfield image showing the intraspecific variability in anterior head morphology of *Conostigmus madagascariensis* Mikó and Trietsch sp. nov.

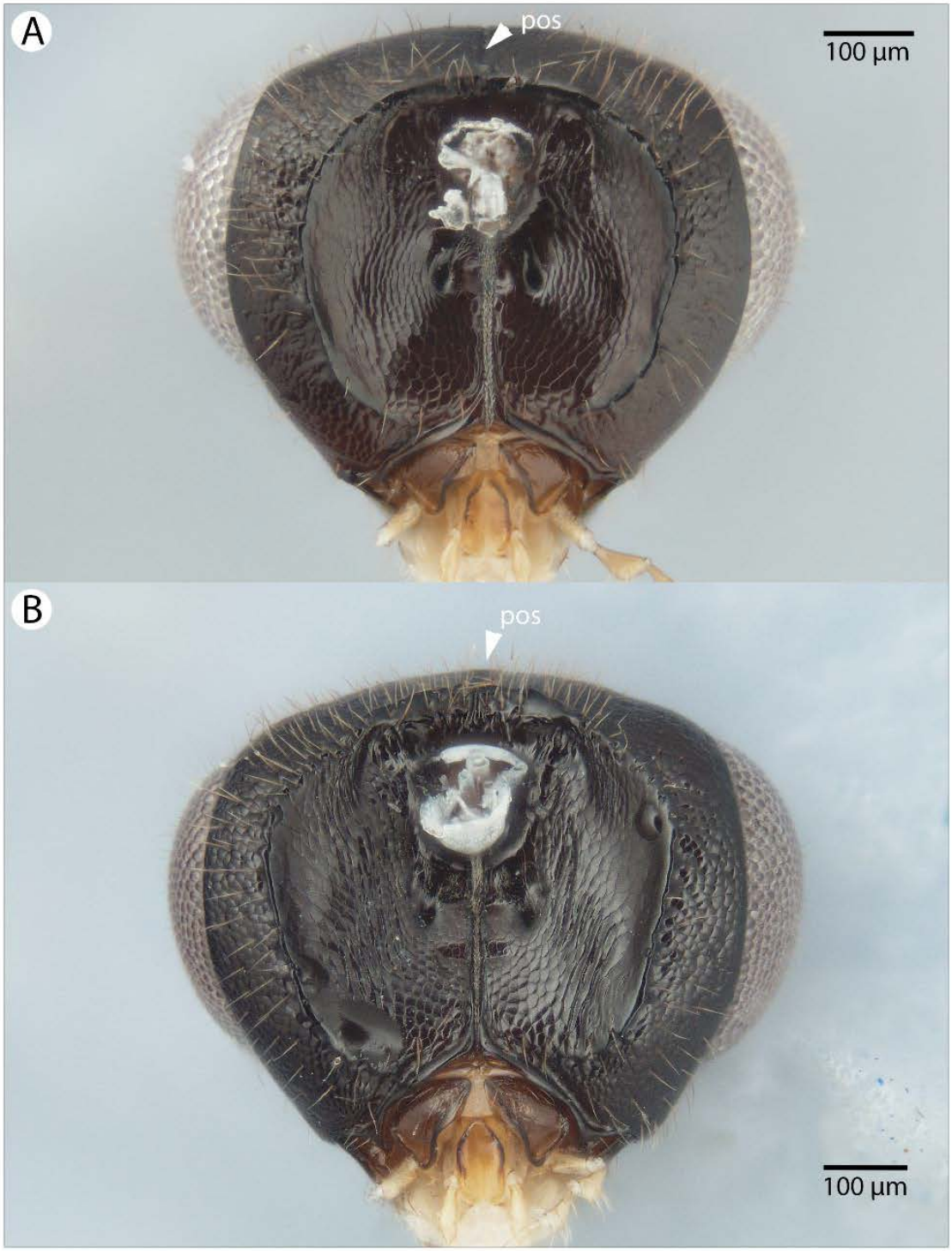

Figure 39. Brightfield image showing the head of Conostigmus species, posterior view A. *Conostigmus madagascariensis* Mikó and Trietsch sp. nov. B. *Conostigmus fianarantsoaensis* Mikó and Trietsch sp. nov. (pos=preoccipital furrow).

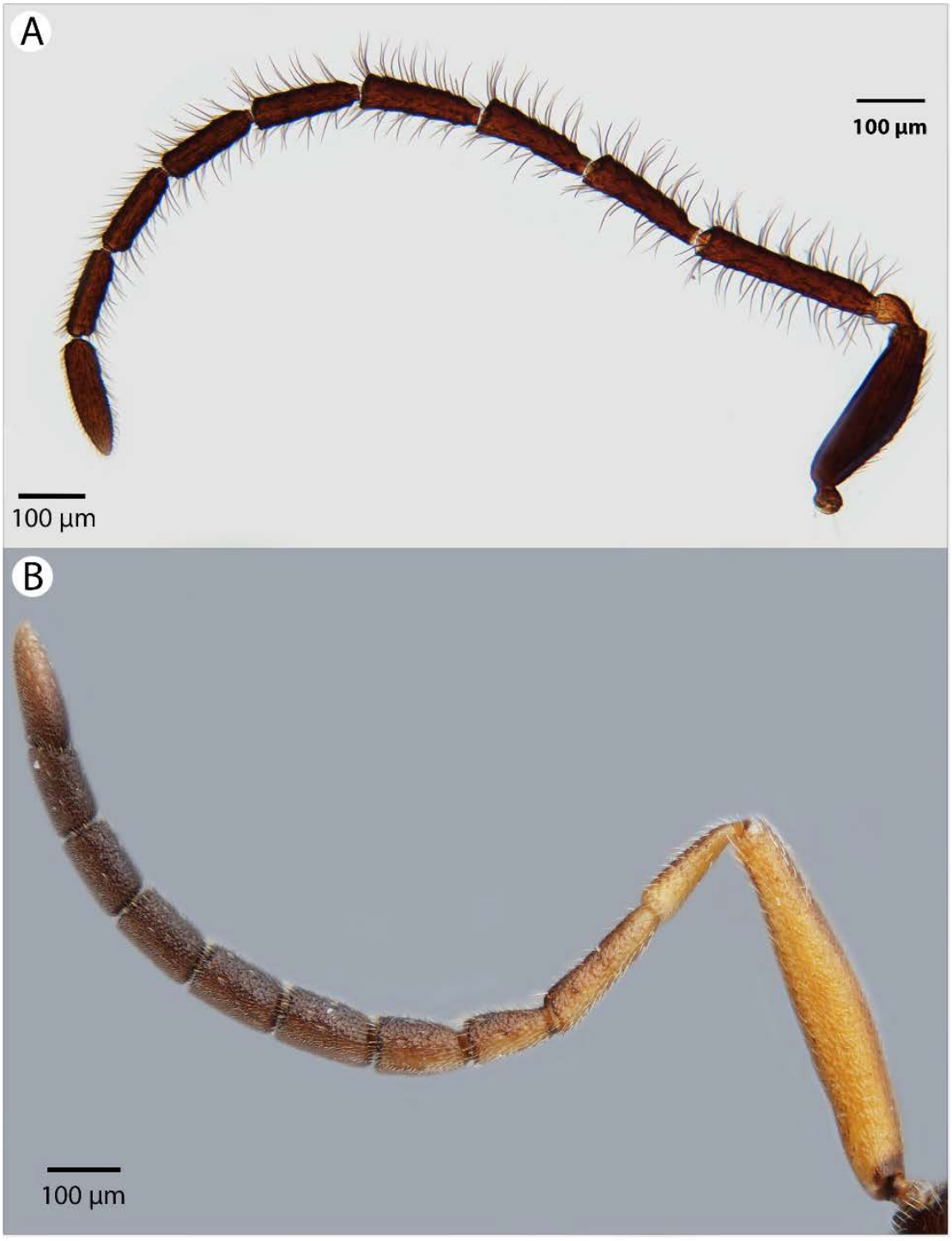

Figure 40. Brightfield image showing the antenna of *Conostigmus madagascariensis* Mikó and Trietsch sp. nov. A. Male. B. Female.

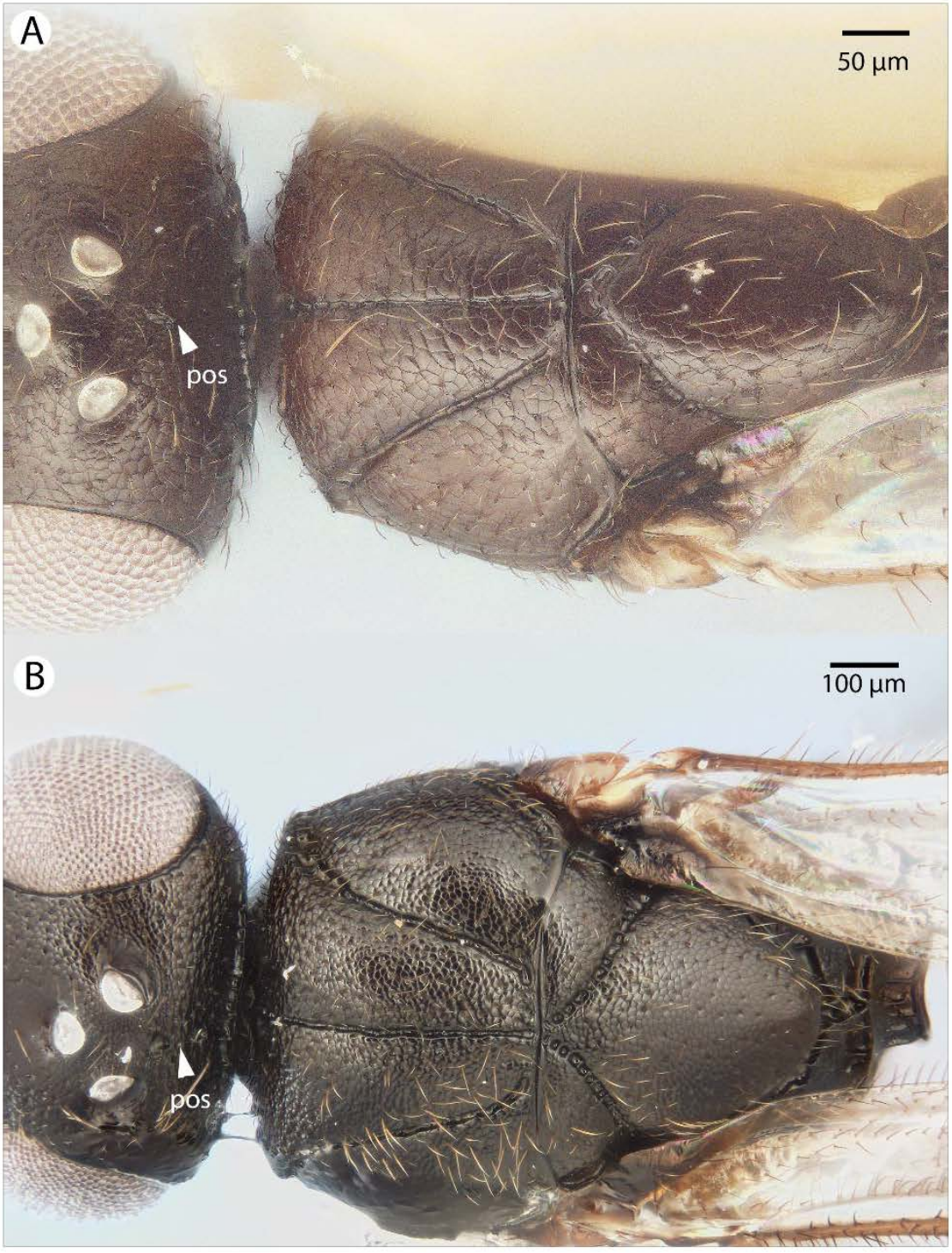

Figure 41. Brightfield image showing the inraspecific variability of the mesosoma of *Conostigmus madagascariensis* Mikó and Trietsch sp. nov., dorsal view. A. Smaller specimen. B. Larger specimen (pos= postocellar sulcus).

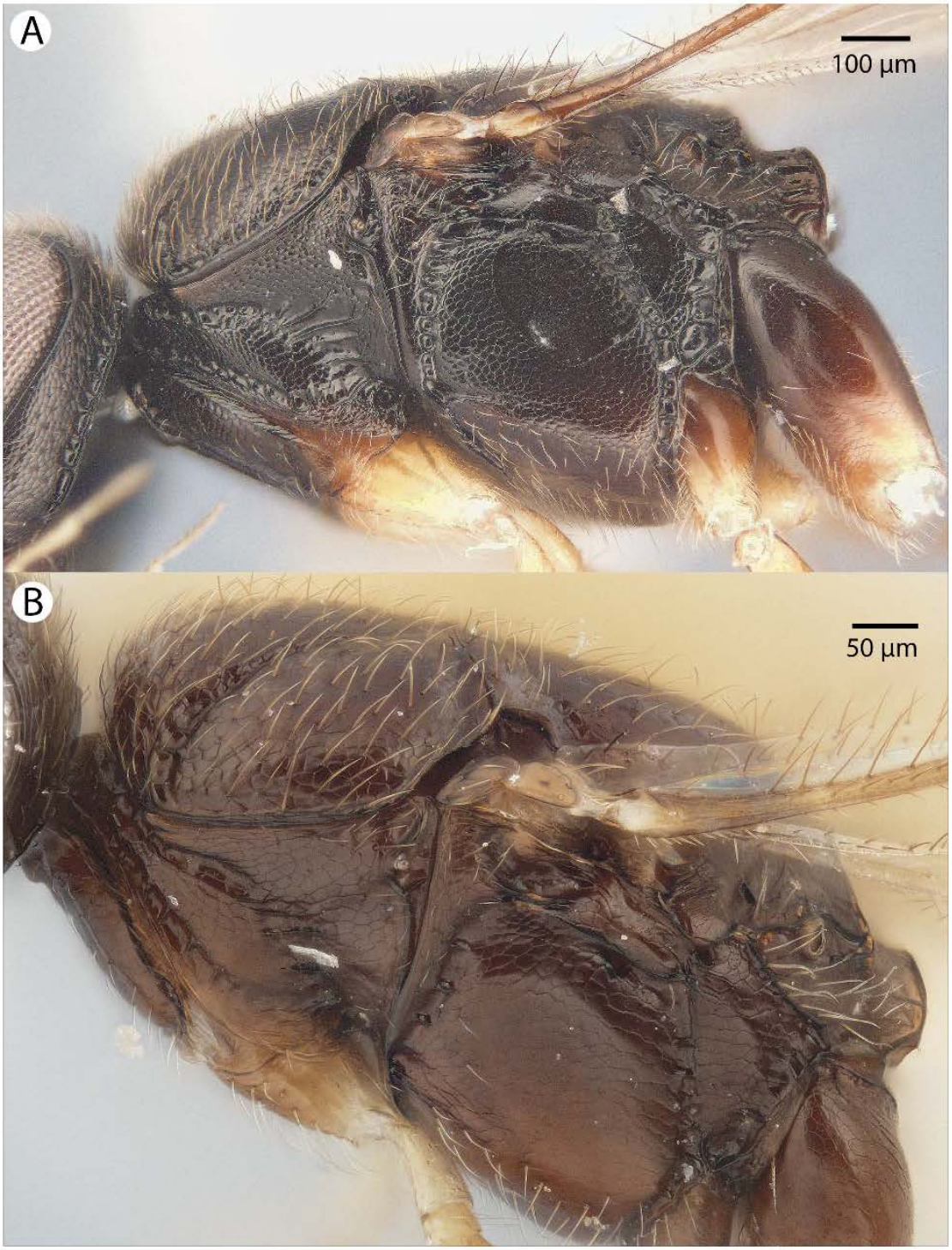

Figure 42. Brightfield image showing the inraspecific variability of the mesosoma of *Conostigmus madagascariensis* Mikó and Trietsch sp. nov., lateral view. A. Larger specimen. B. Smaller specimen.

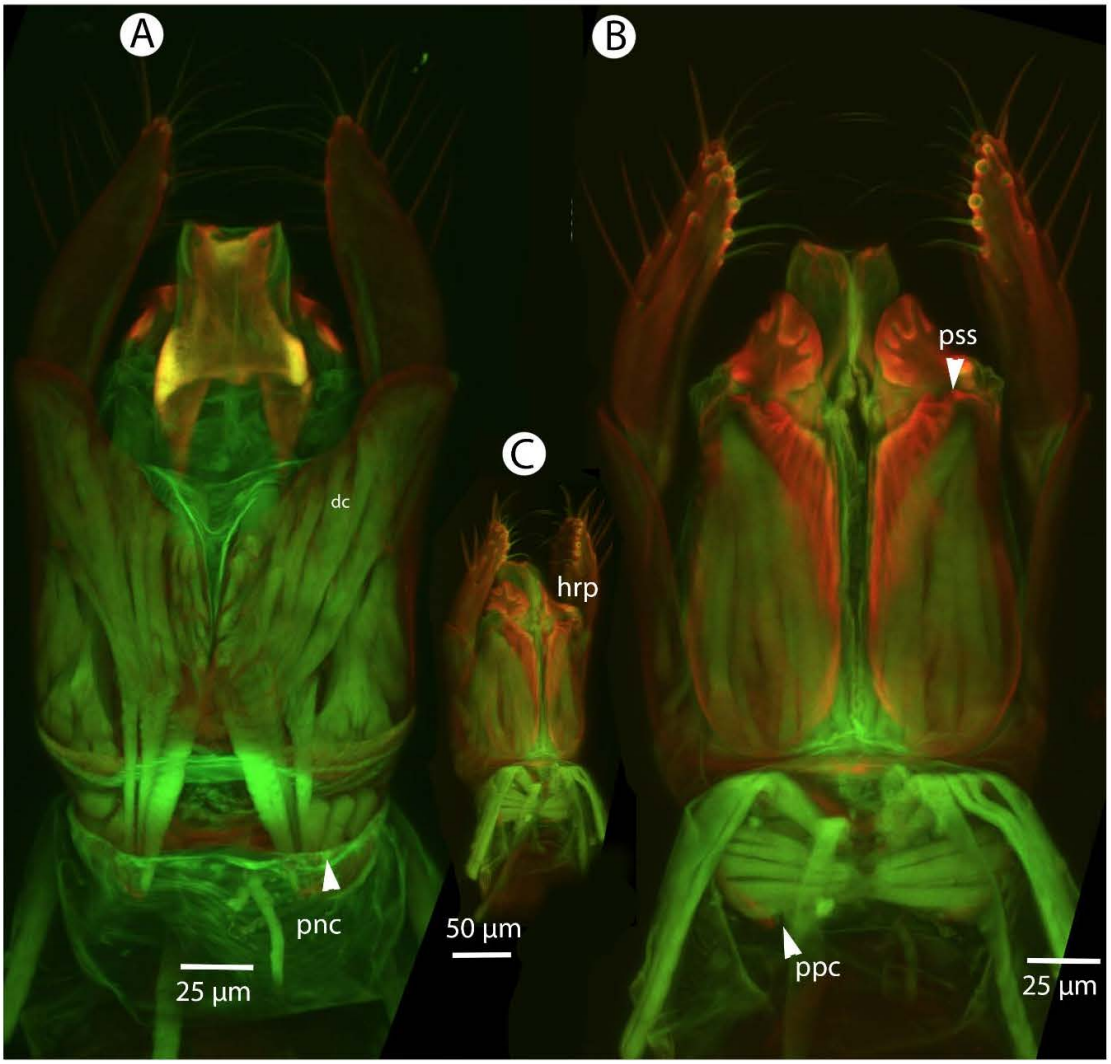

Figure 43. CLSM volume rendered micrographs showing the male genitalia of *Conostigmus madagascariensis* Mió and Trietsch sp. nov. A. Ventral view. B. Dorsal view (dc=dorsomedian conjunctiva of gonostyle/volsella complex, hrp=harpe, pdc=proximodorsal notch of cupula, ppc= proximlateral projection of cupula, pss= parossicular seta).

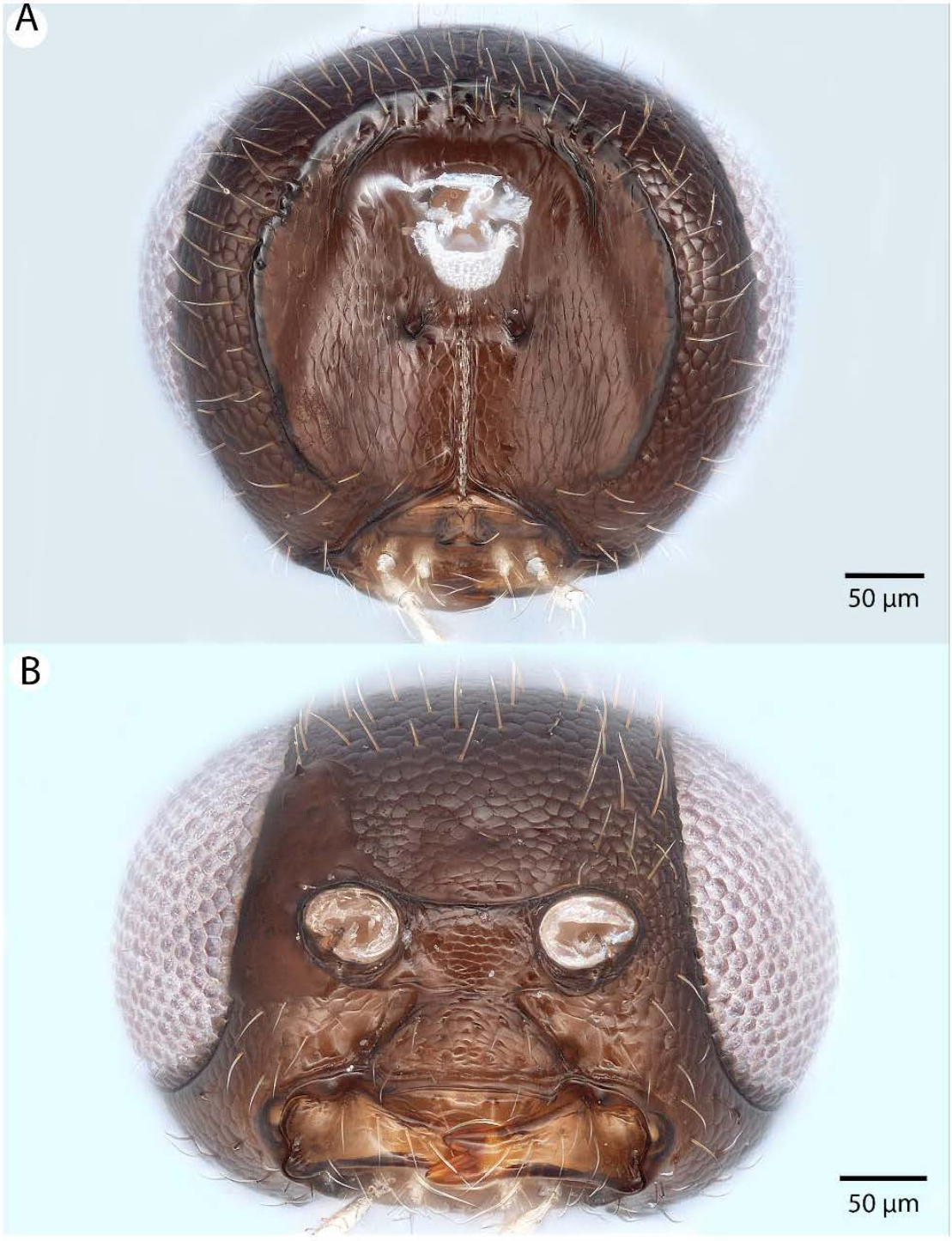

Figure 44. Brightfield image showing the head of *Conostigmus missyhazenae* Mikó and Trietsch sp. nov. A. Posterior view. B. Ventral view.

Figure 45. Brightfield image showing the antenna of *Conostigmus missyhazenae* Mikó and Trietsch sp. nov. A. Male. B. Female.

Figure 46. Brightfield image showing the head and mesosoma of *Conostigmus missyhazenae* Mikó and Trietsch sp. nov. A. Dorsal view. B. Lateral view.

Figure 47. CLSM volume rendered micrographs showing the male genitalia of *Conostigmus missyhazenae* Mió and Trietsch sp. nov. A. Ventral view. B. Dorsal view (hrp=harpe, dhs=dorsomedial setae of harpal setal ring).

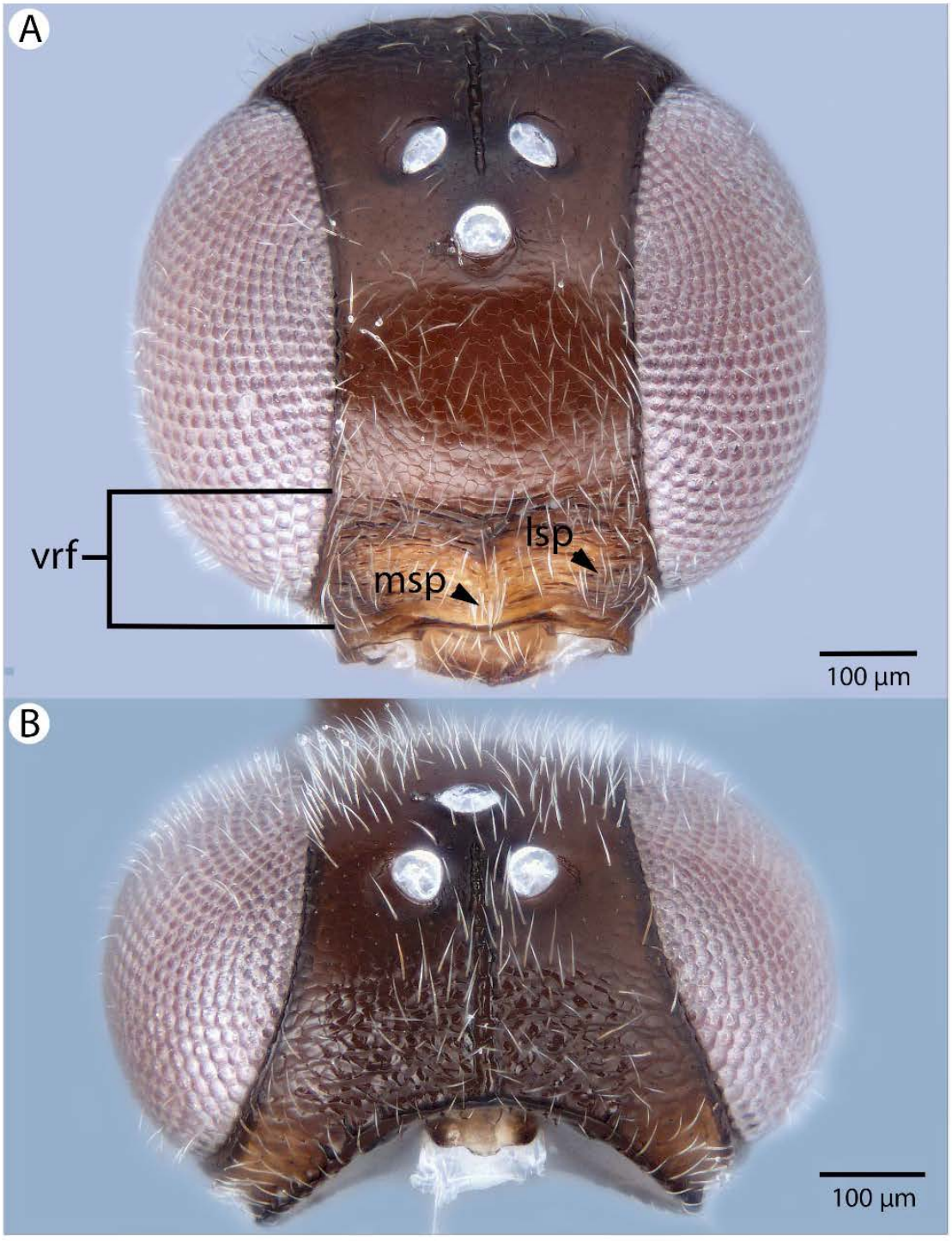

Figure 48. Brightfield image showing the head of *Conostigmus pseudobabaiax* Mikó and Trietsch sp. nov. A. Anterior view. B. Dorsal view.

Figure 49. Brightfield image showing the antenna of *Conostigmus pseudobabaiax* Mikó and Trietsch sp. nov. A. Female. B. Male.

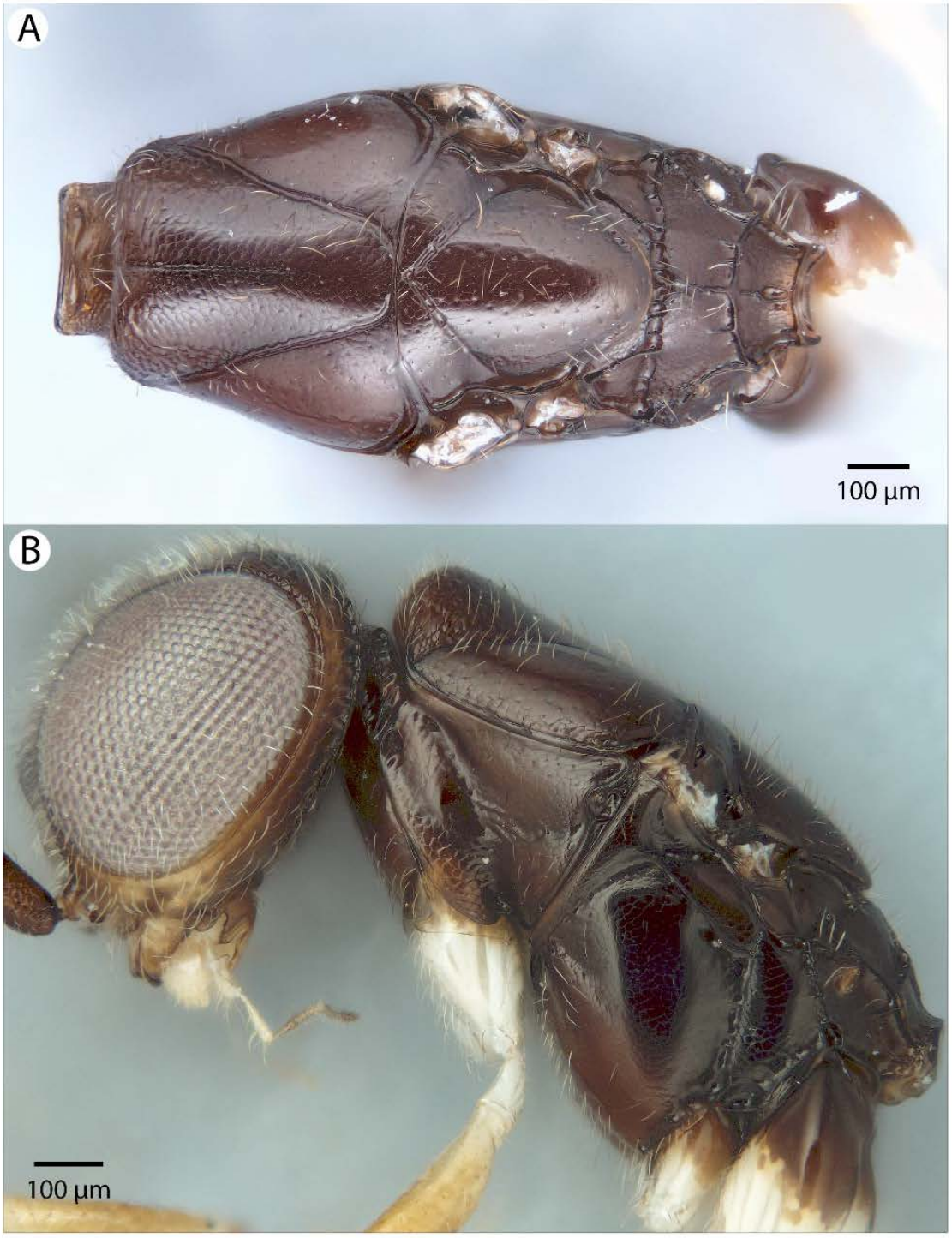

Figure 50. Brightfield image showing the head and mesosoma of *Conostigmus pseudobabaiax* Mikó and Trietsch sp. nov. A. Mesosoma, dorsal view. B. Head and mesosoma, lateral view.

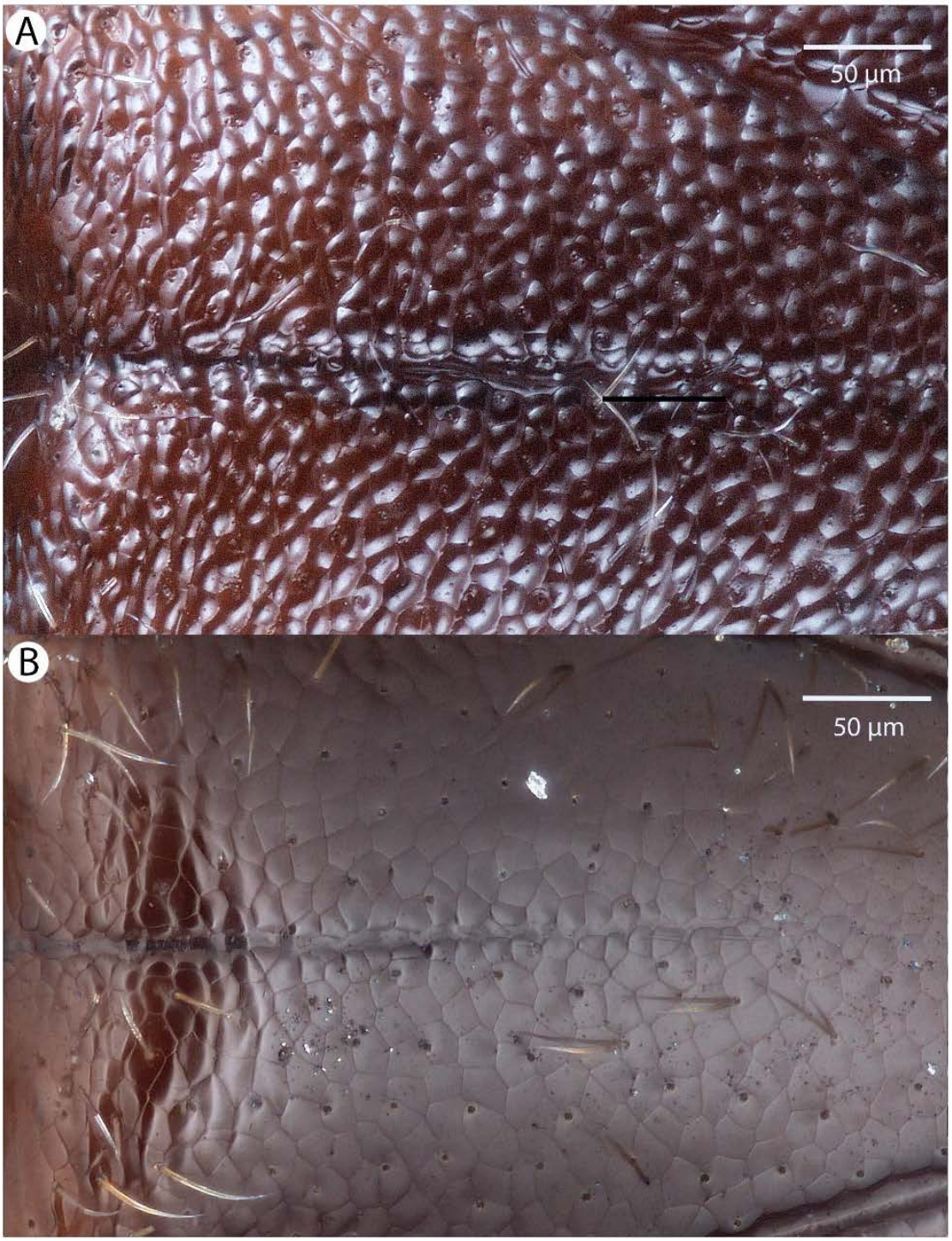

Figure 51. Brightfield image showing the middle anteromesoscutum of *Conostigmus* species, dorsal view. A. *Conostigmus toliaraensis* Mikó and Trietsch sp. nov. B. *Conostigmus pseudobabaiax* Mikó and Trietsch sp. nov.

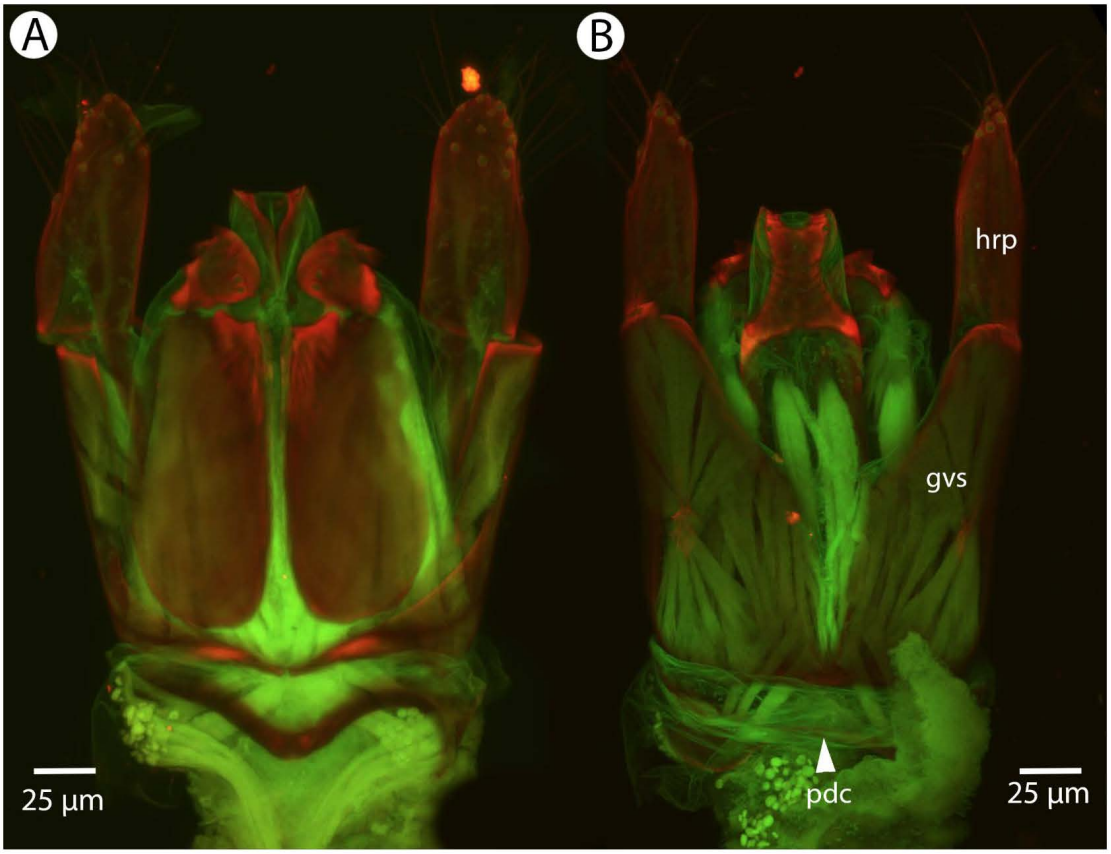

Figure 52. CLSM volume rendered micrographs showing the male genitalia of *Conostigmus pseudobabaiax* Mikó and Trietsch sp. nov. A. Ventral view. B. Dorsal view (dhs=dorsomedial setae of harpal setal ring, gvs=gonostyle/volsella complex, hrp=harpe, pdc=proximodorsal notch of cupula).

Figure 53. Brightfield image showing the antenna of *Conostigmus toliaraensis* Mikó and Trietsch sp. nov. A. Female. B. Male.

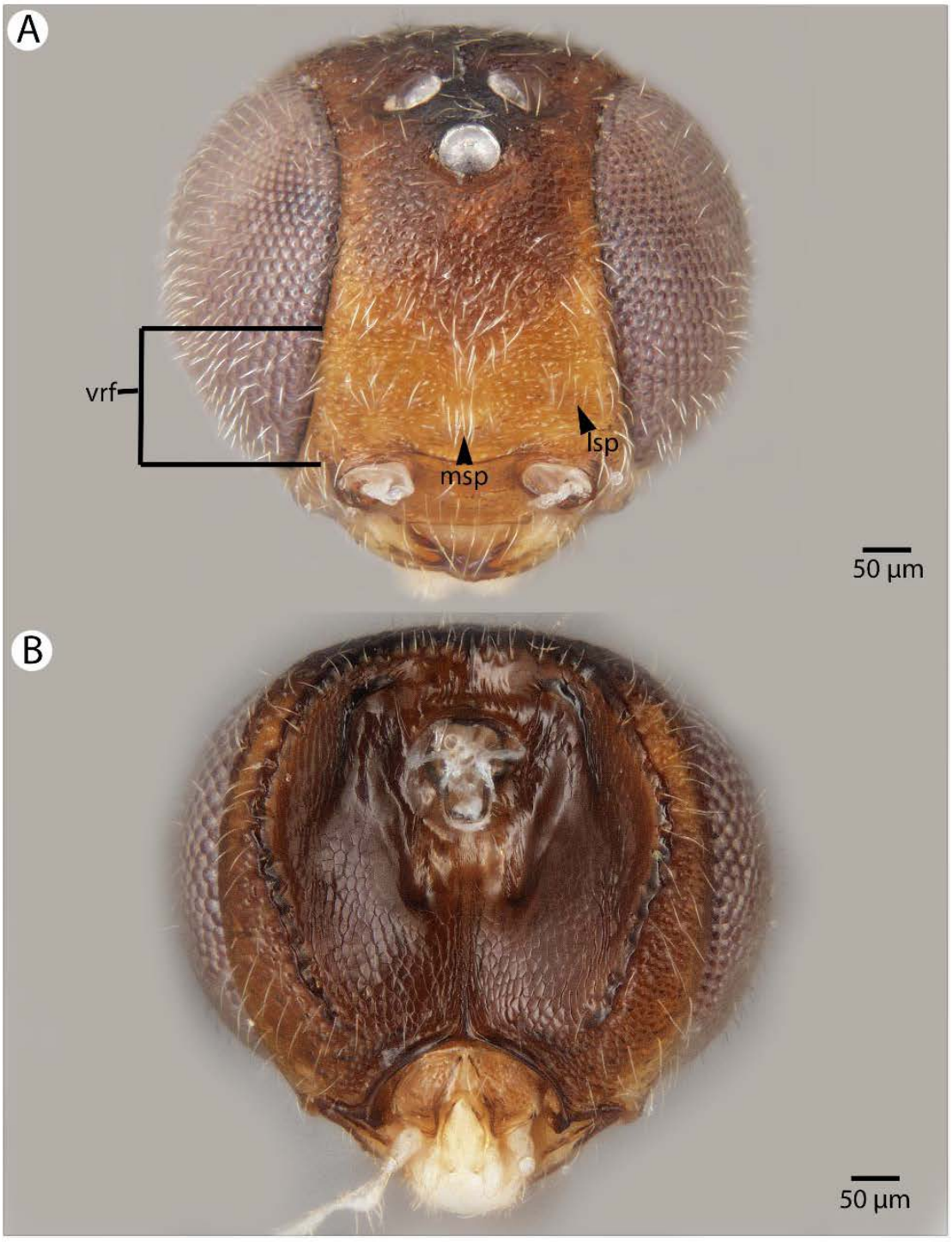

Figure 54. Brightfield image showing the head of *Conostigmus toliaraensis* Mikó and Trietsch sp. nov. A. Anterior view. B. Posterior view.

Figure 55. Brightfield image showing the mesosoma of *Conostigmus toliaraensis* Mikó and Trietsch sp. nov., dorsal view (mml= median mesoscutal line).

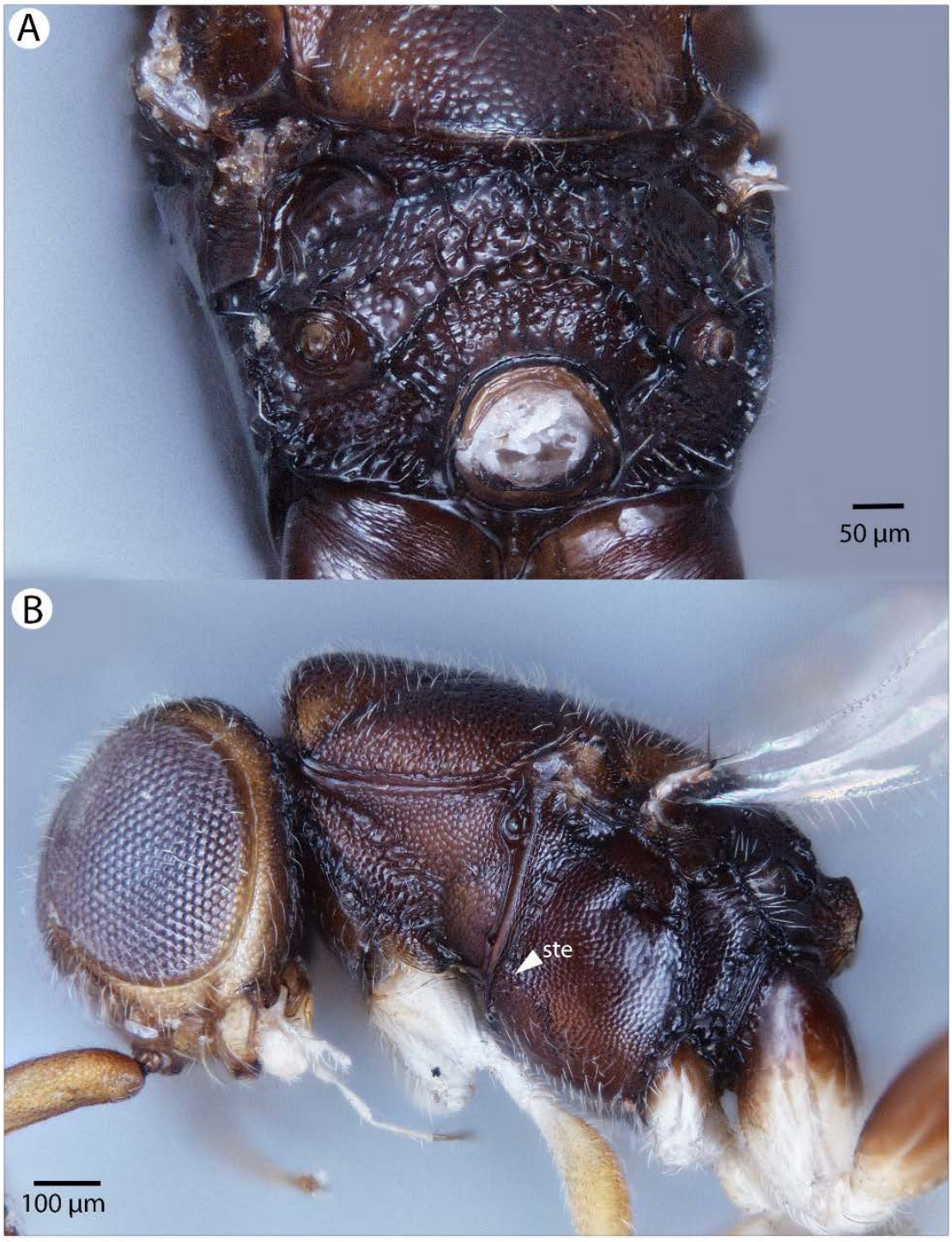

Figure 56. Brightfield image showing the head and mesosoma of *Conostigmus toliaraensis* Mikó and Trietsch sp. nov. A. Mesosoma, posterior view. B. Head and mesosoma, lateral view. (ste=sternaulus).

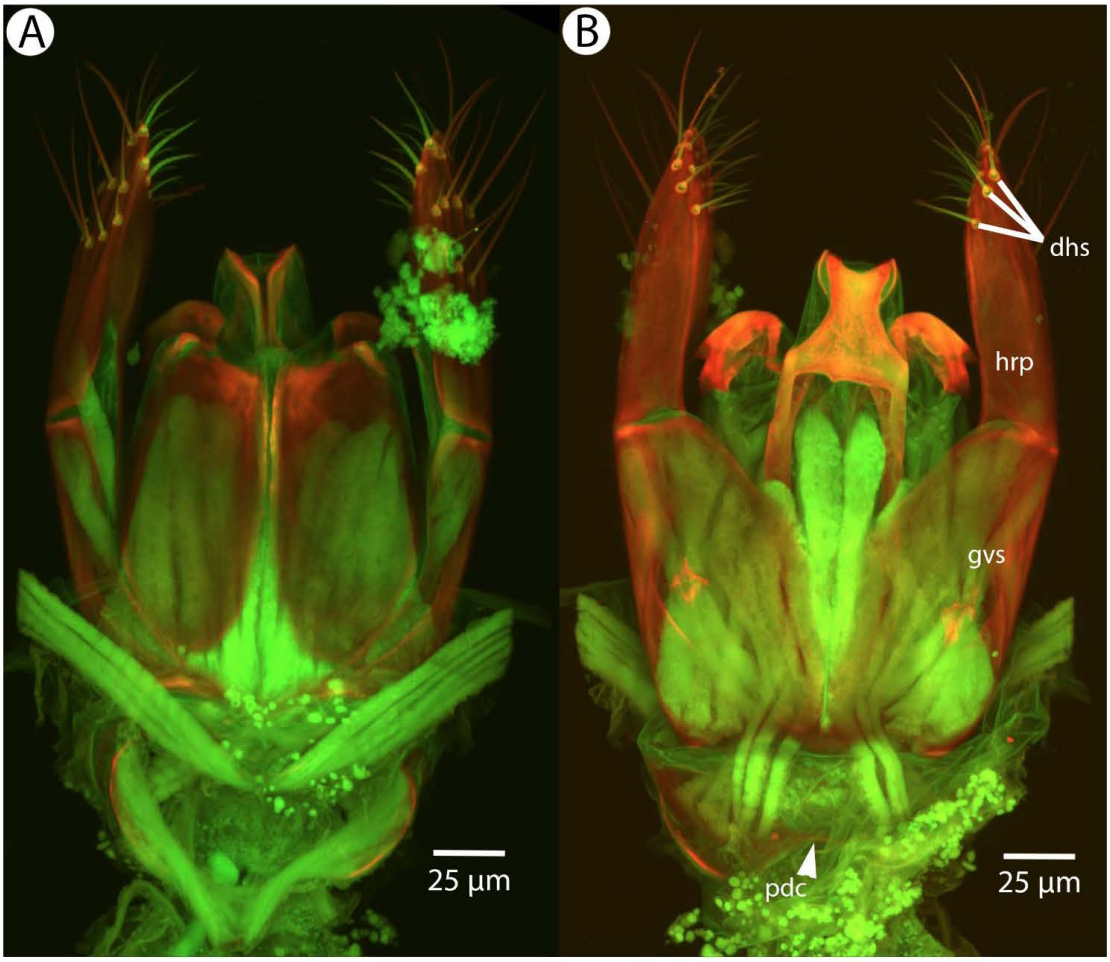

Figure 57. CLSM volume rendered micrographs showing the male genitalia of *Conostigmus toliaraensis* Mikó and Trietsch sp. nov. A. Ventral view B. Dorsal view (hrp=harpe, dhs=dorsomedial setae of harpal setal ring, gvs=gonostyle/volsella complex, pdc=proximodorsal notch of cupula).

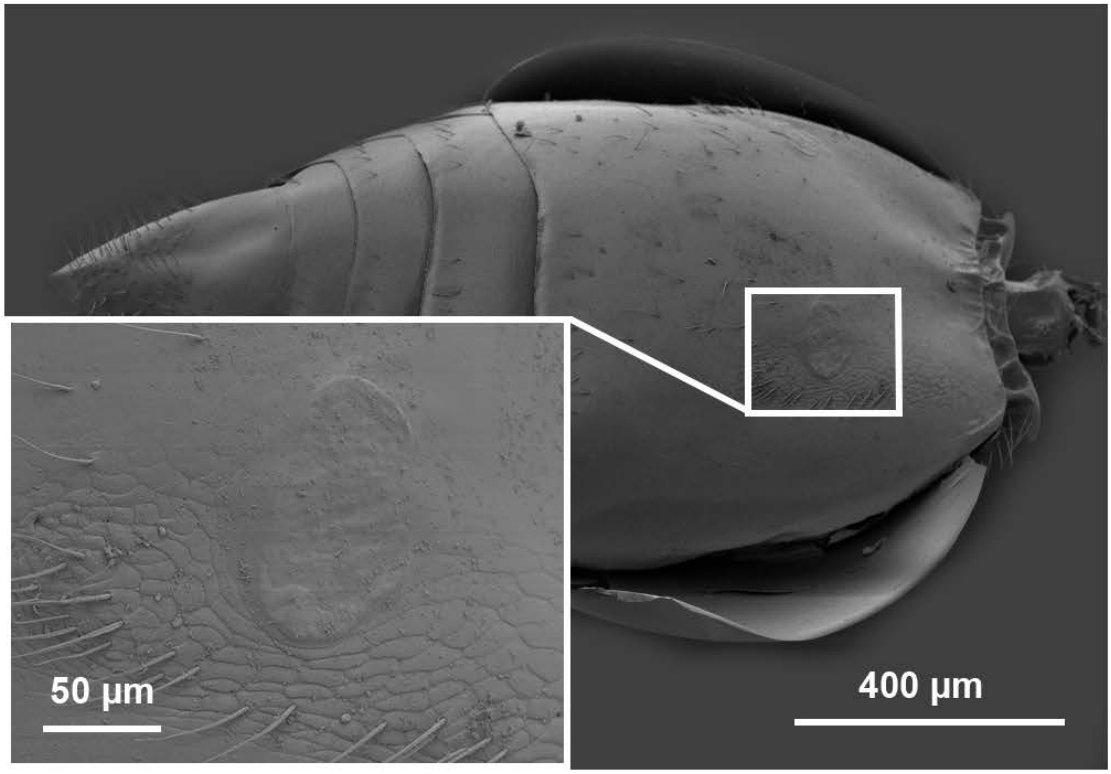

Figure 58. SEM micrograph of the metasoma of *Trichosteresis glabra* (Boheman 1831) in ventral view showing scutes corresponding to a possible exocrine gland.